PROCEEDINGS OF THE WORKSHOP
EXTERNAL SULFATE ATTACK

PORTUGAL • LISBON • LNEC
November 3-4, 2016

Editors:
Véronique Baroghel-Bouny
Isabel Martins
Esperanza Menéndez

PROCEEDINGS OF THE WORKSHOP EXTERNAL SULFATE ATTACK

Editors:
Véronique Baroghel-Bouny
Isabel Martins
Esperanza Menéndez

Preface

External sulfate attack (ESA) affects the long-term durability of various types of concrete structures. Although ESA has been studied for many years, it remains a controversial, confusing, and complex topic.

This volume contains the abstracts and full-length papers of contributions presented at the Workshop on External Sulfate Attack in concrete structures (ESA 2016) held on the 3rd and 4th of November 2016 at LNEC, Lisbon, Portugal. ESA 2016 is part of the activities of the RILEM TC 251-SRT on external sulfate attack, but was also open to other researchers. 12 countries were represented at the Workshop. As an important event of this TC, the Workshop focused on novelties in the understanding of basic mechanisms, as well as in the development of test methods dedicated to the evaluation of the resistance of concrete exposed to ESA. New binders (e.g. incorporating SCM and/or recycled materials) were in particular taken into account. In addition, the link between field performance and lab tests in accelerated conditions was addressed in the keynote lecture. The Workshop program included 18 contributions, which were articulated in 3 themes:

- Testing & influence of mix-parameters,
- Field aspects,
- Mechanisms and modeling.

This workshop provided a forum in which people from around the world came together to share their ideas and experience. For example, the most recent advances in research related to ESA and new developments on test methods were presented, as well as real case studies of concrete structures affected by external sulfate attack. All of this will constitute valuable matter to complement the STAR, one of the main deliverables of the RILEM TC.

Our sincere thanks go to the speakers and authors who have contributed to the scientific quality of the Workshop as reflected in the proceedings. We also gratefully acknowledge the LNEC for the organization of the event. Moreover, we express our gratitude to all the attendees for their interest and active contribution to fruitful discussion during the Workshop.

Paris, the 25th of April 2017

The Editors,
Véronique Baroghel-Bouny (Chair of RILEM TC-251-SRT)
Isabel Martins (LNEC)
Esperanza Menéndez (Secretary of RILEM TC-251-SRT)

ABSTRACT INDEX

PROCEEDINGS INDEX

KEYNOTE LECTURE

Perspectives on testing related to field performance

K. Scrivener[1]

ABSTRACT

This presentation will review work on external sulfate attack conducted at EPFL over the past ten years. This work has enabled us to determine the mechanism by which the ingress of sulfate ions lead to expansions and / or spalling of surface layers. It also shows that the types of tests applied in the laboratory bear little relation to the type of degradation seen in field. This led us to design new test methods, which also be presented.

---

1 EPFL, Switzerland

TESTING AND INFLUENCE
OF MIX-PARAMETERS

External sulphate resistance of low pH concrete

A.Cabrerizo[1], F. Cassagnabère[1], L. Lacarrière[1]

ABSTRACT

In the context of radioactive waste disposal in a deep geological repository in clay, low-alkalinity and low heat of hydration concretes referenced "low pH" have been designed with a specific matrix (OPC-silica fume-slag) by ANDRA (French National Radioactive Waste Management Agency). The physicochemical interactions between concrete and the environment (Argilite and Bentonite clay) can generate degradation of the concrete. The present study focuses the resistance of the material to ESA. The accelerated test method consisted of an immersion test of concrete specimens pre-saturated by the attack solution (T=25°C pH=7). The sodium sulfate concentration used for the test was 8.9 g/L.

To characterize the impact of accelerated SRT on concrete, various characteristics were measured before, during and after 12 weeks of immersion: dimensional and mass variation, and transfer properties.

The results show that, in comparison with current concretes (OPC and binary binder), low pH concrete presents a high resistance to ESA, similar to that of a concrete designed with SR cement.

1   Université de Toulouse, UPS, INSAT; LMDC, Toulouse, France, email: cassagnabère@insa-toulouse.fr

Combination of immersion and semi-immersion test to evaluate concretes manufactured with sulfate resistance cements

E. Menéndez[1], R. García-Roves[2], V. Baroghel-Bouny[3], B. Aldear[4], S. Ruíz[5]

ABSTRACT

Usually the regulation defines the concentration of sulfates to consider aggressive soil or water. There are different standards to evaluate the resistance of concretes to the external sulfate attack. Most of these tests are based on the immersion of samples in solutions with high concentration of sulfates. But in the field, the concretes are exposed also to wet-dry cycles and the crystallization of salts can occur. In this work sixty five concretes manufactured with sulfate resistance cements are tested. The cores are tested in immersion during 1 year in sodium and calcium solutions analysing aspect, expansion and variation of weight. After this, the cores are exposed to same solutions semi-immersed for 2.5 years. After one year of semi-immersion some of the concretes are showing alterations. After 2.5 years, around the 15% of cores are showing cracks and loss of material, due to formation of ettringite and thaumasite.

1   IETcc-CSIC, Spain; email: emm@ietcc.csic.es

2   IETcc-CSIC, Spain; email: ricardo@ietcc.csic.es

3   IFSTTAR, France; email:veronique.baroghel-bouny@ifsttar.fr

4   IETcc-CSIC, Spain; email:beaaldea@ietcc.csic.es

5   Dragados, S.A., Spain.

Influence of recycled coarse aggregates on concrete under external sodium sulphate attack

L. Carranca[1], I. M. Martins[2], J. de Brito[3]

ABSTRACT

Concrete is the building material most widely used in the world and has been the focus of increased research efforts in what concerns the sustainable use of resources in its production, as well as on the performance and durability of concrete structures.

In this study, the above outlined areas were considered by analysing the effect of substituting natural aggregates with coarse recycled concrete aggregates, at 25%, 50% and 100%, on the durability of concrete subjected to external attack by sodium sulphate.

The degradation due to the immersion of the specimens in solutions with different concentrations of sulphates, with and without pH control, was assessed by monitoring the variations in mass and length over time and comparing them with those from a reference concrete.

Other physical characteristics of the concrete compositions, like compressive strength and tensile strength, permeability, porosity and water absorption, were also monitored to investigate relationships with sulphate attack.

1   IST, Instituto Superior Técnico, Portugal; e-mail: luis_msc@hotmail.com

2   LNEC, Laboratório Nacional de Engenharia Civil, Portugal; e-mail: imartins@lnec.pt

3   CERIS-ICIST, Instituto Superior Técnico, Universidade de Lisboa, Portugal; e-mail: jb@civil.ist.utl.pt

External sulfate attacks: advanced testing and performance specifications

G. Massaad[1], E. Rozière[2], A. Loukili[3], L. Izoret[4]

ABSTRACT

In this work, a new monitoring approach was developed to enhance the analysis of performance tests and provide new criteria for the sulfate resistance of cement-based materials. Even in the case of low expansion, the method allows detecting microscopic evolutions of materials exposed to external sulfate attacks via a set of easily accessible monitored parameters.

The main phenomena induced by external sulfate attack are leaching, precipitation, aggregates loss and cracking. Based on the monitoring of mass, hydrostatic weighing, elongation and the amount of leached OH- the method provides the decoupling of micro-elemental mass variations corresponding to each phenomenon.

The phenomena decoupling and the other monitoring strategy outputs allow the proposition of new potential performance indicators: the averaged density and the deformation path. The indicators showed an interesting sensitivity to the microstructural and macroscopic evolutions for different tested cements composition.

1   Institut de Recherche en Génie Civil et Mécanique (GeM), UMR-CNRS 6183, Ecole Centrale de Nantes, 1 rue de la Noë, 44321 Nantes, France; email: georges.massaad@ec-nantes.fr

2   Institut de Recherche en Génie Civil et Mécanique (GeM), UMR-CNRS 6183, Ecole Centrale de Nantes, 1 rue de la Noë, 44321 Nantes, France; email: emmanuel.roziere@ec-nantes.fr

3   Institut de Recherche en Génie Civil et Mécanique (GeM), UMR-CNRS 6183, Ecole Centrale de Nantes, 1 rue de la Noë, 44321 Nantes, France; email: ahmed.loukili@ec-nantes.fr

4   Association Technique de l'Industrie des Liants Hydrauliques (ATILH), 7 place de la Défense, 92974 Paris La Défense, email: l.izoret@atilh.fr

Sulfate resistance testing, mortar vs. concrete testing

F.Moro[1], A.Leemann[2]

ABSTRACT

The sulfate resistance of mortar and concrete was investigated using two accelerated tests. The ASTM-C1012 mortar test is based on immersion in sulfate solution, while the concrete in SIA 262-1/D is subjected to drying-immersion cycle before a constant immersion period. While the former test intends to evaluate the potential sulfate resistance of a binder, the latter is designed to assess the sulfate resistance of job-site concrete. In addition to nine cements based on ordinary Portland cement, sulfate activated and alkali activated slag cements were used. The comparison of the test results reveals a correlation between the length changes of the mortars and the concrete with a water-to-binder-ratio (w/b) of 0.65. This correlation is much weaker, when the results of the mortar test are compared to the results obtained with the concrete produced with a w/b of 0.40. Obviously, the impact of w/c is stronger for certain binders applied in concrete than the impact of cement composition.

1   LafargeHolcim Research Centre, Durability & Modelling Department, France; email: fabrizio.moro@lafargeholcim.com

2   Empa, Swiss Federal Laboratories for Materials Science and Technology, Dübendorf, Switzerland; email: Andreas.Leemann@empa.ch

Degradation of cement paste immersed in sodium sulfate solutions

Xu Ma[1], Oğuzhan Çopuroğlu[2], Erik Schlangen[3], Ningxu Han[4] and Feng Xing[5]

ABSTRACT

External sulfate attack is a slow degradation process that may cause expansion and cracking in cementitious materials. The underlying mechanism is still under debate. In this paper, hollow cement paste cylinders with a wall thickness of 2.5mm were made and immersed in sodium sulfate solutions with concentrations of 1.5 g/L and 30 g/L SO_4^{2-}. Changes in pore size distributions were investigated by mercury intrusion porosimetry (MIP) before exposure and after 21-day, 70-day and 105-day immersion. Also the reaction products were analyzed through energy dispersive spectrometry (EDS) elemental mapping. The effects of solution concentration and immersion time were discussed. A mixture of ettringite and gypsum was found in the low sulfate concentration, while high sulfate concentration resulted in much more gypsum precipitation. It was also found that the pores with diameters between 10 nm and 70 nm were continuously filled during the immersion tests which can support the crystal growth pressure theory.

---

1   Delft University of Technology, Microlab, the Netherlands; e-mail: X.Ma-1@tudelft.nl

2   Delft University of Technology, Microlab, the Netherlands; e-mail: O.Copuroglu@tudelft.nl

3   Delft University of Technology, Microlab, the Netherlands; e-mail: Erik.Schlangen@tudelft.nl

4   Shenzhen University, Guangdong Province Key Laboratory of Durability for Marine Civil Engineering, PR China; e-mail: nxhan@szu.edu.cn

5   Shenzhen University, Guangdong Province Key Laboratory of Durability for Marine Civil Engineering, PR China; e-mail: xingf@szu.edu.cn

Comparative study on the sulfate milieu attacks effect on concrete based on limestone additions at curing temperature

I. A. Bella[1], N. Bella[2], A. Asroun[3]

ABSTRACT

The aggregates factory consumes a big quantity of energy; by consequence, it costs money, in the other hand it produces a lot of waste material or SCM (sustainable concrete material).

The results obtained in this study summarize up the importance of SCMs aggregates on behavior of the concrete, this different kind of SCM aggregate offered different behavior at the fresh state of the batch and by consequence its result with different mechanical behavior at the hardened state of concrete. The principal aim of adding rolled or crushed SCM is makes a concrete, which can resist to exhaustive environment (at curing temperature).

The results obtained in this study summarize up the importance of the use of waste material or sustainable concrete material to minimize the transfer mechanisms' in concrete in sulfate milieu and at curing temperature, than finally minimize down the permeability of concrete which leads to durable concrete.

1   FIMAS, Civil engineer department, Algeria; e-mail: Ilham_aguida@yahoo.fr

2   FIMAS, Civil engineer department, Algeria; e-mail: bella5dz@yahoo.fr

3   University of Djilaly Liabess, Civil engineer department, Algeria; e-mail: a_asroun@yahoo.fr

External sulfate attack – Influence of an early age exposure, coupling with the cement composition

R. Ragoug[1,2], O. Omikrine-Metalssi[1], J-M. Torrenti[1], F. Barberon[2], L. Divet[1], N. Roussel[3]

ABSTRACT

External sulfate attack (ESA) is one of the main causes of deterioration for concrete structures. It is currently studied on saturated samples. However, in pratice, concrete structures are exposed as soon as the formworks are removed. The aim of this study is to highlight the effect of an early age exposure on the degradation mechanisms of the ESA. For this study, two cements were used (CEM I and CEM III). The microstructure changes are monitored by using several experimental techniques such as NMR (^{27}Al), ICP, XRD and SEM. These analyses showed a neutral effect of an early age exposure on the sulfate ingress in both cement types. A negative effect of slag cement is observed after only 3 months of exposure at early age and a positive one for the mature pastes. Conversely, Portland cement paste resist very well and long to ASE, for an early age exposure and fail for the cured specimens.

1   Université Paris Est, IFSTTAR, MAST, FRANCE

2   Bouygues Travaux Publics, Pôle Ingénierie Matériaux, FRANCE

3   Université Paris Est, IFSTTAR, Laboratoire Navier, FRANCE

Performance of limestone calcined clay blends in sodium sulphate attack on mortars

F. Suma[1], M. Samthanam[1]

ABSTRACT

Limestone blended cements are increasingly emerging as a choice for good long-term durability of concrete. In this category of cements, limestone-calcined clay cement blends present a major advantage owing to the high reactivity of the calcined clay and the synergistic effects brought about by the aluminate – carbonate interactions. The present study reports an experimental evaluation of the resistance to sodium sulphate attack of limestone calcined clay cement mortars in comparison with OPC and fly ash blended cement mortars. Results up to 60 weeks of immersion confirm that both limestone calcined clay cement blend and fly ash cement blend perform far superior to the OPC. Expansions are almost nil in the case of the limestone calcined clay cement mortar despite the long period of immersion in 5% sodium sulphate solution. The details of the microstructural analysis conducted using SEM and XRD are also reported in the paper.

1   Department of Civil Engineering, IIT Madras, Chennai, INDIA, email: manus@iitm.ac.in

FIELD ASPECTS

External sulfate attack in Japan: A review

Y. Kawabata[1], N. Yoshida[2], S. Ogawa[3], K. Yamada[4]

ABSTRACT

External sulfate attack (ESA) is one of the pathologies in which concrete is physically or chemically degraded, leading to loss of performance of the structure affected. Although the damage level by ESA is strongly influenced by climate conditions such as temperature history and wetting/drying cycles as well as sulfate concentration of the exposed site, the relation of laboratory tests to field performance remains unclear.

In order to bridge the knowledge gap between laboratory and field performance, it is beneficial to summarize cases of ESA damage to real concrete structures in the field. This paper reviews the real cases in Japan, including some current cases related to ESA.

1   Port and Airport Research Institute, Structural Engineering Department, Japan; email: kawabata-y@pari.go.jp

2   General Building Research Corporation of Japan, Materials laboratory, Japan; e-mail: n-yoshida@gbrc.or.jp

3   Taiheiyo Consultant, Sales and Marketing Division, Japan; e-mail: Shoichi_Ogawa@taiheiyo-c.co.jp

4   National Institute for Environmental Studies, Radiological Contaminated off-site waste Management Section, Japan; e-mail: yamada,kazuo@nies.go.jp

Sulfate attack on residential concrete foundations in Japan

N. Yoshida[1]

ABSTRACT

Deterioration of concrete structures caused by external sulfate attack was found in many residential concrete foundations in Japan. In residential concrete foundations constructed on sulfate-bearing ground, sodium sulfate solution contained in the soil penetrates the above-ground area of the concrete, and a scaling of the area occurs with white crystals of thenardite or mirabilite. The deterioration mechanism is known as "physical sulfate attack" or "salt weathering". The deterioration cases were usually observed in sites where the ground comprised of marine deposits that contained sulfides; these soil conditions are common in large part of Japan. This paper describes the concrete deterioration phenomenon based on field investigations and analysis results of soil and concrete samples. A rapid test method to estimate the risk of physical sulfate attack is proposed.

1   General Building Research Corporation of Japan, Materials laboratory, Japan; e-mail n-yoshida@gbrc.or.jp

Sulfate ingress in recycled concrete immersed in sodium sulfate solution for 10 years

L.R. Santillán[1], Y.A. Villagrán Zaccardi[2], D.E. Benito[3], C.J. Zega[4]

ABSTRACT

Sulfate ions ingress into concrete matrix through pore solution, and interact with hydration products resulting in potential detrimental effects. A main concern regarding this deterioration process is the rate at which sulfate can penetrate into concrete, and for the particular case of recycled concrete, the increased porosity due to attached mortar in aggregate particles is a potential disadvantage. Moreover, hydration products within recycled aggregate particles can react with ingressing sulfates, causing more internal damage. This paper presents sulfate ingress profiles in conventional and recycled concrete specimens immersed in 50 g/l sodium sulfate solution for 10 years. Four concretes with w/cm= 0.35 and with 0%, 50%, 75% and 100% of coarse recycled aggregate were tested. Sulfate content was determined up to 3 cm depth by chemical analysis and XRF. Complementary thermogravimetric analyses were also performed. Limited influence of recycled aggregate was obtained and not in correspondence with the increased porosity.

1   LEMIT, CONICET, Área Tecnología del Hormigón, Argentina; email: lautarorsantillan@gmail.com

2   LEMIT, CONICET, Área Tecnología del Hormigón, Argentina, Magnel Laboratory for Concrete Research, Ghent University, Belgium; email: yuryvillagran@conicet.gov.ar

3   LEMIT, Área Tecnología del Hormigón, Argentina; email: benitodamian@hotmail.com

4   LEMIT, CONICET, Área Tecnología del Hormigón, Argentina; email: cj.zega@conicet.gov.ar

Sulfate attack in concrete: State of art in Brazil

R.Schmalz[1], F.G.S.Ferreira[2], A.I. Castro[3], J.P.Moretti[4], A. Sales[5]

ABSTRACT

Sulfate ions are among the main concrete deterioration agents. When in contact with cement hydration products ($Ca(OH)_2$ and C-S-H), they chemically react causing expansion and cracking of the cement matrix, which facilitates the ion penetration and accelerates the degradation process. Fairly is known about the effects of this aggressive agent, however some issues still raise doubts and controversy. Among them, which is the most effective method to analyze the deleterious potential of these ions and which variables can interfere in the results. Therefore, the present papers presents the state of art of Brazilian research about sulfate attack and thus, seeks to analyze and discuss the factor that can influence the degradation process, the laboratory tests results and, at last, show Brazilian standards that define the requirements for concrete exposed to sulfates.

1   Department of Civil Engineering, Federal Universityof São Carlos, Brazil; email: rosanaschmalz@gmail.com

2   Department of Civil Engineering, Federal Universityof São Carlos, Brazil; email: fgianotti@ufscar.br

3   Department of Structure Engineering, Federal Universityof São Paulo, Brazil; email: alcastro@sc.usp.br

4   Department of Civil Engineering, Federal Universityof São Carlos, Brazil; email: julianamoretti88@ufscar.br

5   Department of Civil Engineering, Federal Universityof São Carlos, Brazil; email: almir@ufscar.br

Sulfate resistance in blended cements with fired clay-based additions

E. Asensio[1], C. Medina[2], I.F. Saéz[2], B. Cantero[2], M. Frías[1], M.I. Sánchez de Rojas[1]

ABSTRACT

Binders should be judged not only in terms of their ability to develop hydraulic properties, but also of their interaction with potentially aggressive agents, which may affect their characteristics and performance during service life.

This study analysed the effect of different types of fired clay-based industrial by-product or waste additions on cement sulfate resistance. The additions were characterised both physically and chemically. Blended cement pastes were prepared and, using the Köch-Steinegger method, the durability of the new materials was assessed on the grounds of their corrosion index. New hydration products that might induce specimen mineralogical and morphological decay were also studied by comparing the pastes before and after soaking in a sodium sulfate solution for different test periods. With a few exceptions, the findings showed that including such waste as alternative pozzolans improved cement paste durability.

---

1   Eduardo Torroja Institute for Construction Sciences (IETcc – CSIC). 28033 Madrid, Spain

2   School of Engineering, UEX – CSIC Partnering Unit, University of Extremadura. 10003, Caceres, Spain

MECHANISMS
AND MODELLING

Experimental study of stresses induced in model cement-based materials by in-pore crystallization

N.N.Bui[1] , M. Vandamme[2], J-M. Pereira[3], R. Barbarulo[4]

ABSTRACT

Ingress of sulfates in ordinary cement-based materials induces in-pore crystallization of ettringite and/or gypsum, which may lead to an expansion or even damage of the material. Here we aim at better understanding how in-pore crystallization induces mechanical stresses at the scale of the sample.

We used well-hydrated cement pastes, which we grind and compact into macroscopic cylindrical specimens which are significantly more permeable than regular cement pastes. Upon testing, the specimens are located in a so called isochoric cell, which prevents the sample from expanding, but it is instrumented such that the mechanical stresses exerted by the specimen on the walls of the cell can be measured. Each experiment consists in flushing a specimen in its isochoric cell with solutions of sodium sulfate of various concentrations and measuring how these stresses evolve over time.

In parallel to the experimental campaign, thermodynamical modelling is performed, to estimate how the phase assembly of the specimens evolves over the injections. We find that the stresses that are measured are directly correlated to the volume of crystals formed. We discuss a mechanism that can explain the observed correlation and therefore how, in our compacted ground cement-based specimens in-pore crystallization translates into macroscopic mechanical stresses.

1   Université Paris.Est, Laboratoire Navier (ENPC, IFSTTAR), 6-8 Av. B. Pascal, 77420 Champs sur Marne; email: nam-nghia.bui@enpc.fr

2   Université Paris.Est, Laboratoire Navier (ENPC, IFSTTAR), 6-8 Av. B. Pascal, 77420 Champs sur Marne; email: matthieu.vandamme@enpc.fr

3   Université Paris.Est, Laboratoire Navier (ENPC, IFSTTAR), 6-8 Av. B. Pascal, 77420 Champs sur Marne; email: jeanmichel.pereira@enpc.fr

4   LafargeHolcim Centre de Recherche, 95 rue de Montemurier, 38291Saint-Quentin-Fallavier ; email: remi. barbarulo@lafargeholcim.com

Artificial neural network modeling of the expansion behaviour of recycled concrete aggregate under external sulphate attack

S. Boudali[1,6], B. Boukhatem[2], B. Abdulsalam[3], S. Poncet[4], A.M. Soliman[5], D. E. Kerdal[6]

ABSTRACT

Evaluating expansion of self-compacting concrete (SCC) incorporating recycled concrete aggregates (RCA) during production is a commonly used criterion. However, monitoring expansion is a complicated process. In this research, an Artificial Neural Network (ANN) model was developed to predict the expansion of self-compacting concrete (SCC), incorporating recycled concrete aggregates (RCA) and fine recycled aggregates (FRA) as replacement of natural aggregates (NA) and natural pozzolana (NP), respectively, while being exposed to external sulphate attack. For the ANN model, nine input parameters including water content, water-binder ratio, mineral additives (NP,FRA), sand, natural aggregate (NA) ,recycled concrete aggregates contents and immersing period in sodium sulphate (Na_2SO_4) solution. The output parameter of the developed ANN is the expansion change for an investigated period (up to 1 year). The developed ANN model exhibited excellent capability in capturing complex effects and interactions among model inputs on the expansion change of SCC for different levels of RCA replacement.

1   Université de Sherbrooke, Department of Mechanical Engineering,Canada; email: sara.boudali@usherbrooke.ca

2   Université de Sherbrooke, Department of Civil Engineering, bakhta.boukhatem2@usherbrooke.ca

3   Western University, Departent of Civil and Environmental Engineering, email: babdulsa@uwo.ca

4   Université de Sherbrooke, Université de Sherbrooke, Department of Mechanical Engineering, Canada; email: Sebastien.Poncet@USherbrooke.ca

5   Concordia University, Departent of Building, Civil and Environmental Engineering, email: ahmed.soliman@concordia.ca

6   Oran University of Science and Technology, Department of Civil Engineering, email: djkerdal@yahoo.fr

Simplified model to assess the durability of elements subjected to external sulfate attack: Influence of shape and size of the elements

Ikumi, T.[1], Cavalaro, S.[1], Segura, I.[1, 2], de la Fuente, A.[1], Aguado, A.[2]

ABSTRACT

The mitigation of the external sulfate attack from the standpoint of the design of concrete structures is usually based on the use of cement with limited content of aluminates. Nevertheless, other parameters may affect the final durability, such as the cement content, the geometry and size of the structure. The consideration of these factors is highly complex. Few straightforward methods are available to verify the durability of structures subjected to sulfate ingress. The objective of this paper is to present a simplified model for the verification of the durability, considering variables related with the composition, the exposure and the geometry of the structure. First, a model to simulate the chemical-physical- mechanical phenomenon is proposed and validated. Then, this model is simplified to make it easy to apply. Finally, a parametric study is performed to evaluate the influence of the shape and size of the element on the durability

1   Department of Civil and Environmental Engineering, Universitat Politècnica de Catalunya, Barcelona Tech, Jordi Girona 1-3, C1, Barcelona, Spain

2   Smart Engineering Ltd., C/Jordi Girona 1-3, Parc UPC – K2M, 08034, Barcelona, Spain

Sand mineralogy effects on external sulfates resistance of concrete cured in hot climate

A.Ben Ammar[1], A. Merbouh[2], N. Bella[3], I.A. Bella[4], B. Glaoui[5]

ABSTRACT

ACI 305 defined hot climate concreting as mixing, placing and cured concrete with any combination of the flowing conditions that trend to impair concrete: high ambient temperature, high concrete temperature, high wind velocity and solar radiation. In these cases, concrete is subjected principally to plastic shrinkage and concrete differential settlement cracks which lead the penetration of aggressive agents. External sulfate attack is one of the main chemical aggression of concrete. In this research, three different mineralogies of sands (limestone, silica-calcareous and silica) are used to prepare specimens cured in simulate hot climate, and conserved in solutions of $MgSO_4$ and Na_2SO_4 for 12 months. Concrete micro-structure was analysed by SEM and XRD analysis. Results showed that the mineralogy of sand has a significant effect on the mechanical performance and micro-structure of concrete subjected to hot weather conditions and exposed to different sulfate solutions.

1   University of Tahri Mohamed, FIMAS Laboratory, Algeria; email: babdelhafid16@yahoo.fr

2   University of Tahri Mohamed, FIMAS Laboratory, Algeria; email: mmerbm@yahoo.fr

3   University of Tahri Mohamed, FIMAS Laboratory, Algeria; email: bella5dz@yahoo.fr

4   University of Tahri Mohamed, FIMAS Laboratory, Algeria; email: ilham_aguida@yahoo.fr

5   University of Tahri Mohamed, FIMAS Laboratory, Algeria; email: glaoui_bachir@yahoo.fr

Sulfate attack on cement paste with volcanic ash: Durability analysis

M. Johnston[1], K. Kupwade-Patil[2], R. Masmoudi[3], A. Bumajdad[4], O. Buyukozturk[5]

ABSTRACT

The aim of this study is to investigate the effect of volcanic ash cements when exposed to different forms of sulfate attack, specifically to sodium and magnesium attack. This study reports the microstructural and mechanical characterization of cement pastes with volcanic ash when exposed to accelerated sulfate attack. Application of applied eletrokinetics was used to expedite the sulfate attack treatment. The test specimens were exposed to sodium and magnesium sulfate solutions for a period of 30 days. The effect of gradual decomposition of calcium-silicate-hydrate (C-S-H) gel along with phases related to magnesium-silicate hydrate (M-S-H) was examined using Raman spectroscopy, Magic Angle Nuclear Magnetic Resonance (MAS NMR) and syncrothron X-Ray Diffraction. Mechanical properties were determined using nano-identation and compression tests. A new insight towards sulfate resistance was determined by partial substitution of Portland cement with volcanic ash considering the resulting mechanical, micro and pore structure characteristics of hardened cement pastes.

1   Massachusetts Institute of Technology, USA; email: maranda@mit.edu

2   Massachusetts Institute of Technology, USA; email: kunalk@mit.edu

3   Kuwait University, email: reehab.m@live.com

4   Kuwait University. . email: bumajdad@ku.edu.kw

5   Massachusetts Institute of Technology, USA

PROCEEDINGS

TESTING AND INFLUENCE
OF MIXING PARAMETERS

Influence of recycled coarse aggregates on concrete under external sodium sulphate attack

L. Carranca[1], I. M. Martins[2], J. de Brito[3]

ABSTRACT

Concrete is the building material most widely used in the world and has been the focus of increased research efforts in what concerns the sustainable use of resources in its production, as well as on the performance and durability of concrete structures.

In this study, the above outlined areas were considered by analysing the effect of substituting natural aggregates with coarse recycled concrete aggregates, at 25%, 50% and 100%, on the durability of concrete subjected to external attack by sodium sulphate.

The degradation due to the immersion of the specimens in solutions with different concentrations of sulphates, with and without pH control, was assessed by monitoring the variations in mass and length over time and comparing them with those from a reference concrete.

Other physical characteristics of the concrete compositions, like compressive strength and tensile strength, permeability, porosity and water absorption, were also monitored to investigate relationships with sulphate attack.

KEYWORDS: Recycled aggregate / Sulphate attack / Concrete

1.   INTRODUCTION

Concrete is the second most consumed material in volume by Mankind, right after potable water. The high consumption and transformation of raw materials for concrete production have relevant impact on the depletion of material resources and damage to the environment. With the growing environmental consciousness, it is imperative to make a careful management of the exploitation of raw material in the construction sector, delaying the shortage of the deposits of natural aggregates at local and regional level and using alternative resources [1]. Within this framework, the high number of concrete structures in an increasing process of aging represents a window of opportunity for the construction sector, which should be prepared to receive and transform the used materials from the demolition of these structures into secondary raw materials. Moreover, most of the volume of concrete is made up of aggregates and their substitution by aggregates processed from construction and demolition wastes presents itself as a solution, which has been slowly applied. To promote the use of construction and demolition waste, a significant number of recommendations has been developed, including the use of recycled aggregates in concrete. Normally, these recommendations establish a maximum content of recycled coarse aggregate, obtained from crushing concrete, between 20% and 35%.

---

[1]   IST, Instituto Superior Técnico, Portugal; e-mail: luis_msc@hotmail.com

[2]   LNEC, Laboratório Nacional de Engenharia Civil, Portugal; e-mail: imartins@lnec.pt

[3]   CERIS-ICIST, Instituto Superior Técnico, Universidade de Lisboa, Portugal; e-mail: jb@civil.ist.utl.pt

In what concerns the mechanical performance, several studies indicate that the compressive strength levels achieved in concrete with recycled aggregates is similar to that of concrete with natural aggregates [2-4]. Nevertheless, durable performance of concrete with recycled aggregates is still a topic of concern due to the variability of results published and the different conclusions, particularly under severe exposure conditions [5-9].

It is known that concrete with recycled aggregates tend to be more porous than the equivalent concrete with natural aggregates, mainly due to the mortar adhered to the recycled aggregates surface [10]. This feature, influenced by the recycled aggregates' grading and replacement ratio, affects the ingress of aggressive specimens, thereby having an influence on the degradation of concrete.

Different approaches to assess the resistance of concrete to sulphate attack have been used in the European Union but consensus on a specific test has not been reached [11]. The degradation due to the interaction of cement hydrates of concrete with sulphate solutions depend on several factors, namely the diffusion coefficient of the cementitious matrix, the sulphate content, the total or partial or cyclic immersion, the cation associated to sulphate. The sulphate attack involves physical and chemical features that are difficult to separate. Nevertheless, some authors claim that for it to occur the concrete needs to be permeable and placed in contact with an environment rich in sulphates and water[12].

The present study, through the use of wetting and drying cycles followed by immersion in sodium sulphate solutions, intends to verify, in a short time, how the performance of concrete will be, with and without coarse recycled concrete aggregates, when exposed to aggressive environment of sodium sulphate. To achieve this objective, the variations in mass and length were followed over time and the mechanical behaviour was also assessed. Oxygen permeability was also monitored to investigate relationships with sulphate attack.

2. EXPERIMENTAL

The experimental program was designed to study the sulphate resistance of concrete with different percentages of coarse recycled concrete aggregates substituting natural aggregates. Concrete mixes were produced taking into account the cement content, water/cement ratio and strength classes prescribed in Specification LNEC E 464 [13] for concrete degradation by chemical attack. An accelerated test [14], comprising dry/wet cycles and immersion of concrete in a high sulphate concentration solution, and a natural test, consisting of concrete immersion in a low sulphate concentration solution that simulates the real field condition were performed.

2.1   Materials

A total of four concrete mixes were produced. The reference concrete, BR, was produced only with natural aggregates. The remaining three compositions used coarse recycled concrete aggregates prepared from crushing in laboratory a C30/37 concrete The recycled aggregates replace 25%, 50% and 100% of coarse natural aggregates in concrete B25, B50 and B100 respectively.

As recycled aggregates have higher water absorption, compared to natural aggregates, the percentage of water absorption over time was accessed. As shown in Fig. 1, the high water absorption occurs in the first 10 min.
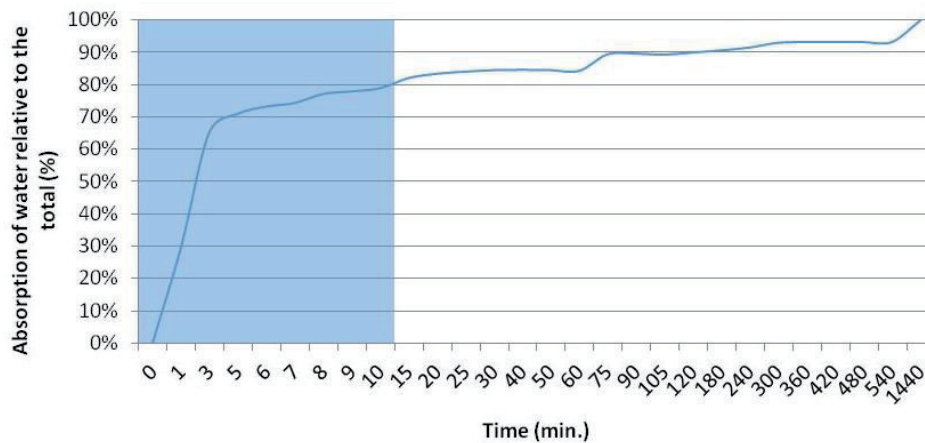
Figure 1: Water absorption of recycled aggregates

For the recycled aggregates, the water absorption at 10 min, w_{a10}, was estimated, in percentage, using Equation (1):

$$w_{a10} = \frac{(m_{10} - m_0)}{m_0} \times 100 \qquad (1)$$

where m_0 is the initial mass and m_{10} is the mass after 10 min.

Table 1 resumes the tested concrete compositions. All mixes used cement type CEM II A-L 42.5R, with a constant water-to-cement ratio (w/c) of 0.5. Due to the water absorption of recycled aggregates, the volume of water added during mixing was adjusted as indicated in the last line of the table.

Table 1: Concrete compositions

Constituents		BR	B25	B50	B100
Cement (kg/m³)		387.5	387.5	387.5	387.5
Water (kg/m³)		193	193	193	193
Natural fine aggregate (kg/m³)	0.05-0.3	114.28	114.28	114.28	114.28
	1.2-4.8	562.64	562.64	562.64	562.64
Natural coarse aggregate (kg/m³)	2-5	237.51	178.13	118.75	-
	4-16	141.65	106.24	70.83	-
	11-22	685.91	514.43	342.95	-
Recycled coarse aggregate (kg/m³)	4-22	-	237.31	474.62	949.23
Water added to the mix (kg/m³)		-	9.29	18.59	37.18

37

The cement used (CEM II A-L 42,5R), produced in Outão cement plant of SECIL, meets the requirements of NP EN 197-1 and its chemical characteristics are presented in Table 2.

Table 2: CEM II A-L 42,5R - Chemical characteristics

	Test standard	Percentage of the mass of cement
Sulphate content (SO_3)	NP EN 196-2	≤ 4.0%
Chloride content		≤ 0.10%

2.2 Testing procedures

Concrete constituents were mixed according to standard EN 206-1:2000 [12]. Cubic (150x150) mm^2 and cylindrical (ϕ100x200) mm^2 specimens were cast, and were demoulded after 24 h and moist cured, for 28 days, at a temperature of 20 ºC and 95% relative humidity, based on standard EN 12390-2:2000 [13]. Cylindrical samples, with (ϕ28x150) mm^2, were cored from each cube, to be tested for sulphate resistance and gauge studs were at both ends.

Three sulphate attack protocols were applied:

1) Natural immersion test: concrete specimens were totally immersed in a solution with a low concentration of sodium sulphate (200 mg SO_4^{2-}/l), using a ratio v_c/v_s=4, where v_c is the volume of concrete specimens and v_s is the volume of solution;

2) Accelerated test without pH control: all concrete compositions were exposed to four dry/wet cycles, i.e. dried in an oven at 50 ºC for 5 days and then immersed in a solution of 5% of sodium sulphate (34g SO_4^{2-}/l), for 2 days, after which the specimens remain completely immersed in the solution using a ratio v_c/v_s=4;

3) Accelerated test with pH control: protocol similar to 2) was applied only to reference concrete, BR, and concrete with 25% replacement of coarse concrete aggregates, B25, but with control of the solution pH, within the range 6 - 8, to simulate field conditions.

The accelerated testing protocols intend to obtain results within a reasonable testing time span in the laboratory although the used sulphate concentration is very high when compared to field exposure conditions.

After the cycles, the specimens remain in solution for 8 weeks. During that time, for each mix, specimens were removed from solution and tested after 7, 14, 28, 42 and 56 days. The specimens were subjected to the following tests:

- Visual inspection (ϕ28x150): throughout the test;

- Oxygen permeability (ϕ100x50): in the beginning of the test and after 56 days immersion, according to Specification LNEC E 392;

- Capillary water absorption (ϕ100x50): in the beginning of the test and after 56 days immersion, according to Specification LNEC E 393;

- Water absorption by immersion (ϕ100x50)): in the beginning of the test and after 56 days immersion, according to LNEC E 395;

- Resistance to compression and splitting tensile strength (ϕ28x150): after the end of the cycles, and after 28 and 56 days of immersion, following EN 12390-3 and EN 12390-6, respectively;

- Mass and length variations (ϕ28x150): after the end of each cycle, and after 7, 14, 28, 42 and 56 days of immersion, according to Specification LNEC E 398. For the mass measurements, specimens were surface dried before weighting in a balance with a precision of ±0.01 g. For the length measurements, an invar cylinder was used as reference to zero a length comparator, with sensitivity of 1 µm, before and after the measurement of concrete specimens.

3.   RESULTS AND DISCUSSION

3.1   Before exposure to sulphate environment

The compressive and splitting tensile strengths of all concrete compositions are shown in Fig. 2.
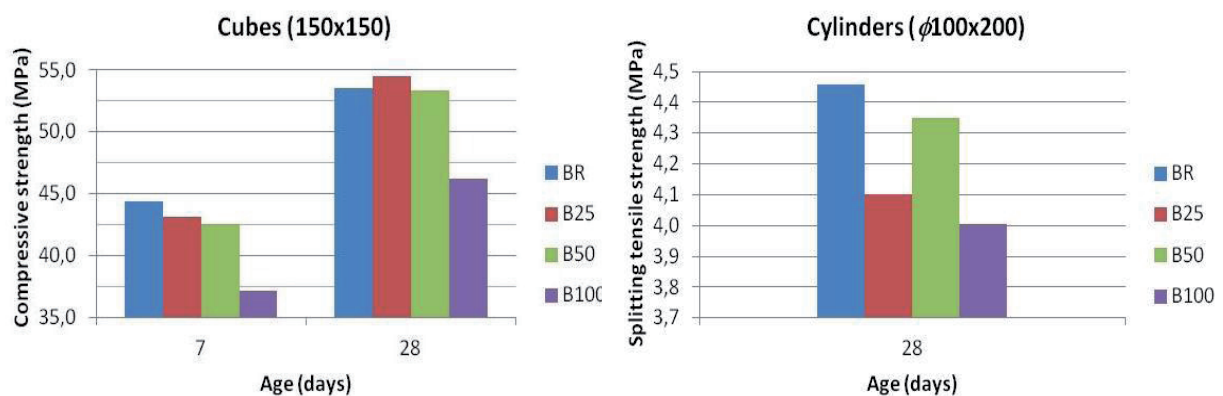
Figure 2: Compressive and splitting tensile strength, before immersion.

Usually, the compressive and splitting tensile strengths tend to increase with curing age. At 28 days, mixes BR, B25, B50 and B100 exhibited a compressive strength of 53 MPa, 54 MPa, 53 MPa and 46 MPa, respectively. These values are more than 20% of the compressive strength at age 7 days. According to Specification LNEC E 464, for a lifetime of 50 years, the minimum compressive strength required is 45 MPa for a concrete exposed to chemical attack, namely sulphate attack. All concrete compositions at 28 days satisfy this condition.

Replacing natural aggregates with recycled aggregates, in the same volume and size and at the same w/c ratio, affects the strength of concrete. This is justified by the two interfacial transitions zones, ITZ, in the concrete with recycled aggregates: the ITZ between the original aggregate and the old mortar, and the ITZ between the old mortar and the new mortar. Ryu argues that the ITZ between the original aggregate and the old mortar is almost the same as for natural aggregate [15]. But the interfacial zone between the old and the new mortar will significantly affect the mechanical performance [15].

3.2 After exposure to sulphate environment

3.2.1 Compressive and splitting tensile strength

Fig.3 shows the results of compressive and splitting tensile strength in accelerated test with and without pH control.

It is expected that the compressive and splitting tensile strength decrease with the duration of immersion in sulphate solutions. This decline is related to sulphate attack that results in the formation of ettringite and gypsum, which can cause concrete expansion due to the limited space available for mineral crystallization leading to internal stresses that cause cracking, lowering the mechanical resistance.
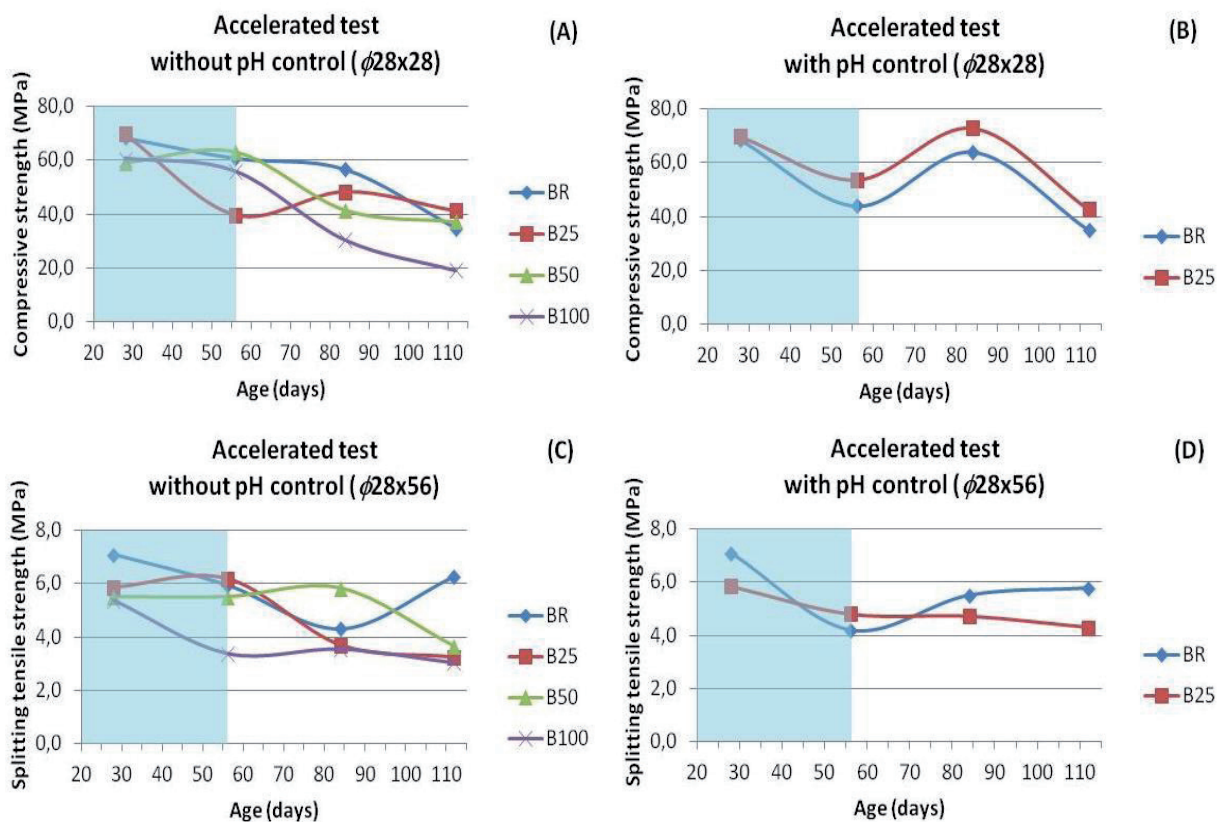
Figure 3: Compressive and splitting tensile strength for specimens, after dry/wet cycles and immersion in a solution of 5% Na_2SO_4.

During the dry/wet cycles, i.e. in the first 56 days, all mixes, in the test with and without pH control, show analogous trend, i.e. there is a decrease in compressive strength. However, after the cycles the specimens immersed in the sulphate solution with pH control almost recover the values of the strength at 28 days. After 56 days of immersion and with pH control, the values of the compressive strength converge to similar values, 40 MPa.

Comparing the final compressive strengths of the mixes exposed to sodium sulphate solutions with and without pH control, it seems that the pH has not significantly affected their mechanical performance. It should be noted that there is a marked decrease of compressive strength for concrete incorporating 100% of coarse recycled concrete aggregate, as shown in Fig. 3 (A). This reduction is in accordance with the visual degradation observed for this mix: at 98 days, Fig. 4 shows several macro cracks on these specimens surface.
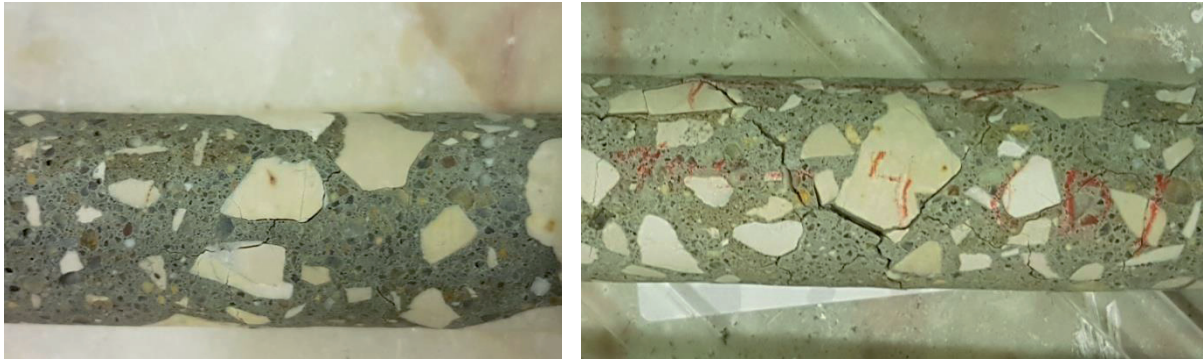
Figure 4: B100 specimen immersed in solution of 5% Na₂SO₄. On the right cracking at 98 days, and on the left cracking at 167 days.

3.2.2 Mass and length variation

For the period of the test, the specimens of all concrete compositions, immersed in different solutions of 5% Na₂SO₄ solution, showed a greater variation of the mass during dry/wet cycles (Fig. 5) when compared to the immersion after cycles. In Fig. 5, after dry/wet cycles, the mass variation was similar for all specimens, except for concrete containing 100% recycled concrete aggregates, B100, in the sulphate solution without pH control. This variation can be attributed to an increase of formation of ettringite, due to the chemical reaction between the cement hydrates and sulphate ions in the voids of concrete.
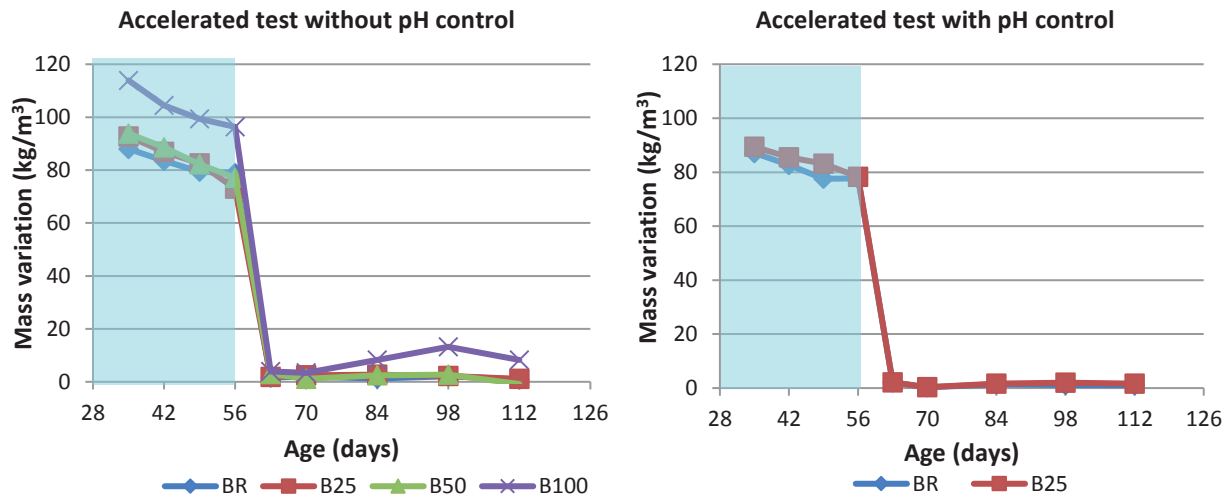
Figure 5: Mass variation during cycles and after immersion in a solution of 5% Na₂SO₄

The total mass variations in the accelerated tests were compared to those observed in specimens immersed in a solution of low sulphate concentration, 400mg/lSO_4^{2-}), is shown in Fig.6. The control of pH in the accelerated test does not seem to have a relevant effect in what concern the mass increase in concrete containing up to 25% of recycled concrete aggregates.
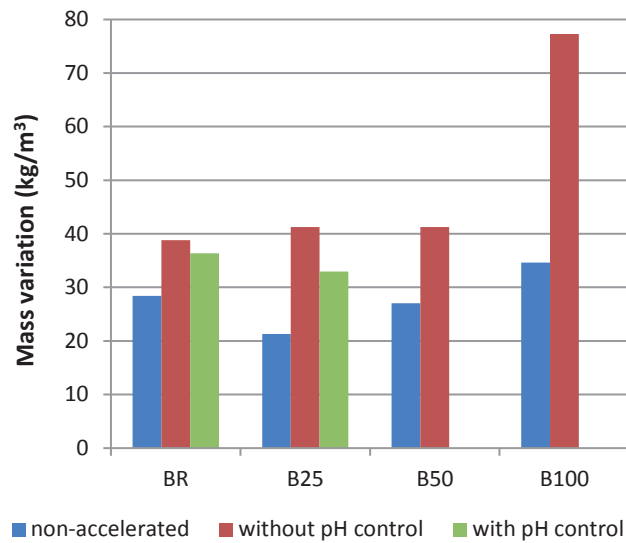
Figure 6: Total mass variation after immersion in a low concentration solution of Na$_2$SO$_4$ (400mSO_4^{2-}g/l).

Since the sulphate attack increases the internal stresses, leading to cracking, it is normal to observe considerable length variations. Fig. 7 and Fig. 8, shows the length change of the different concrete specimens in sulphate solutions without and with pH control. As it was observed for other properties, the specimens with 100% recycled concrete aggregates, B100, for the solution without pH control, stand out presenting the higher variation of length and allowing observing cracking from week 10 (Fig. 4).
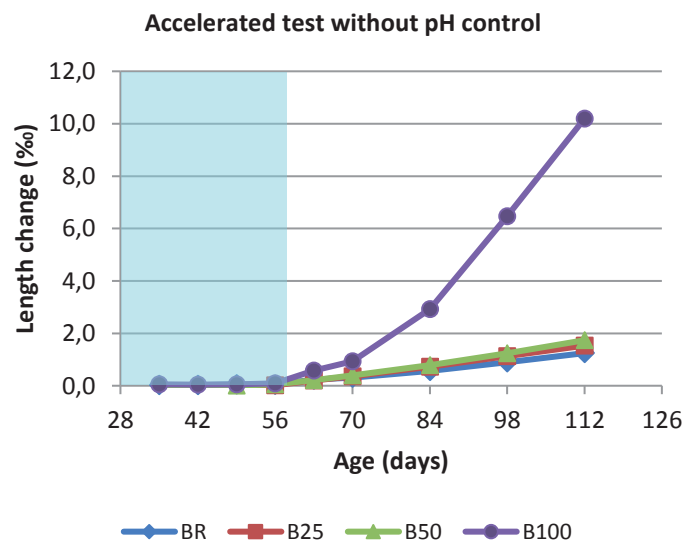
Figure 7: Length change during cycles and after immersion without pH control in solution of 5% Na$_2$SO$_4$
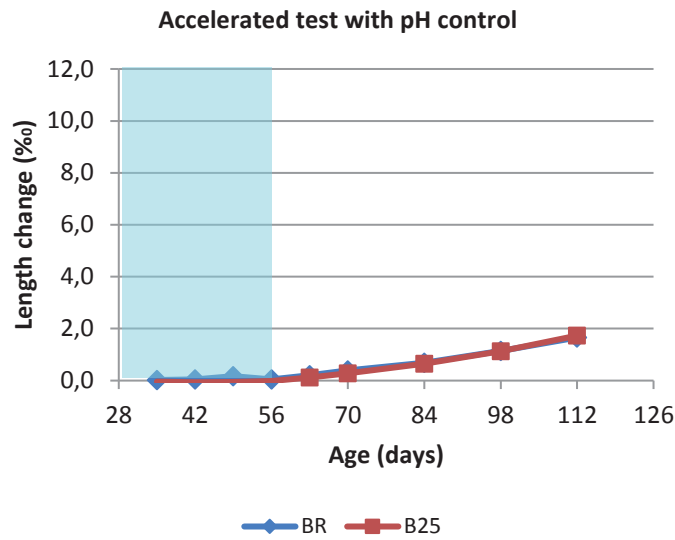
Figure 8: Length change during cycles and after immersion with pH control in solution of 5% Na_2SO_4

It is known that mixes with recycled coarse aggregates tend to produce concrete with more voids, compared to concrete with natural aggregates, which can accommodate a higher volume of ettringite. Most likely, the results of B100, in solution without pH control, could be related to this fact. As a matter of fact, the open porosity, evaluated by water absorption (Table 1) validates the increase of porosity with increasing the recycled aggregates content. Nevertheless, according to the theory of crystallization pressure the formation of ettringite from oversaturated solution must occur within small pores to cause expansion. Therefore, this suggests a finer porosity in the concrete with 100% recycled concrete aggregates.

Table 1: Open porosity of concrete specimens

Open porosity	BR	B25	B50	B100
Before immersion	13.5	14.1	15.2	17.1
After immersion (Accelerated test without pH control)	12.7	13.5	14.5	16.9
After immersion (Accelerated test with pH control)	12.5	13.5		

Comparison of length changes for specimens under sulphate attack, with low and high concentration of sulphate ions is displayed in Fig.9. Higher length change occurs for mix B100, for the accelerated test without pH control and the expansion appears to be only slightly accelerated in sulphate solution with pH control, highlighting the low influence of controlling pH.
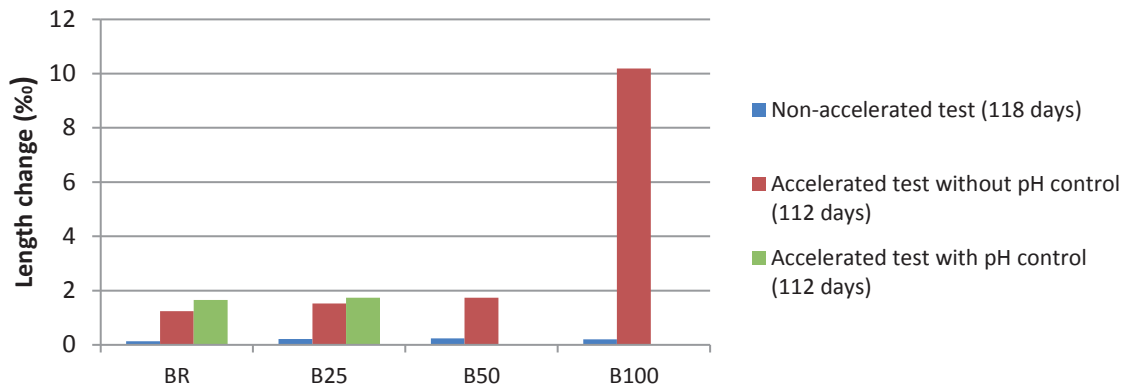
Figure 9: Length change for specimens, after immersion in the three different solutions.

3.2.3 Oxygen permeability

As a trend, the mixes with higher percentage of recycled coarse aggregates tend to have higher oxygen permeability, as seen in Fig. 10. For concretes with recycled aggregates content up to 50%, the oxygen permeability is lower or quite similar to concrete produced with natural aggregates even after sulphate attack.
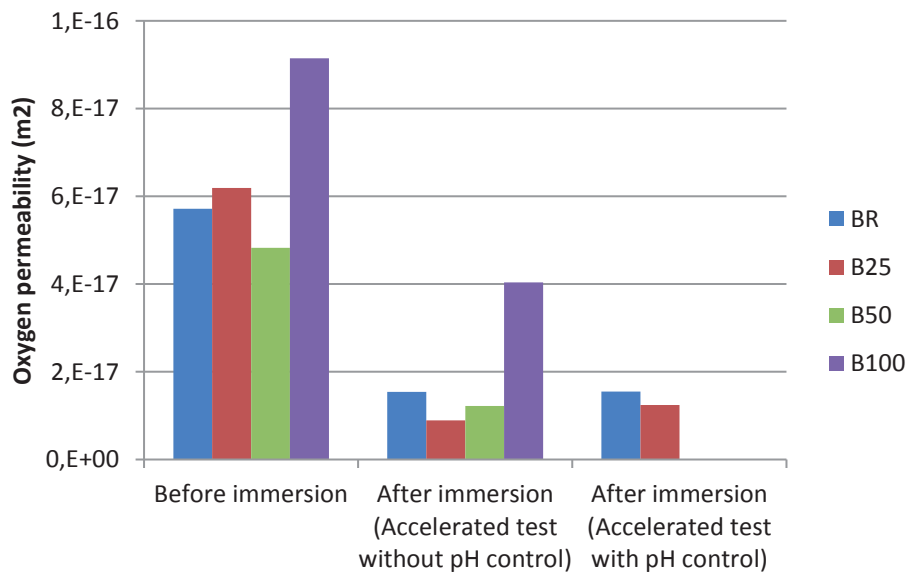
Figure 10: Oxygen permeability, of all specimens before and after immersion.

After 56 days of full immersion, the specimens were placed in an oven at 50 ºC for drying. This procedure allowed the evaporation of water inside the pores, and crystallization of sodium sulphate. This phenomenon along with the formation of ettringite during the accelerated tests decreases reduces the porosity and the oxygen permeability of concretes.

4   CONCLUSION

This work aimed to assess the resistance to sulphate attack of concrete produced with recycled concrete coarse aggregates. Within the accelerated exposure conditions the distinct behaviour of the mix with 100% coarse recycled concrete aggregates, B100, should be noted when compared to the reference concrete, BR, and to mixes with replacement of 25% and 50% of natural aggregates, B25 and B50, respectively.

For mix B100, surface cracking was detected by visual inspection in specimens with 98 days, a mass increase was found from 70 days onwards and the expansion evaluated by length change was observed after 56 days of age although a steeper change occurs after 70 days. Moreover, a sharper decrease in compressive strength was found for B100.

The results achieved until now point to the feasibility of using coarse concrete recycled aggregates, up to 50%, without impairing the resistance to sulphate ingress into concrete. These results will be supplemented with the results of external sulphate attack on concrete specimens immersed in low sulphate solutions and microstructural analysis.

REFERENCES

[1]   Khatib, J., *Sustainability of Construction Materials*: Elsevier Science. 2009. 9781845695842.

[2]   Tabsh, S.W. and A.S. Abdelfatah, *Influence of recycled concrete aggregates on strength properties of concrete.* Construction and Building Materials, **23**(2): p. 1163-1167. 2009.

[3]   Pedro, D., J. de Brito, and L. Evangelista, *Influence of the use of recycled concrete aggregates from different sources on structural concrete.* Construction and Building Materials, **71**(0): p. 141-151. 2014.

[4]   Corinaldesi, V., *Mechanical and elastic behaviour of concretes made of recycled-concrete coarse aggregates.* Construction and Building Materials, **24**(9): p. 1616-1620. 2010.

[5]   Tam, V. and C. Tam, *Assessment of durability of recycled aggregate concrete produced by two-stage mixing approach.* Journal of Materials Science, **42**(10): p. 3592-3602. 2007.

[6]   Thomas, C., et al., *Durability of recycled aggregate concrete.* Construction and Building Materials, **40**(0): p. 1054-1065. 2013.

[7]   Bravo, M., et al., *Durability performance of concrete with recycled aggregates from construction and demolition waste plants.* Construction and Building Materials, **77**(0): p. 357-369. 2015.

[8]   Kwan, W.H., et al., *Influence of the amount of recycled coarse aggregate in concrete design and durability properties.* Construction and Building Materials, **26**(1): p. 565-573. 2012.

[9]   Gonçalves, A., A. Esteves, and M. Vieira, *Influence of recycled concrete aggregates on concrete durability*, in *International RILEM Conference on The use of recycled materials in building and structures*, C.F.H.i. E. Vázquez, G.M.T. Janssen (Ed.), Editor. 2004.

[10]   Gómez, J.M., L. Agullo, and E. Vasquez, *Cualidades físicas y mecánicas de los agregados reciclados de concreto.* Construcción y Tecnología, **XIII**(157): p. 10-22. 2001.

[11]   Alexander, M., A. Bertron, and N. De Belie, *Performance of Cement-Based Materials in Aggressive Aqueous Environments: State-of-the-Art Report, RILEM TC 211 - PAE*: Springer Netherlands. 2012. 9789400754133.

[12]   Collepardi, M., *A state-of-the-art review on delayed ettringite attack on concrete.* Cement and Concrete Composites, **25**(4-5): p. 401-407. 2003.

[13]   Laboratório Nacional de Engenharia Civil, LNEC-E464 Betões. Metodologia prescritiva para uma vida útil de projecto de 50 e de 100 anos face às acções ambientais. LNEC, 2007.

[14]   SIA 262/1; SN 505262/1, Betonbau - Ergänzende Festlegungen. 2013.

[15]   Ryu, J.S., *An experimental study on the effect of recycled aggregate on concrete properties.* Magazine of Concrete Research, **54**(1): p. 7-12. 2002.

Comparative study on the sulfate milieu attacks effect on concrete based on limestone additions at curing temperature

I. A. Bella[1], N. Bella[2], A. Asroun[3]

ABSTRACT

The aggregates factory consumes a big quantity of energy; by consequence, it costs money, in the other hand it produces a lot of waste material or SCM (sustainable concrete material).

The results obtained in this study summarize up the importance of SCMs aggregates on behavior of the concrete, this different kind of SCM aggregate offered different behavior at the fresh state of the batch and by consequence its result with different mechanical behavior at the hardened state of concrete. The principal aim of adding rolled or crushed SCM is makes a concrete, which can resist to exhaustive environment (at curing temperature).

The results obtained in this study summarize up the importance of the use of waste material or sustainable concrete material to minimize the transfer mechanisms' in concrete in sulfate milieu and at curing temperature, than finally minimize down the permeability of concrete which leads to durable concrete.

1.   INTRODUCTION

Durability is defined as the ability of a material, component, or structure to remain serviceable for a desired period within its environment. Serviceability refers to the ability of a material, component, or structure to fulfil its design function, for example to retain water. A required property of concrete is long-term durability, and here aggregates and mineral admixture have a role [1].

The results of compression tests according to the temperature show clearly the increase of the compressive strength (around 20%), compared with the value obtain for specimen saturated with water. The increase on resistance of cement matrix can attribute to two phenomena: the first one is the effect of capillary suction; it causes a compression of the solid skeleton, which leads to a "pre-stress" of the material becomes more resistant. This phenomenon is also found in rocks; in this case, even without water gradient there is increases in the compressive strength. The second phenomenon is related to water gradients created in the specimen during the desiccation process: the edges of the specimen shrink in the direction of the heart of this one, causing a micro-cracking and also a confinement of the heart of the specimen [2,3].

However, the experimental results on the effect of the temperature are very variables; the initial fast rate of hydration at curing temperature causes non-uniform distribution of the

---

[1]   FIMAS, Civil engineer department, Algeria; e-mail: Ilham_aguida@yahoo.fr

[2]   FIMAS, Civil engineer department, Algeria; e-mail: bella5dz@yahoo.fr

[3]   University of Djilaly Liabess, Civil engineer department, Algeria; e-mail: a_asroun@yahoo.fr

hydration products inside the paste. In this case, the products do not have sufficient time to precipitate uniformly in interstitial space (like the case at low temperature) [4.5].

The results obtained in this study summarize up the importance of the use of waste material or sustainable concrete material to minimize the transfer mechanisms' in concrete in sulfate milieu and at curing temperature, than finally minimize down the permeability of concrete which leads to durable concrete. In addition, this study summarize up the importance of the curing temperature at 55°C during the development of the mechanical characteristics of concrete mainly compressive strength.

2. EXPERIMENTAL INVESTIGATION

2.1 Cement

Cement used in this study is CEM II/A 42.5, the mineral analyze and chemical composition are summarized in table 1 and 2.

Table 1. Mineralogical analysis of cement.

C_3S (%)	C_2S (%)	C_3A (%)	C_4AF (%)
60	14	6	10

Table 2. Chemical composition of Portland cement.

Loss on ignition (%)	Insoluble part (%)	SO_3 (%)	MgO (%)	Chloride (%)	Alkalis(%)
5.9	1.1	2.1	1.7	0.01	0.40

2.2 Admixture

The chemical admixture results from the technology of chemical products development and the new generation of superplasticizer based on acrylic copolymer (Table 3).

Table 3: Properties of Admixture.

Specific gravity	1.06 ± 0.01
pH	6 ± 1
Chloride content	$< 0.1\,\%$
Alkali content	$\leq 1\,\%$
Dry extract	$30,2 \pm 1,3\,\%$

2.3 Mineral admixture

The limestone addition or SCM limestone used is a finely divided limestone, obtained by crushing limestone from the southern region of the city of Bechar reddish. The limestone addition is a hard reddish product mainly composed of carbonate (79.43%). Tables 4 summarize the results chemical analyzes made on the limestone addition. SCM limestone used as mineral admixture with amount of 15%, 25% and 35% by substitution from cement.

Table 4: Chemical analyzes of SCM limestone.

Lime (%)	SO_3 (%)	Chloride (%)	Insoluble part (%)
79.43	Trace	0.0085	20.40

2.4 Sand and gravel

Bechar City (southwest of Algeria) benefit of a large number of building materials, the main choice is the nearly site, the used sand is the principal existing sand in this region. To attain the desired objectives we use crushed limestone sand result from crushed aggregate manufactories. Crushed sand used is characterized by its high water absorption and high percentage of fine element (size < 80µm) for this reason the sand used in the concrete composition is composed by 30% of dune sand and 70% of crushed sand (table 5 and figure 1).

Table 5: Physical Characteristics.

	Bulk density	Specific gravity	Fineness modulus	property	MBt***	Origin
Sand	2.66	1.5	2.8	60.81*	0.95	Limestone
Gravel	2.85	1.32	-	1.62**	0.4	Limestone
* Sand equivalent test; ** property test; ***the methylene bleu test.						
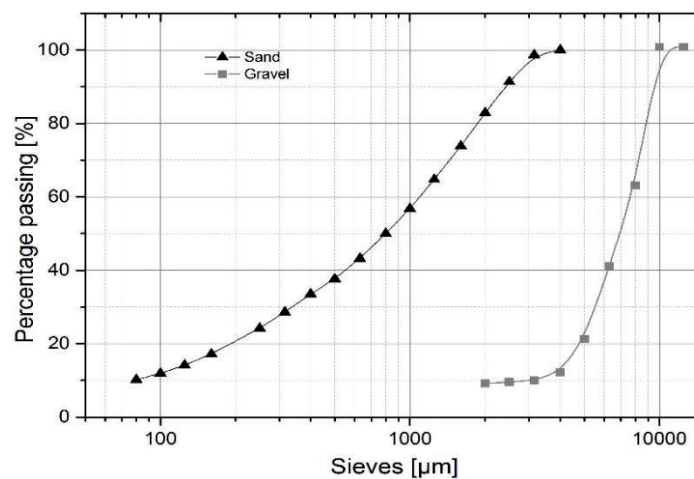
Figure 1: The cumulative sieving curve.

2.5   Mixture

In this study, for environmental and economics' consideration we suggest the use of fine limestone by substitution form cement, the different mixes used are by substitution of fine limestone by cement with the amount of 15%, 25% and 35% percentage of substitution. The aims desired is studying the influence of this kind mineral admixture on the behavior of concrete in exhaustive environment (at normal temperature in sulfate attacks for 7 days and curing temperature around 55°C for 1 day). We notice, one cycle of conservation mains conservation 7days in sulphate milieu then one day in curing temperature at 55°C.

Table 5: Mixture composition.

Sand (Kg/ m³)	Gravel (Kg/ m³)	Cement (Kg/ m³)	Water (Kg/ m³)	Superplasticizer (%)
952	784	350	185	2,5*

2.6   Curing method

In order to better studies the effect of sulphate attacks and curing temperature on the concrete. We chose two cases of curing method; the first one is conservation in saturated sulphate milieu at 25°C for 7 days and the second one is conservation in dry milieu at curing temperature at 55°C (figure 2), after 6 cycle of maturation in exhausted milieu the specimens will be tested for physical and mechanical characterization. It is noticed the choosing of this different case of conservation is based on the aim to studies the effect of the environment on the mechanical behavior of concrete.
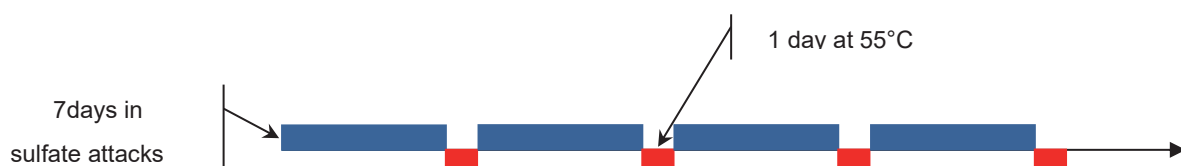
Figure 2: Mode of specimens' conservation at curing temperature (55°C).

The main purpose of choosing this mode of conservation is to studying the durability of concrete by the influence of physical characteristic related to the receptivity of concrete, by physical parameter with cycle of shrinkage and swelling. In this case the shrinkage is obtain by conservation at curing temperature, swelling and chemical attack is promoted in saturated sulphate milieu , where several research use this kind of conservation to expect the concrete behavior in short period of time.

3. RESULTS AND DISCUSSIONS

3.1   The effect of the conservation milieu on the mechanical resistance

In this study, after 6 cycle of conservation in saturated milieu for 7 days and in sealed milieu at curing temperature around 55°C for total 42 days, the specimens are tested on the compressive and traction strength (EN 196-1 test method of cement: determination of compressive strength test).
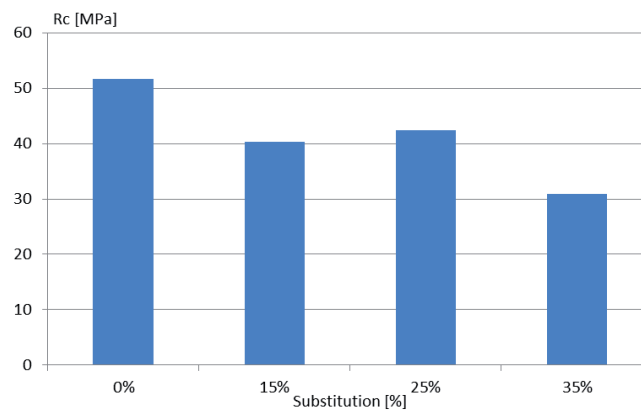
Figure 3: the variation of compressive strength as function of percentage of substitution.

 The use of mineral admixture especially fine limestone is based on the valorization of local material and environmental consideration. The main purpose of using this kind of menial admixture is to increase the compactness of the concrete even if this kind of admixture is characterized by its high water demand. In our case of study and like it is show in Figure 3, it is very clear that the limestone substitution do not have effect on compressive resistance until we attain 35% of substitution [4, 6].
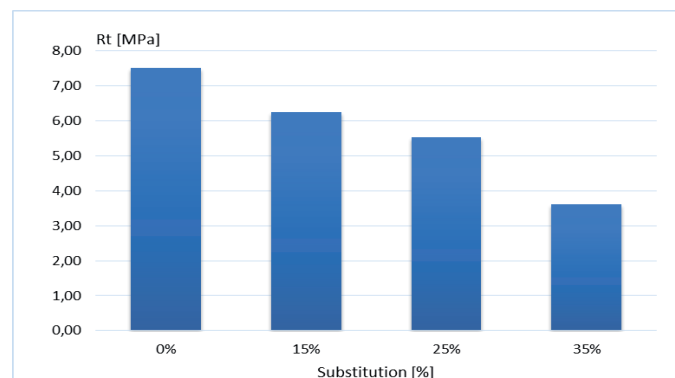
Figure 4: the variation of traction strength as function of percentage of substitution.

After 6 cycle of conservation, we simply remark that the tensile strength decrease by the augmentation of the percentage of substitution, even if the decreasing is not significant until 35% of substitution is attain (figure 4). Notice the addition of fine limestone is based on the substitution by cement for sustainable consideration.

3.2   The effect of the conservation milieu on the weight variation

In this part, we describe the variation of the weight of concrete after very cycle of conservation in sulphate milieu. we notice the cycle of conservation mains 7 days of conservation in sulphate saturated milieu and then 1 day at temperature about 55°C.
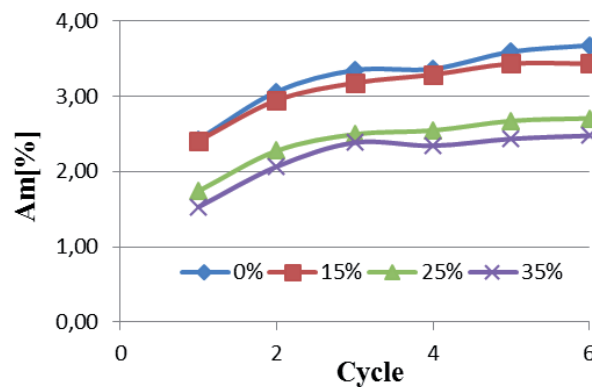
Figure 5: weight variation as function of cycle of conservation.

After six cycle of conservation, we notice that the weight of concrete increase each cycle of conservation in sulphate milieu, where the weight gain of concrete based on 35% of substitution is less than the concrete with 0% substitution, which leads the addition of fine limestone minimise the augmentation of weight gain in sulphate milieu (figure 5). Might explain by the changing in chemical hydration processes by the sulphate attacks.

3.3   The effect of the conservation milieu on the depth deteriorate

The depth deterioration is based on colorimetric method used in this research to determinate the depth by spraying phenolphthalein indicator on the concrete surface, which detects the changing in the PH-values in the concrete surface after 6 cycle of conservation in sulphate milieu (figure 6).
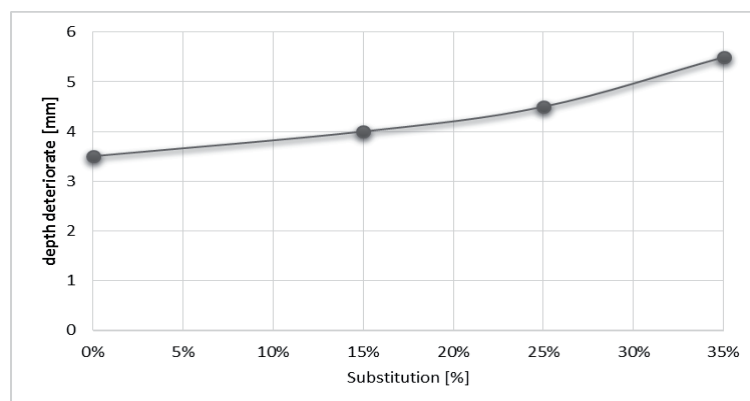
Figure 6: Depth deteriorate as function of percentage of substitution.

As the below represent, we can easily remark that the depth deterioration is stable between 0% and 25% of substitution which change from 3.5 to 4.5 mm.

3.3   The effect of the conservation milieu on diffusion coefficient

The transports mechanisms presented that are normally associated with the ingress of deleterious material into concrete. The transport mechanisms also serve as the theoretical models to evaluate the transport characteristics of concrete in different test methods one of this test is the diffusion coefficient in non-steady state (figure7) [8].

Figure 7: Penetration profounder of chloride ions; left) 25% substitution ; right) 0% substitution.

The use of fine limestone permit it is possible to eliminate an important percentage of vacuums, which can create a significant capillarity forces might explain the decreasing of the penetration profounder of chloride ions.
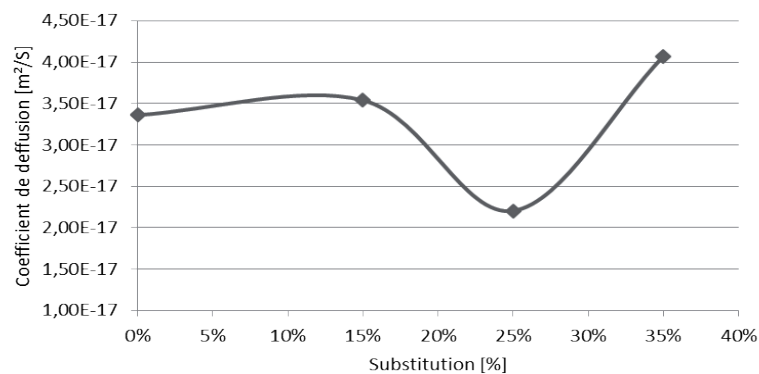
Figure 8: coefficient diffusion as function of percentage of substitution.

By definition, the diffusion coefficient is an indicator of the concrete permeability and it's very clear in Figure 8, 25% of substitution seems to be an optimum of compactness or vacuums filling. The mineral admixture based on limestone by its size, it make possible to subdivide the pores structure between sand and cement, by consequence it's rise up the compactness of concrete and finally decrease the coefficient of diffusion and the concrete want be more durable.

3.   CONCLUSION

A variety of different physical and/or chemical mechanisms may govern the transport of the media into the concrete, depending on the environmental conditions, the pore structure of concrete, the pore radius, the degree of saturation of the pore system and the temperature. Considering the wide range of pore sizes and a varying moisture concentration in the concrete as a function of the climatic exposure conditions, the transport of media into concrete in most cases is not due to one single mechanism. However, several mechanisms may act simultaneously.

Concrete durability means the summation of the effect of physical (shrinkage and swelling), chemical (sulphate of acid attack) and mechanical parameter influence on the concrete behavior during life cycle of concrete (more than 1 year). Actually, it can be possible to expect the durability of concrete if the concrete is subject under the effect of combined milieu of conservation between saturated and sealed milieu. In our case of research we those to study the combination between curing temperature around 55°C and saturated sulphate milieu, this kind of conservation can make possible to stimulate the durability of concrete in a short period of time base on the use of sustainable concrete material.

The main purpose of using of limestone is the amelioration of concrete durability or the cycle life of concrete in exhausted milieu. The addition of limestone by substitution of cement can increase the compactness on cement matrix and minimize the percentage of vacuums' or subdividing the size of the pores structure between cement and sand. In addition, according to other research it might change the hydration process.

Moreover, the main aim of this research is the use of SCM by substitution to rise up the density of concrete composition therefore resulting the rising up of the compactness and without a significant decreasing of the compressive strength, even if sealed in exhaustive environment at curing temperature about 55°C. This fact cannot be possible without the use of SCM characterized by their good aggregate/matrix cement adherence.

Furthermore, the use of SCM rise up a parameter related directly with the durability, which is the diffusion coefficient. Maybe explain by the summation of capillarity forces obstruct the transport mechanism by the decreasing of the size of the pores structure (decreasing of open porosity).

REFERENCES

 [1]   Mark Alexander & Sidney Mindess, Aggregates in Concrete, Modern concrete technology 13, Taylor & Francis, Simultaneously published in the USA and Canada, 2005.

[2]   I. A. Bella, A. Asroun & N. Bella, Effect of Curing Temperature on Mortar Based on Sustainable Concrete Material's and Poly-Carboxylate Superplasticizer. Journal of Civil Engineering and Architecture, 8(1), pp. 66-72, (2014).

[3]   Ismail Yurtdas, Nicolas Burlion, Frederic Skoczylas, Hydrous damage of cementious materials, in: 16th Mechanics French Congress, Nice, France, 2003.

[4]   Jaques Baron and Raymond Sauterey, Hydraulic concrete practice and knowledge, the National school of bridges and roads Press, Paris, France, 1982.

[5]   Adam M. Neville, Concrete Property, Eyrolles edition, Paris, France, 2000.

[6]   G. Dreux, New guide of concrete, Eyrolles 8th edition, Paris, France, 1999.

[7]   J. Plank, C. Schroefl, M. Gruber, M. Lesti, R. Sieber, Effecteness of poly-carboxylate superplasticizers in ultra-high strength conrete: The importance of PCE compatibility with silica fume, Journal of Concrete and Advanced Technology 7 (1) (2009) 5-12.

[8]   H. Hilsdorf, J. Kropp, Performance Criteria for Concrete Durability, Taylor & Francis, London, 2005.

External sulfate attack – Influence of an early age exposure, coupling with the cement composition

R. Ragoug[1,2], O. Omikrine-Metalssi[1], J-M. Torrenti[1], F. Barberon[2], L. Divet[1], N. Roussel[3]

ABSTRACT

External sulfate attack (ESA) is one of the main causes of deterioration for concrete structures. It is currently studied on saturated samples. However, in pratice, concrete structures are exposed as soon as the formworks are removed. The aim of this study is to highlight the effect of an early age exposure on the degradation mechanisms of the ESA. For this study, two cements were used (CEM I and CEM III). The microstructure changes are monitored by using several experimental techniques such as NMR (^{27} Al), ICP, XRD and SEM. These analyses showed a neutral effect of an early age exposure on the sulfate ingress in both cement types. A negative effect of slag cement is observed after only 3 months of exposure at early age and a positive one for the mature pastes. Conversely, Portland cement paste resist very well and long to ASE, for an early age exposure and fail for the cured specimens.

1.   INTRODUCTION

Long-term behaviour of concrete structures is still a major challenge for civil engineers. Usually, concrete structures are exposed to various physical and chemical aggressions as soon as their formwork is removed. This early age exposure has an obvious influence on the structural element future transport properties, which are first order parameters affecting the durability of the material. More specifically, transport properties influence the ability of the material to sustain deterioration mechanisms due to the penetration of deleterious ions and aggressive elements from external environment into the inner porous microstructure of the cementitious matrix. However, most standards and laboratory investigations are based on mortar or concrete samples studied after 28 days or 91 days curing.

One of the more hazardous phenomena leading to the degradation of concrete structures is External Sulfate Attack (ESA) which is considered as the second cause of deterioration and the most frequently cited causes of service life reduction of concrete structures after corrosion [1-7]. It is generally attributed to the formation of secondary ettringite and/or gypsum from the interaction between sulfate and alumina-bearing phases in the cement [8-10]. The formation of these new elements in the cement matrix is usually thought to be responsible for significant expansion and cracking in the concrete structures leading to the stiffness, strength decrease, surface spalling and finally the general structural damage during sulfate attack [4, 11, 12].

Furthermore, ESA is considered as a complex phenomenon involving physical, chemical and mechanical processes [4, 10, 13-15]. Indeed, various investigations have consistently indicated that ESA is a complicated, multiscale and multiphysics process involving the

---

1   Université Paris Est, IFSTTAR, MAST, FRANCE

2   Bouygues Travaux Publics, Pôle Ingénierie Matériaux, FRANCE

3   Université Paris Est, IFSTTAR, Laboratoire Navier, FRANCE

coupling of chemical, physical and mechanical interactions [4, 10]. These coupling phenomena remain unclear and highly controversial even for the CEM I where the results are at least provided. Moreover, the use of supplementary cementitious materials (SCMs) like slag and fly ash changes necessarily the chemical and physical properties of cement matrix in contact with sulfate solution [16]. In brief, despite some publications and research about the ESA process, there still exist some open questions especially on the use of SCMs and the early age conditions of structure exposure to ESA which are far to be understood and require some extensive research.

This work aims to investigate the kinetics of sulfate ingress and its consequences on microstructure of ordinary cement paste (OCP) and to compare its behaviour with that of cement paste with slag (SCP). Sulfate concentration profiles are measured both at early ages and for matured cement paste (after 1 year of curing in water). These measurements are combined with some investigations of the microstructural changes using the SEM analysis. Moreover, other investigations using NMR (^{27}Al) and XRD are used to highlight the chemical nature of the elements formed during the ESA. Finally, a visual comparison of samples degradation between the two kinds of cements and for different curing conditions was analysed and discussed.

2. EXPERIMENTAL STUDY

2.1 Material and exposure conditions

Two cements with the same clinker were used for this study (CEM I and CEM III with 62% of slag). The composition of the clinker is given in table 1.The clinker phase contents are calculated according to Bogue's approach and shown in Table 2. This calculation highlights the high quantity of aluminate in C_3A and C_4AF favoring the formation of secondary ettringite after reaction with a high quantity of sulfate ions.

For the laboratory specimens manufacturing, cylindrical samples of 10 cm diameter were cast with cement pastes (OCP for CEM I) and (SCP for CEM III) prepared with a water-to-cement mass ratio W/C equal to 0.6. This high W/C ratio was chosen in order to enhance sulfate diffusion inside the porous media of the material. A sample slow rotation device was used during setting to prevent bleeding of cement paste and to produce homogenous samples (Fig 1-a). After 24 hours, all specimens were removed from their molds and were cut into 5 cm thick cylinders. Then, a third of samples were kept directly in sulfate solution (early age case), and the second third of samples were cured in non-renewed water for one year (matured case). After this long curing period of one year, this second third of samples were kept in the sulfate solution tanks in the same conditions of the early age case. An epoxy resin was applied on the peripheral surface of all the samples in order to insure unidirectional diffusion of sulfate ions (Fig 1-b). Only one side of the specimens was in contact with the test solution (semi-immersion) (Fig 2), which was prepared with 15 g/L of sodium sulfate in deionized water (10 g/L of sulfate). The surface area of samples to the solution volume ratio was 25. The pH of the sulfate solution was adjusted to (8 ±0,1), as explained later by the pH regulator. Finally, the last third of samples were kept in water as reference cases.

Table 1: Chemical composition of CEM I cement by using ICP-AES and TGA

Chemical composition (%)		
CaO	62,81	49.46
SiO_2	20,22	29.58
Al_2O_3	4,85	8.93
Fe_2O_3	2,92	1.51
CaO (free)	1,58	-
MgO	0,84	4.57
SO_3	2,88	1.46
S	0	0.58
K_2O	0,77	0.62
Na_2O	0,34	0.48
Ignition Loss	2,59	1.12

Table 2: The main cement clinker phases according to Bogue's analysis

Cement	C_3S	C_2S	C_3A	C_4AF
CEM I	65.2	8.8	7.9	8.9

Figure 1: Specimens used for the study (a) and a slow rotation device used during the setting (b)

2.2   Accelerated test for ESA

As described above, the constant value of the pH=8 ±0,1 (pH lower than the one of the pore solution) in the study of ESA resistance of the cementitious materials appears to be a desirable feature of testing, since it permits simulation of field exposure conditions (e.g. seawater) and it allows accelerating the sulfate degradation process [17]. Thus, experimental conditions provided in our proposed accelerated test method are more representative of field conditions because the sulfate concentration and the pH of the solution remain constant and similar to field conditions. Thereby, a schematic of the test apparatus is given in Fig 2.
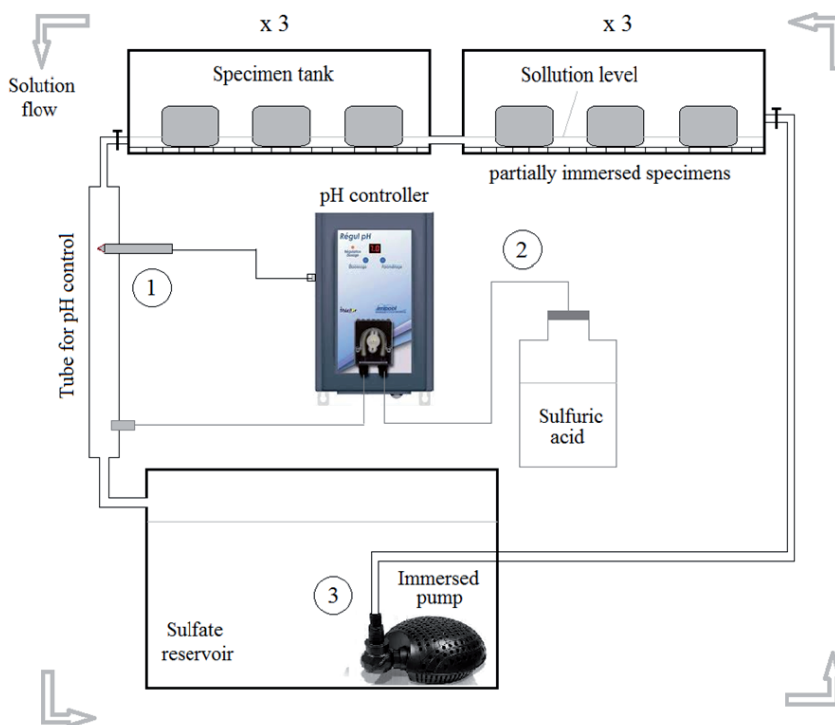
Figure 2: Schematic of pH-control for ESA accelerated test

The simplified device consists of one big tank containing approximately 60L of sulfate solution with a concentration of 15g/L which acts as a reservoir. A pump with a maximum flow rate of 750 L/h was immersed in this big tank in order to move the sulfate solution to others six specimens' tanks containing 10 L each (Figs 2). At the output of these tanks, the pH of the solution is checked into a cylindrical tube using a solution treatment controller that constantly monitors the pH of the solution before it flows into the tanks containing the specimens. The test applies a titration system to maintain the pH of the sodium sulfate at 8 ± 0.1 by means of a continuous titration with sulfuric acid H_2SO_4 (0,05%). It consists of a pH controller that measures the pH of the sulfate solution in a cylindrical tube thanks to an electrode (process 1 in Fig 2), and when the value of pH increases due to the leaching process, the valve of the pH controller apparatus opens to allow a dilute solution to sulfuric acid to flow until a selected pH (value of 8 in this study representing the pH value of the seawater) is reached (process 2). This added sulfuric acid is well mixed in the sulfate solution as this one is continuously moving between the sulfate reservoir and the specimens tanks (process 3).

In the six tanks, semi-immersed samples of similar chemistry are arranged on mesh allowing the exposure of maximum of surfaces to the ESA which increases potential for reaction between the cement paste and the sulfate ions. The volume ratio of the specimens and the sulfate solution in each tank is adjusted to disturb as little as possible the variation of the sulfate concentration. This parameter remains approximately constant because of the weekly renewing of the solution. Moreover, the use of sulfuric acid instead of another acid in the titration ensures that the sulfate ion concentration of the solution remains almost constant over time.

2.3   Experimental techniques for investigation

Several test methods were used in this study to investigate the kinetics of sulfate ingress in the porous media of the two cement pastes (OCP and SCP) and its consequences on their microstructures. Indeed, Inductively Coupled Plasma, ICP-AES was used to quantify sulfate content and/or sulfate ingress into the samples. The output from this experimental method is the total sulfur concentration, from which sulfate concentration is computed. In this study, specimens were grinded starting from the exposed surface. The obtained amount of powder corresponding to a 1 mm thick sample displayed an average particle size of 315 µm. All sulfates present in this powder were ionized by an acid attack. The resulting solution was then tested using ICP-AES.

Otherwise, Scanning electron microscopy (SEM) was also used as a technique for qualitative characterization of cement pastes to obtain information on the spatial distribution of different cement paste phases. In this study, even if this technique is qualitative. However, the SEM image can give us the ability to separate the phases crystallizing in confined pores as compressed ettringite, to those well-crystallized, causing no damage at the microstructure scale.

Furthermore, the X-ray diffraction (XRD) was used in this experimental study. This technique is a reliable method for the identification of cement paste hydrates and especially crystallographic phases as portlandite, ettringite, or Friedel salt. At each measurement time, powders, previously drawn from exposed samples, are manually ground and sieved to obtain a uniform particle size less than 80 µm. These powders are then analyzed to draw the mineralogical profile evolution and to identify the evolution of different mineralogical phases depending on the type of exposure. Another method, also added in this investigation to confirm the results given by XRD is Nuclear Magnetic Resonance (NMR (^{27} Al)). This technique leads to determine the quantity of aluminate in the cementitious materials and then, to deduce the quantity of different phases (AFm and Aft) in the cement after the spectra decomposition.

Finally, some observations of swelling, cracks or material loss were performed on samples after different exposure durations to the sulfate solution for the two studied cements.

3.   RESULTS AND DISCUSSION

Figure 3 shows the evolution of the sulfate content in OCP material, in g/g of the cement paste, as a function of depth for the early age exposure sample. All the curves can be divided into two parts: the first one which presents the sulfate diffusion part and the second one where the sulfate concentrations are stabilized at the average value of the reference cement without any exposure to the sulfate solution (of order 2 % g/g of cement).

In the first part, the sulfate content increases with the time exposure duration until stabilization at a maximum value of about 13 % g/g of cement. This value stays far above what could be expected from a simple equilibrium between the internal pore solution and the external sulfate solution (of order 0.2 % g/g of cement). This suggests that physically or chemically bound sulfates fully dominate any free sulfates in solution that explains the decrease of the sulfate content with the depth. In addition, the extremely high ratio (of order 60) between sulfates content and free sulfates in solution (considering that free sulfates in solution shall be at most of the order of the external solution sulfates concentration) suggest that the energy involved in the fixation process is extremely high. The binding shall therefore be mostly chemical as this ratio is too high for a simple and reversible sulfate physical adsorption alone. This is in agreement with the amount of sulfate adsorbed on C-S-H

considered as being of the order of 1% g/g in [18] far lower than the average 13 % g/g of sulfate content measured here. Another important point to note here is that the penetration depth increases slightly with the exposure time. It is about 4.5 mm after two weeks of exposure to the sulfate solution, and it becomes about 7.5 mm after about 6 months of exposure.
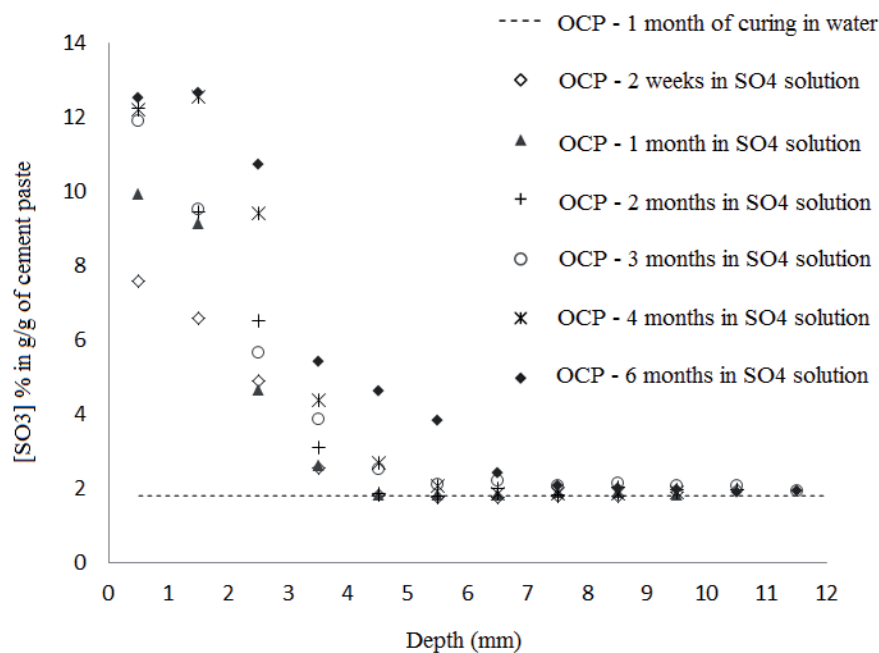

Figure 3: Sulfate profiles for CEM I (OCP) at early age, measured using ICP-AES, for different exposure duration to the sulfate solution.

Furthermore, Figure 4 shows the evolution of the sulfate content in OCP material, in g/g of the cement paste, as a function of depth for the two cases of exposure to the sulfate solution (early age and matured cases). The sulfate profiles are similar in the two cases, after two months of sulfate exposure, with a difference in the maximum value of sulfate content reached at this duration. It is more important in the case of the early age exposure at the first three millimeters because of the high porosity and permeability of the material at this early age. Beyond this depth (in area near the propagation front) this difference is negligible. Therefore, those observations suggest that although a diffusion process due to concentration gradient is initially at the origin of sulfate ingress in the porous medium, sulfate ions get physically and chemically trapped in the paste microstructure with a higher kinetic. Another factor that can initiate the sulfate ingress is the capillary adsorption, especially for an exposure of samples at early age.

It is also noted a small increase in the penetration depth of the sulfate in the case of the matured samples. This can be due to the appearance of some cracks at the exposed surface of the samples after two months of exposure. These cracks could facilitate the penetration of the sulfate ions and other deleterious ions.

On the other hand, Figure 5-a shows the comparison of the sulfate profiles between the two cement pastes used in this study (OCP and SCP) for the matured case. As is clearly shown, these sulfate profile are reduced in the case of SCP cement paste especially at the first millimeters. This can be explained by the finer pore distribution and the low connectivity of the capillary porosity in the case of cement pastes with slag with a higher tortuosity (Fig 5-b).

It can be due also to the low amount of Portlandite and to the availability of aluminium in the case of SCP cement paste.
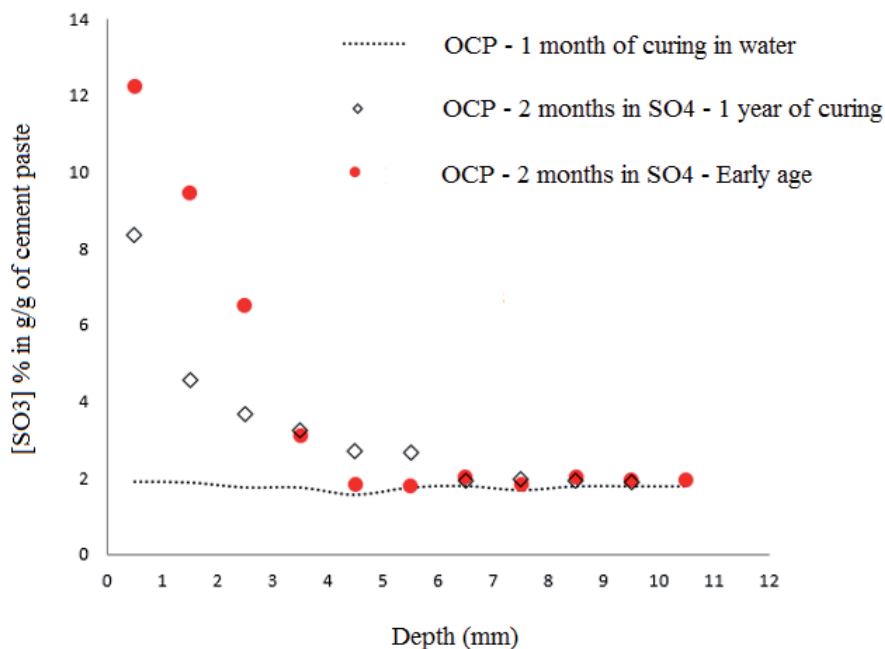

Figure 4: Comparison of the sulfate profiles for CEM I (OCP) between the two exposure conditions: early age and matured cases

(a)

(b)
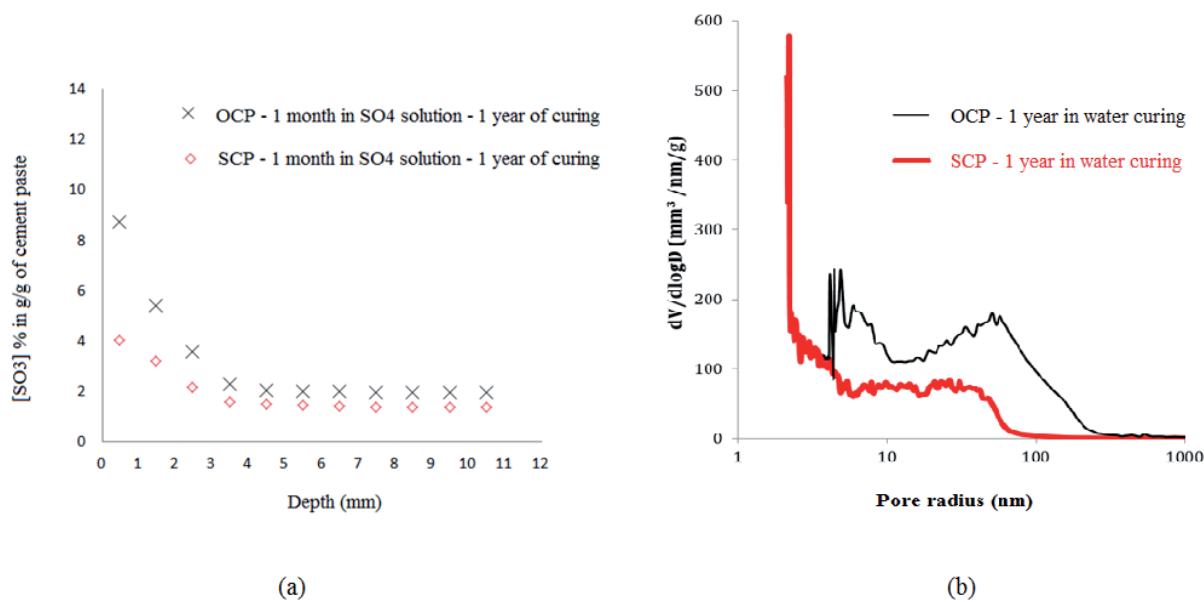
Figure 5: Comparison of the sulfate profiles for the two cements CEM I (OCP) and CEM III (SCP) (a), Pore size distribution for the two cements after 1 year in water curing

The ingress of the sulfate ions inside the cement paste will surely affects the chemical equilibrium of the matrix. Normally, the high quantity of sulfate ions reacts with the other elements of cements to form secondary ettringite and gypsum. The formation of Aft is accelerated by the leaching phenomenon. Indeed, the calcium content increases in the porous solution due to the difference of the pH value between the samples and the sulfate solution. This finding shows the strong coupling and competition between ESA and leaching phenomenon. Figure 6 shows the chemical change in the cement paste after the exposure in the sulfate solution. Both XRD and NMR (^{27} Al) investigations highlight the formation of secondary ettringite from the reactions between portlandite and sulfate ions on the one hand, and the transformation of the AFm to Aft on the other side. However, the investigation using XRD note also the appearance of a quantity of gypsum especially near the exposed surface as this part of samples is almost in equilibrium with the sulfate solution pH (pH=8). At this value of pH, the ettringite remains instable and the gypsum can precipitate in this condition.

The same findings can be shown for the case of SCP samples (Fig 7). The only difference is that we detected by XRD also some quantity of Friedel's salt in this type of cement paste with slag. Also, the aluminate leading to the formation of secondary ettringite can have other sources as the Afm (TAH and CASH).

Figure 6: Determination of elements newly formed by NMR (a) and XRD (b) after exposure of OCP samples to the sulfate solution

Figure 7: Determination of elements newly formed by NMR (a) and XRD (b) after three months of exposure of SCP samples to the sulfate solution

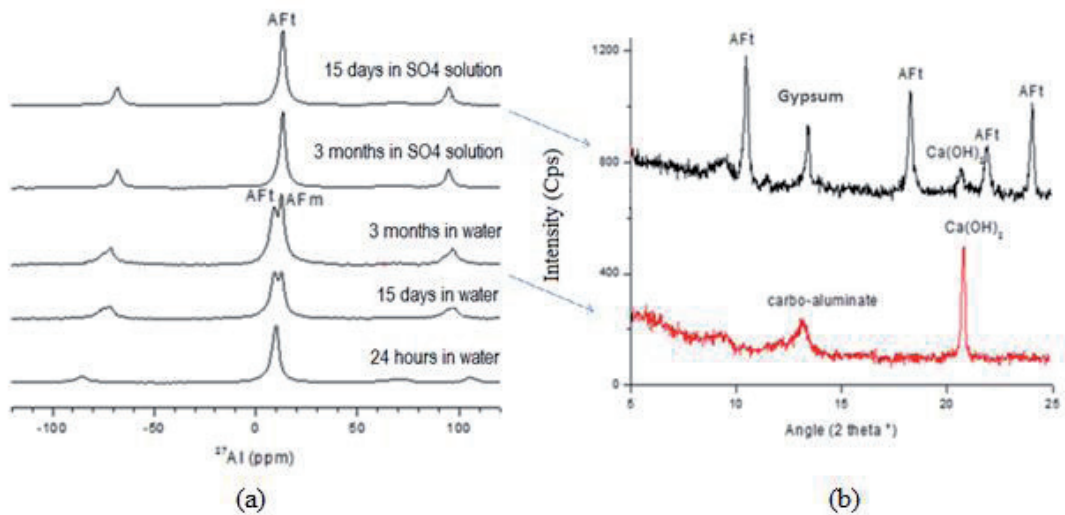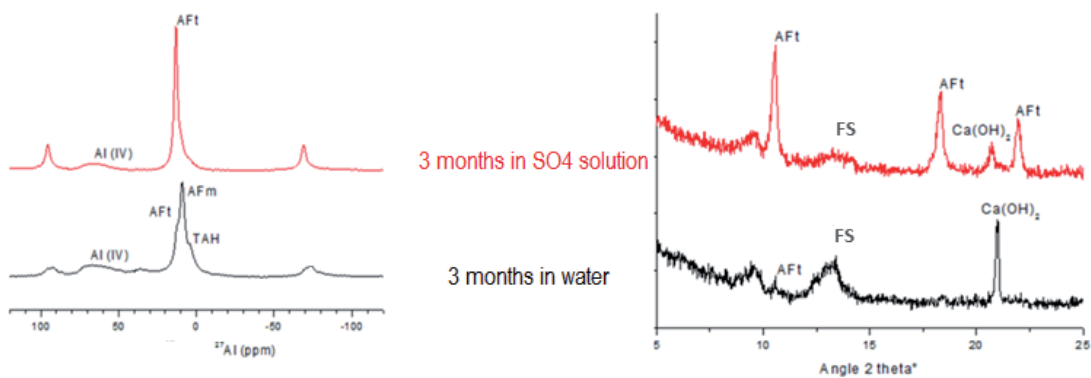As described above, the formation of secondary ettringite and gypsum from the reaction between sulfate, portlandite and alumina phases in the cement matrix is usually thought to be responsible for significant expansion and cracking in the concrete structures leading to the general structural damage during sulfate attack. In this context, some visual investigations on samples after different exposure duration to sulfate solution were carried out to confirm the responsibility of sulfates in damage of cementitious materials. Indeed, Figure 8 shows a comparison between the states of samples at early age (Fig 8-a) and at matured case (Fig 8-b) after two months of exposure to sulfate solution. No apparent degradation and no cracking were observed in the case of exposure at early age. These observations are valid even after 1 year of contact with the sodium sulfate solution. However, there are some cracks after just two month of sulfate exposure for matured samples.

Figure 8: Comparison of observed damage of OCP samples after two months of sulfate exposure: (a) early age, (b) matured sample

These observations suggest that crystallization of AFt phases in the smaller pores and after an advanced hydration reaction (saturated pore in matured samples) is more harmful to the cement paste (the volume of one mole of ettringite is 2.28 greater that AFt phases; 707 cm^3 compared with 309 cm^3). In addition, in the case of matured samples, there is sufficient available portlandite to precipitate gypsum after its dissolution. This is not the case at an early age. Furthermore, the molar volume of gypsum is 2.25 times greater than the molar volume of portlandite (74 cm^3 against 33 cm^3 per 1 mole). Consequently, the elements newly formed after an ESA (AFt and gypsum) can cause the expansion of the cement paste samples when they are confined in porosity in order to exert an internal pressure. This result is confirmed by some SEM tests performed on samples for those two sulfate exposure conditions (early age and matured cases). Those results are given in Figure 9 where the ettringite precipitate in confined spaces in the case of matured samples (Fig 9-a) confirming the expansion and the cracks appearing in the samples, while this ettringite has more spaces in the samples at early age (Fig 9-b).
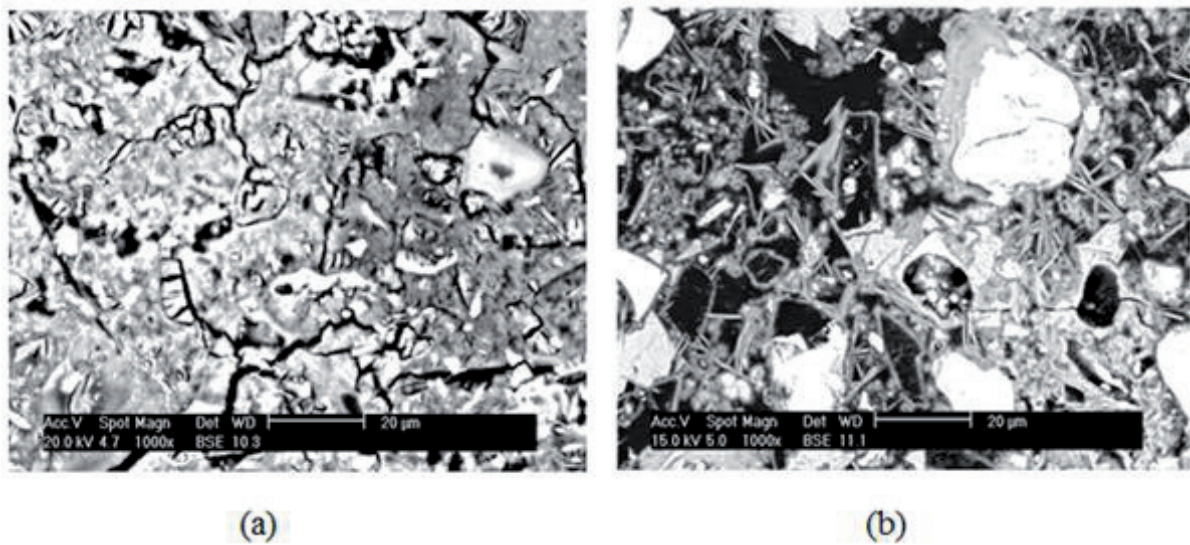
Figure 9: SEM images on OCP samples after two months of sulfate exposure: (a) Compressed ettringite in matured samples, (b) Ettringite in samples at early age

Finally, the behavior of cementitious materials with slag (SCP) seems a little different to the ordinary cement paste (OCP). Indeed, as illustrated in Figure 10 and as already observed in a recent study [10], the degradation due to the ESA in the case of slag binders (SCP) is produced by a material loss at the surface with a slight expansion (Fig 10-a). However, in the case of OPC, this degradation is caused only by macroscopic expansion (Fig 10-b).
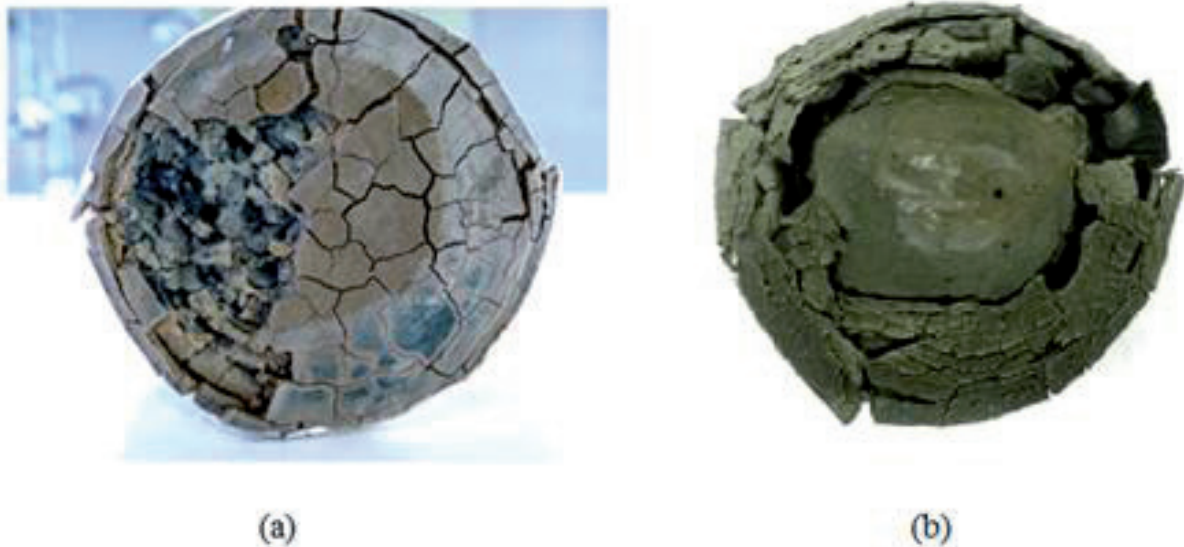
Figure 10: Comparison of observed damage of SCP (a) and OCP (b) samples at an advanced stage of degradation

4. CONCLUSIONS

The objective of this work was to investigate the kinetics of sulfate ingress and its consequences on microstructure of two cement pastes OCP (ordinary cement paste) and SCP (cement paste with slag) and for two different curing time (early age and matured cases). The sulfate profiles are similar in the two cases after two months of sulfate exposure, with a difference in the maximum value of sulfate content reached at this duration. It is more important in the case of the early age exposure at the first three millimeters because of the high porosity and permeability of the material at this early age. Moreover, the curves, given the sulfate profiles, show that sulfate ingress is delayed by chemical interaction with the cement matrix. In the case of slag cement paste, matured samples showed low sulfate binding in the surface. This is due to the low amounts of Portlandite and to the availability of aluminium. Moreover, the sulfate ingress depth is deeper in the case of Portland cement paste. This may be explained by the finer porosity of PCL and also the low calcium ions leached.

Even if a processes of diffusion due to a concentration gradient and capillary adsorption are initially at the origin of the sulfate ions penetration to the cementitious matrix , the physico-chemical interaction with the cement paste hydrates seems to have a higher kinetic. This finding confirms that the ESA is characterized by both diffusion and physicochemical binding of sulfate ions in the cement matrix. Furthermore, it is important to note the strong coupling and competition between ESA and leaching phenomenon. This leaching allows increasing the calcium content in the porous solution leading to the acceleration of the Aft formation during the ESA test.

Although the same sulfate ingress, matured Portland cement paste showed a rapid degradation. Conversely, Portland cement pastes exposed at early age to the sulfate solution showed no craking or spalling during one year after exposure to the ESA. However, slag cement pastes, were cracked rapidly in the early age exposure and resisted better in the matured case.

Finally, the microscopy images have confirmed a large non confined fraction of ettringite present in the porosity for early age exposed cement paste, but a small amount of gypsum was found. Contrary to the matured exposure case, a higher amount of gypsum and a large fraction of confined ettringite are found, after one month of sulfate exposure. The coexistence of an important amount of compressed ettringite and gypsum can explain the degradations observed in the matured samples. The high resistance of Portland cement paste to sulfate attack, at early age, can be explained by the continuous precipitation of ettringite in a large porosity without the monosulfate dissolution.

REFERENCES

[1]   Santhanam, M. et al, Effects of gypsum formation on the performance of cement mortars during external sulfate attack, Cem Concr Res 33 (2003), 325-332

[2]   Sarkar, S. L. et al, Numerical simulation of cementitious materials degradation under external sulfate attack, Cem Concr Compos 32 (2010), 241-252

[3]   Monteiro, P.J.M., Scaling and saturation laws for the expansion of concrete exposed to sulfate attack, Proc Nat Acad Sci USA 103 (31) (2006), 11467–11472

[4]   Neville, A., The confused world of sulfate attack on concrete, Cem Concr Res 34 (2004), 1275–1296

[5]   Monteiro, P.J.M. and Kurtis, K.E., Time to failure for concrete exposed to severe sulfate attack, Cem Concr Res 33 (2003), 987-993

[6]   Schmidt, T. et al, Physical and microstructural aspects of sulfate attack on ordinary and limestone blended portland cements, Cem Concr Res 39 (2009), 1111-1121

[7]   Al-Akhras, N.M., Durability of metakaolin concrete to sulfate attack, Cem Concr Res 36 (2006), 1727-1734

[8]   Santhanam, M. et al, Mechanism of sulfate attack: a fresh look Part 2. Proposed mechanisms, Cem Concr Res 33 (2003), 341-346

[9]   Irassar, E. F. et al, Microstructural study of sulfate attack on ordinary and limestone portland cements at ambient temperature, Cem Concr Res 33 (2003), 31-41

[10]   Yu, C. and Scrivener, K., Mechanism of expansion of mortars immersed in sodium sulphate solution, Cem Concr Res 43 (2013), 105-111

[11]   Ayora, C. et al, Weathering of iron sulfides and concrete alteration: thermodynamic model and observation in dams from central Pyrenees, Spain, Cem Concr Res 28 (1998), 591-603

[12]   Chinchon, J. S. et al, Influence of weathering of iron sulfides contained in aggregates on concrete durability, Cem Concr Res 25 (1995), 1264-1272

[13]   Mehta, P. K., Mechanism of expansion associated with ettringite formation, Cem Concr Res 3 (1973), 1-6

[14]   Marchand, J. and Scalny, J., Materials of concrete: Sulfate attack mechanisms, American Ceramic Society, (1999)

[15]   Planel, D. et al, Long-term performance of cement paste during combined calcium leaching-sulfate attack : Kinetics and size effect, Cem Concr Res 36 (2006), 137-143

[16]   Chabrelie, A., Mechanisms of degradation of concrete by external sulfate ions under laboratory and field conditions, PhD thesis, Swiss Federal Institute of Technology in Lausanne, Lausanne, (2010)

[17]   Brown, P.W., An evaluation of sulfate resistance of cements in a controlled environment, Cem Concr Res 11 (1981), 137-143

[18]   Kunter, W. et al, Influence of the Ca/Si ratio of the C-S-H phase on the interaction with sulfate ions and its impact on the Ettringite crystallization pressure, Cem Concr Res 69 (2015), 37-49

Performance of limestone calcined clay blends in sodium sulphate attack on mortars

F. Suma[1], M. Samthanam[1]

ABSTRACT

Limestone blended cements are increasingly emerging as a choice for good long-term durability of concrete. In this category of cements, limestone-calcined clay cement blends present a major advantage owing to the high reactivity of the calcined clay and the synergistic effects brought about by the aluminate – carbonate interactions. The present study reports an experimental evaluation of the resistance to sodium sulphate attack of limestone calcined clay cement mortars in comparison with OPC and fly ash blended cement mortars. Results up to 60 weeks of immersion confirm that both limestone calcined clay cement blend and fly ash cement blend perform far superior to the OPC. Expansions are almost nil in the case of the limestone calcined clay cement mortar despite the long period of immersion in 5% sodium sulphate solution. The details of the microstructural analysis conducted using SEM and XRD are also reported in the paper.

INTRODUCTION

Several types of supplementary cementing materials (SCM) are used for enhancing different properties of concrete. The blended cements prepared with SCMs provide several advantages over conventional Ordinary Portland Cement (OPC). One of the promising SCMs is limestone powder. A limited addition of limestone powder to Portland cement improves the workability, strength and durability properties of the concrete. Reaction of limestone with alumina in the cement produces monocarboaluminate leading to refinement of pores. In general, up to 5 % limestone addition is acceptable according to various standards for OPC. Many standards accept up to 15% interground limestone in selected cements (ASTM C595-16 and CSA A3000-08).

The hydration reaction of clinker changes with limestone addition. Calcium carbonate from limestone suppresses the conversion of ettringite to monosulphate. A replacement of monosulphate with monocarbonate happens due to higher insolubility and stability of carbonate (Kakali et al. 2000). Limestone addition has a large effect on the permeability of concrete. Tsivillis (2003) tested the permeability of concrete with Portland Limestone Cement (PLC). Water permeability and sorptivity were improved due to limestone addition, in concrete mixes with low w/c. These properties were affected by the size and kind of pores. The factors that affected the pore system were the filler effect and dilution effect. Limestone did not have an effect on the permeability characteristics of concrete at higher w/c ratio.

According to Schutter (2011), limestone filler ensures similar or improved fresh properties to SCC. Very small amount of limestone reacts to form the mono-carboaluminate and the rest is inert to act as filler. Thus the water is completely available for hydration resulting in less dilution of cement. The gap between the coarse particles gets filled by the limestone filler,

---

[1]   Department of Civil Engineering, IIT Madras, Chennai, INDIA, manus@iitm.ac.in

which improves the strength and transport properties of the hardened blend. The hydration is accelerated due to increased possibilities of nucleation by the presence of limestone filler.

In PLC, maximum strength and minimum porosity is achieved when all the aluminates in the cement are consumed to form monocarboaluminate. An optimum amount of limestone facilitates the usage of the entire alumina content provided by SCM. Addition of SCMs with higher alumina content facilitates the use of all available limestone to form monocarboaluminate (Ramezanianpour et al. 2014).
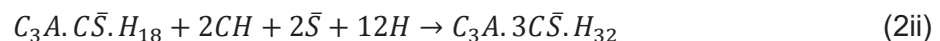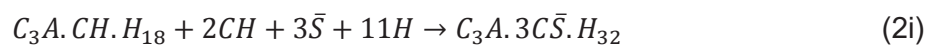
Vance et al. (2013) suggest that the strength gain and capillary porosity of blends with limestone depends on the properties of limestone powder such as fineness and dosage. Again the water-to-powder ratio and the type of powder used influence the capillary porosity and strength gain of the blend. Median particle size of limestone (0.7 to 3 µm) was found to accelerate the early age cement hydration. The higher 28 day strength of ternary blend of OPC-Limestone-Metakaolin is attributed to the carboaluminate formation along with ettringite stabilization and increase in solid volume of the hydrates with the reduction of porosity. Nevertheless, the authors conclude that the synergistic effects of metakaolin and limestone provides improved performance at early ages but at later age the properties are similar to OPC systems. The overall discussion of the chemical compatibility was based on the strength gain while durability aspect was not addressed in the paper.

Metakaolin reacts faster in the system with limestone compared to binary system of Portland cement and metakoalin. Further, limestone reacts faster in the system with metakaolin compared to the binary system of Portland cement and limestone. Compared to 100 % Portland cement, a 45 % substitution of metakaolin and limestone in 2:1 ratio has better properties (Antoni et al. 2012) in terms of strength gain.

The main ingredients of hydrated cement that participate in sulphate attack are portlandite and tricalcium aluminate hydrates. Portlandite reacts with external sulphate to form gypsum and ettringite. Gypsum is formed by the cation exchange reaction as in the equation (1).

$$CH + N\bar{S} + 2H \; \rightarrow C\bar{S}H_2 + NH \tag{1}$$

The gypsum reacts with available C_3A and monosulphate hydrate to form ettringite. In the reaction with calcium hydroxide and external sulphate, the C_3A containing hydrates and the monosulphate hydrates produce ettringite. The reaction is explained by Mehta and Monteiro (2013) as in equation (2)

$$C_3A.CH.H_{18} + 2CH + 3\bar{S} + 11H \rightarrow C_3A.3C\bar{S}.H_{32} \tag{2i}$$

$$C_3A.C\bar{S}.H_{18} + 2CH + 2\bar{S} + 12H \rightarrow C_3A.3C\bar{S}.H_{32} \tag{2ii}$$

Metakaolin addition resists the sulphate attack in Portland cement in three steps. The first step is the reduction of total amount of tricalcium aluminate hydrate in the cement paste. Later due to pozzolanic reaction, portlandite in the system is lowered, thus lowering potential for gypsum and ettringite formation. The third step is the pore size refinement due to both pozzolanic action and filler effect. Due to pozzolanic reaction, large capillary pores are filled by secondary C-S-H and large continuous capillary pores are segmented to small discontinuous pores. The filler action is due to the 1 µm size of metakaolin, relative to around 12 µm size of cement particles (Al-Akhras, 2006).

Studies show that the performance of PLC against thaumasite formation is very poor at certain replacement levels (Irassar et al., 2003), while the partial replacement of PLC with SCMs improves the resistance to thaumasite attack. When PLC reacts with SCM much of the limestone which is a requirement for thaumasite formation is consumed. Ettringite

formation and permeation of sulphate ions is suppressed by the combined effect of pozzolanic action and the synergy of PLC with SCM, which inhibits thaumasite formation (Mirvalad and Nokken, 2015).

MATERIALS AND EXPERIMENTAL PROCEDURE

OPC provided by Penna Cement, Class F Fly Ash procured from North Chennai Thermal Power Station, Metakaolin provided by English Indian Clays Limited were used (LCCC) in this study. LC3 was produced in a factory ball mill intergrinding clinker, calcined clay, limestone and gypsum in a proportion of 50, 30, 15 and 5% respectively. The ingredients of LC3 were interground at Tiranga cements, Virpur, Gujarat. Clinker, limestone and gypsum for LC3 were provided by UltraTech Cement. The calcined clay of 56% kaolinite from Bhuj (Gujarat) was used to prepare LC3.

The mortar was mixed in a planetary mixer following the procedure in ASTM C305. The procedure for sulphate attack study was adapted from ASTM C1012. The cement-to-aggregate ratio was maintained as 1: 2.75 with Indian Standard sand (as per IS 650) as aggregate. Mixing was done in a cabin maintaining temperature of 23 ± 2° C with a relative humidity of 65%. The description of each blend is provided in Table 1. In the case of OPC and FA30, the mix was workable at a water-to-binder ratio of 0.485. LCCC was prepared by blending OPC, metakaolin and limestone in laboratory. LCCC required a water-to-binder ratio of 0.69, to maintain the same flow as OPC. For LC3 the water-to-cement ratio was maintained as 0.485 and to attain sufficient workability, a PCE based superplasticizer was used. 25 x 25 x 285 mm prisms with attached studs at the ends were prepared for length change measurements. After casting, the prism moulds were covered with a polythene sheet and kept at a controlled temperature of 23 ± 2°C with a relative humidity of 65% for 24 hours.

Demoulding was done 24 hours after mixing. After demoulding the prisms were transferred to saturated lime solution. On the 7th day, the initial length was measured. The specimens were then immersed in a 5 % sodium sulphate solution. The volume of solution to volume of prisms was maintained at a ratio of 4:1. For the first four weeks, the length measurements were made along with the renewal of solution on a weekly basis. Thereafter, measurements and renewal of solution were made every two weeks.

Table 1. Description of blends

	Constituents	Weight (%)
OPC	Portland Cement (53 grade)	100
LC3	Limestone Calcined Clay Cement	100
LCCC	Portland Cement (53 grade)	55
	Metakaolin	30
	Limestone Powder	15
FA30	Portland Cement (53 grade)	70
	Class F- Fly Ash	30

RESULTS

Length change

Change in length was measured with reference to an invar bar using a length comparator. The measurement was performed at a temperature of 25±2 °C and relative humidity of 65±5 %. Figure 1 shows the expansion-time plot for each blend. OPC showed an expansion of about 0.32 % after more than 60 weeks of exposure, whereas negligible expansions were registered for the mortars with FA30, LC3 and LCCC. Significant increase in expansion for the OPC mortar occurred after about 30 weeks of exposure. It is interesting to note that both the limestone-calcined clay systems, i.e. LCCC that is prepared in the lab using high purity metakaolin and LC3 that is obtained from an industrial production with a clay containing only 60% kaolin, performed very well in sodium sulphate solution. This clearly shows the benefits of this combination.
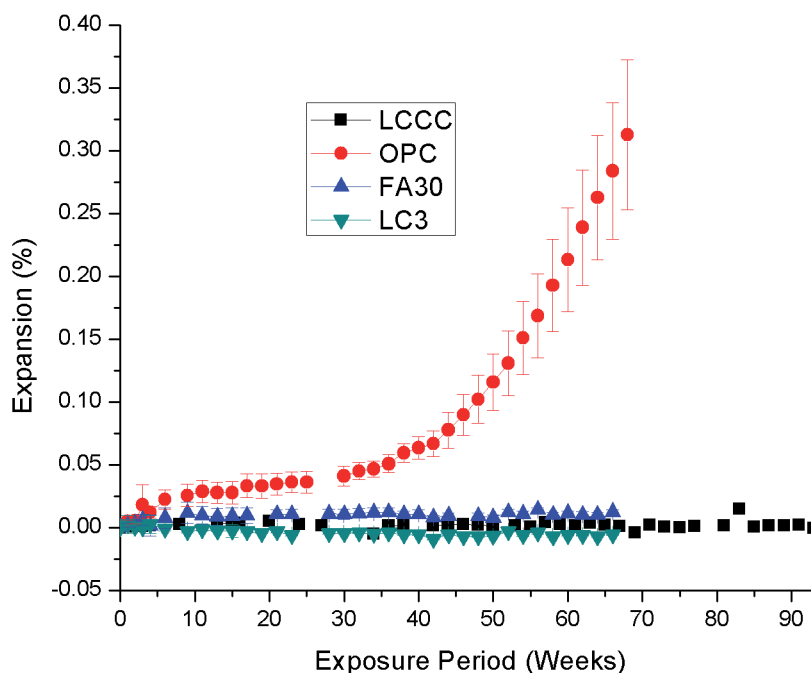
Figure 1. Expansion of mortar prisms in sodium sulphate solution.

X-ray diffraction

Samples of mortar for microanalytical investigations were cut from the sides of the prism to a depth of about 4 mm, in order to obtain a sample from the surface zone. The samples were then immersed in isopropanol for 4 days for removal of water through solvent exchange, and then dried in vacuum. Grinding of samples was done manually using agate mortar and pestle, following which the powder was sieved through a 75 μm sieve. The powder samples passing 75 μm were used for X-ray diffraction on a Bruker instrument using Cu Kα radiation.

XRD patterns for LC3 and FA30 mortars immersed in 5 % sodium sulphate solution for 66 weeks, OPC mortars immersed for 68 weeks and LCCC mortar immersed for 93 weeks are shown in Figure 2. Table 2 shows the qualitative assessment of the expected minerals and

compounds present in the cementitious system. *, **, *** respectively indicate that the compound is present but in very low, moderate and high concentration in comparison to the other three blends.

Intensity of gypsum peaks is higher in the XRD pattern of OPC which shows the clear indication of severe sulphate attack in OPC alone. The second peak of gypsum at 20.733° 2Θ is overlapped by 3rd peak of quartz at 20.861° 2Θ. Main ettringite peaks at 9.08° and 15.79° 2Θ are much clearer for OPC compared to other blends. Thaumasite, if it is available, is very difficult to identify due to the peak overlap with ettringite. LC3 sample immersed in lime for 26 weeks shows the presence of monocarboaluminate, whereas this phase is absent in the case of LC3 sample immersed in sodium sulphate solution (Figure 3). Calcium hydroxide is absent in LC3 samples at an early age itself, indicating a complete consumption due to high reactivity of the calcined clay.
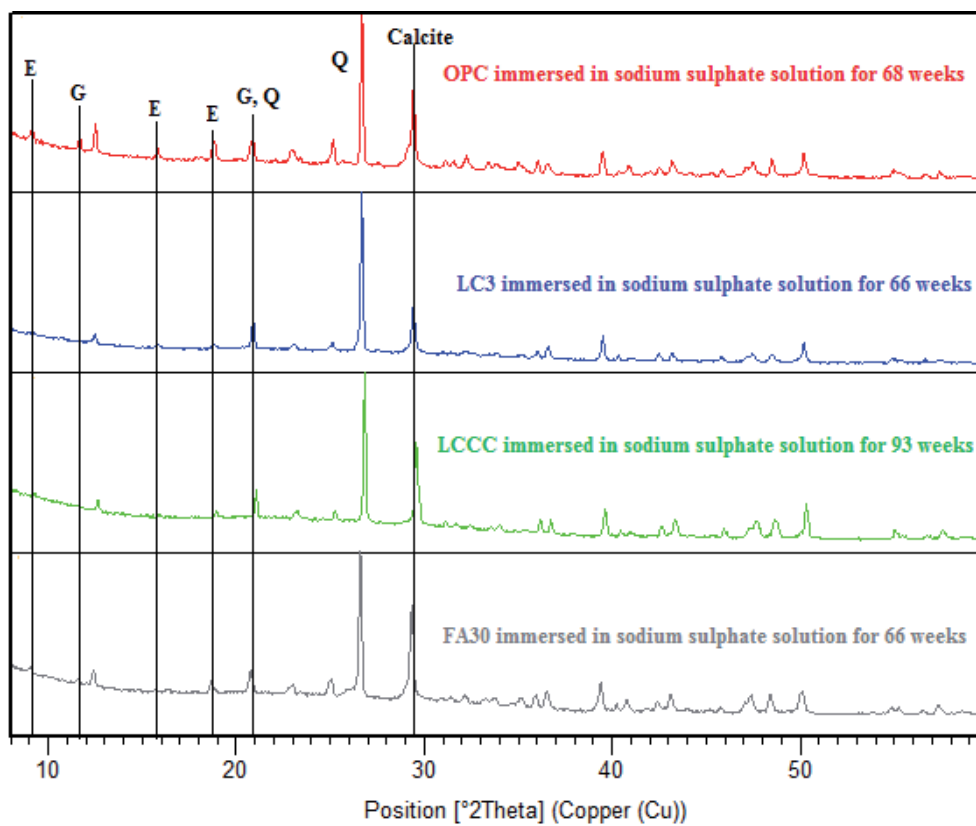
Figure 2. X-ray diffraction patterns for the different mortars after 60 – 90 weeks of exposure in the sodium sulphate solution
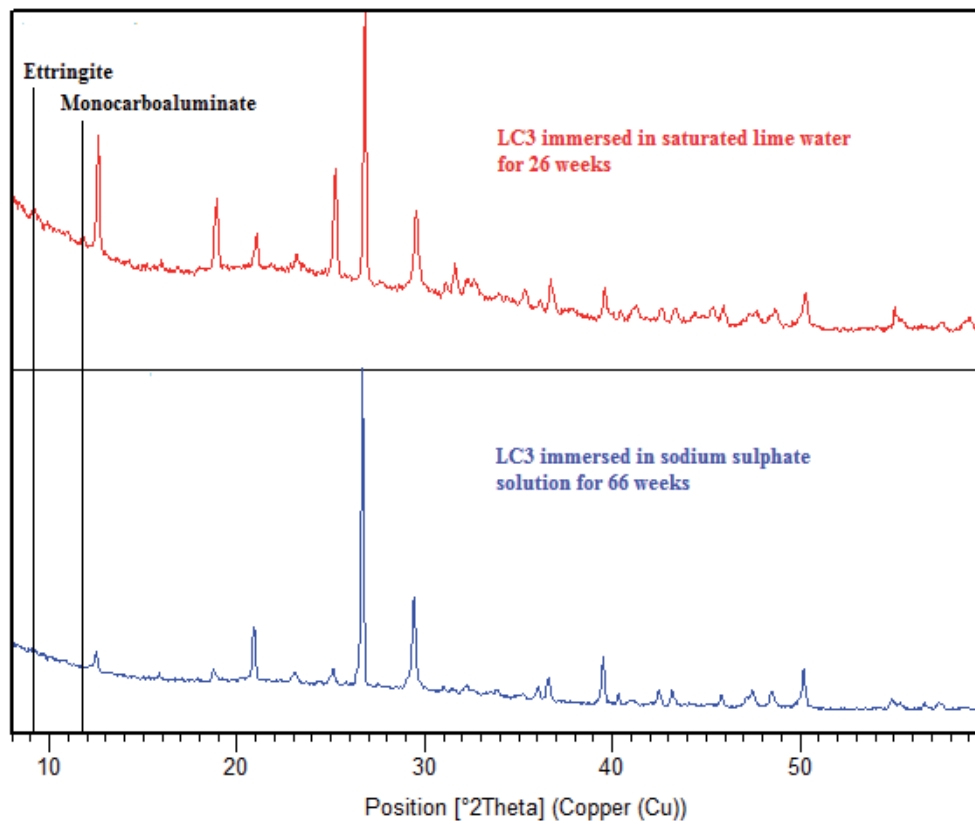
Figure 3. LC3 sample immersed in saturated lime water and sodium sulphate solution

Table 2: Compounds detected by XRD in the specimens subjected to sodium sulphate attack

Mineral/Compound	OPC	LCCC	LC3	FA30
Ettringite	***	*	*	**
Gypsum	***	-	-	*
Calcium hydroxide	-	-	-	-
Monocarboaluminate	-	-	-	-
Calcite	***	***	**	***

Mercury intrusion porosimetry (MIP)

The MIP results for different ages for OPC, LC3 and FA30 are shown in Figure 4 (from an earlier study in the same laboratory). The diameter at which the mercury begins to penetrate into the pores of the specimen (threshold diameter) is significantly lower at 3 days itself for LC3 in comparison to OPC and FA30. As the threshold diameter is comparatively less, the

permeability of LC3 blend can be considered lesser than OPC and FA30. The results show higher pore refinement for LC3 compared to OPC and FA30.
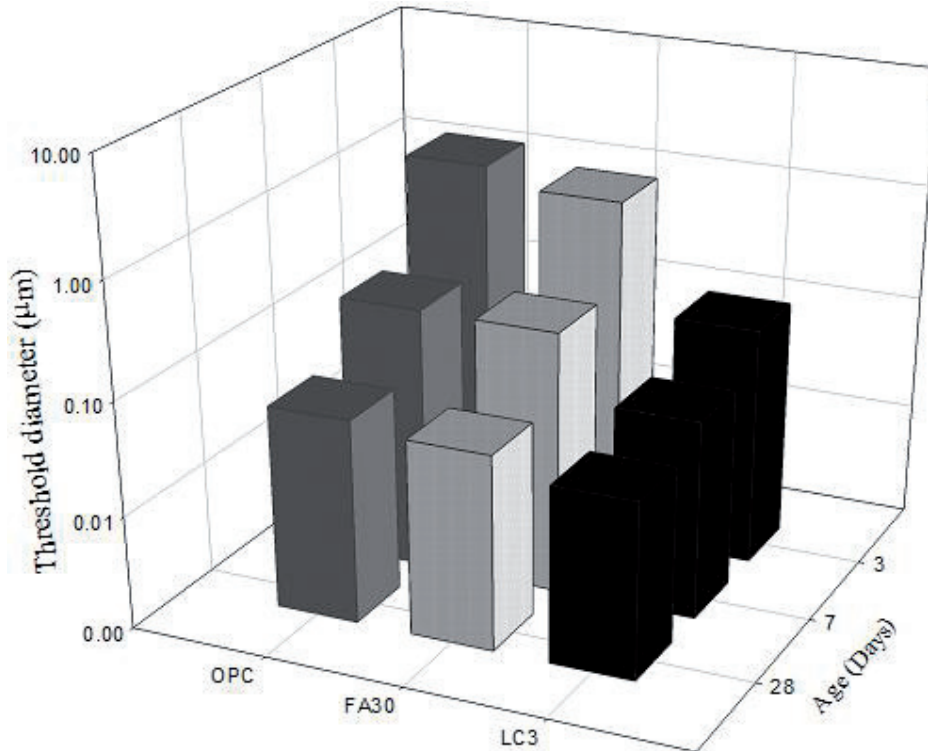
Figure 4. Variations in threshold pore diameter in OPC, FA30 and LC3 (Yuvaraj and Santhanam, 2015)

Scanning Electron Microscopy (SEM)

Visible degradation is observed in OPC specimens. All the OPC specimens were cracked at the edges as shown in Figure 5a. No visible degradation is seen in FA30 specimens (Figure 5b). LCCC and LC3 specimens are intact without any changes (Figure 5c and d).
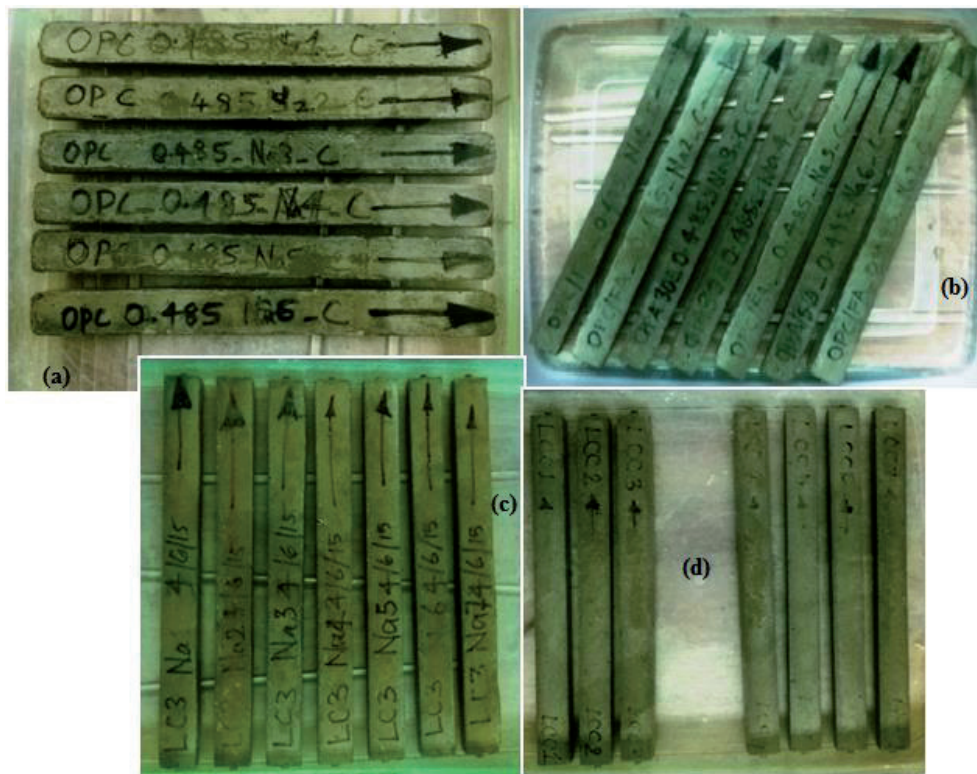
Figure 5. Specimens immersed in sodium sulphate solution
(a) OPC immersed for 68 weeks (b) FA30 immersed for 66 weeks
(c) LC3 immersed for 66 weeks (d) LCCC immersed for 93 weeks

For SEM studies, a sample was cut from the corner of 25 mm x 25 mm cross section prism and immersed in isopropanol for 4 days for removal of moisture through solvent exchange, followed by drying in vacuum. After epoxy impregnation of this sample, coarse and fine polishing were performed using silicon carbide grits and diamond spray of progressively finer sizes. The specimen after polishing was coated with Au-Pd, and then studied in the backscatter mode in the SEM.

Figure 6 shows the elemental mapping for LC3 and OPC system. The high Si content in both the systems is due to siliceous fine aggregate. Ca is prominent in both systems, whereas Al content is very high in LC3 due to the calcined clay in the LC3 system. There is a clear evidence of lower S contents in the LC3 system, indicating negligible presence of sulphate attack products such as gypsum or ettringite. On the other hand, in the case of the OPC mortar, the elemental map shows a band of S, and this is confirmed to be gypsum (Figure 7). This band was seen to extend through a large portion of the surface zone in the OPC mortar specimen. Further, the gypsum band was seen to also go around the aggregate in the interfacial region. The EDS analysis on outer CSH confirms the presence of embedded ettringite in OPC mortars immersed in 5% sodium sulphate solution for 68 weeks (Figure 8).
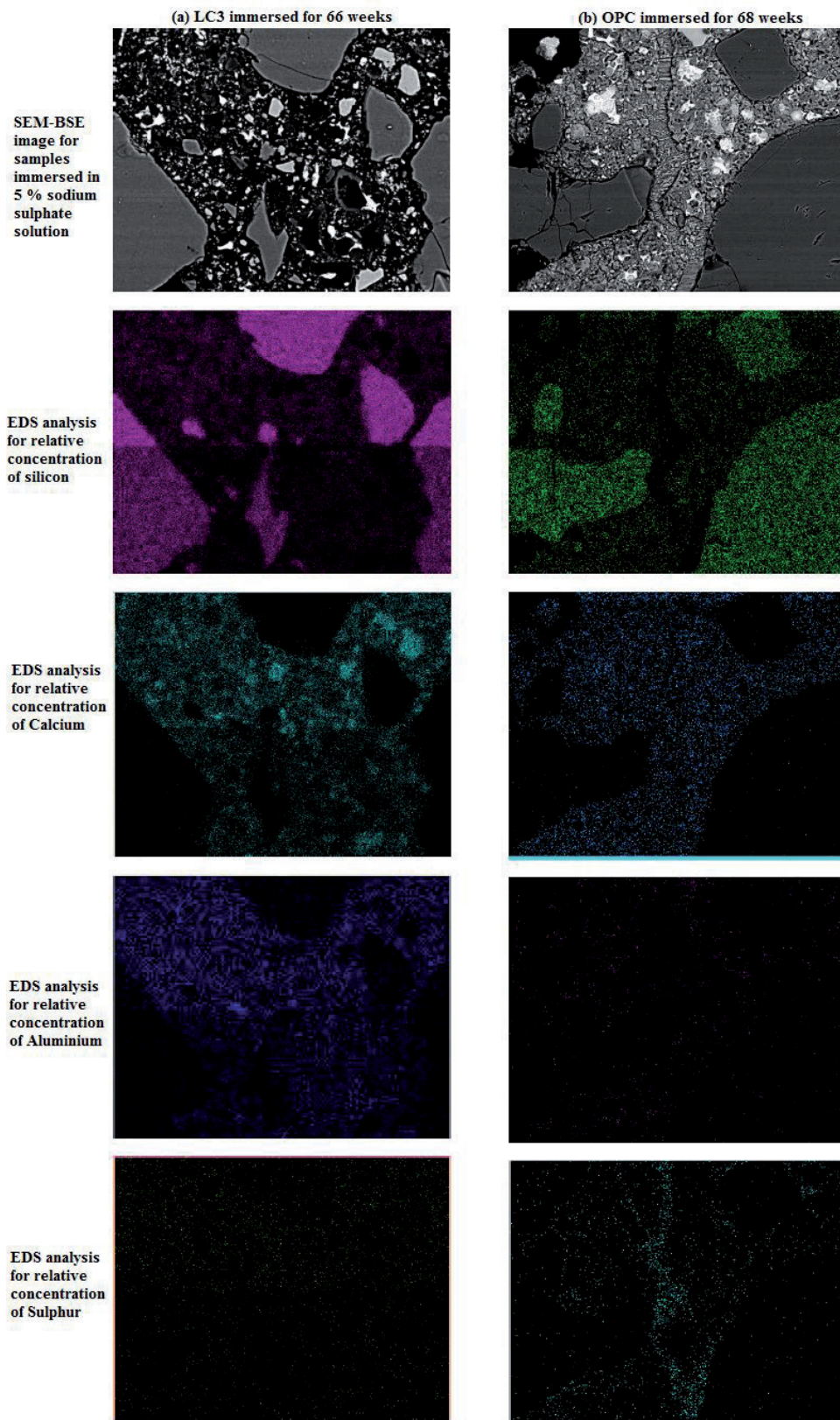
Figure 6. Mapping of elements near the surface of LC3 and OPC mortar sample.
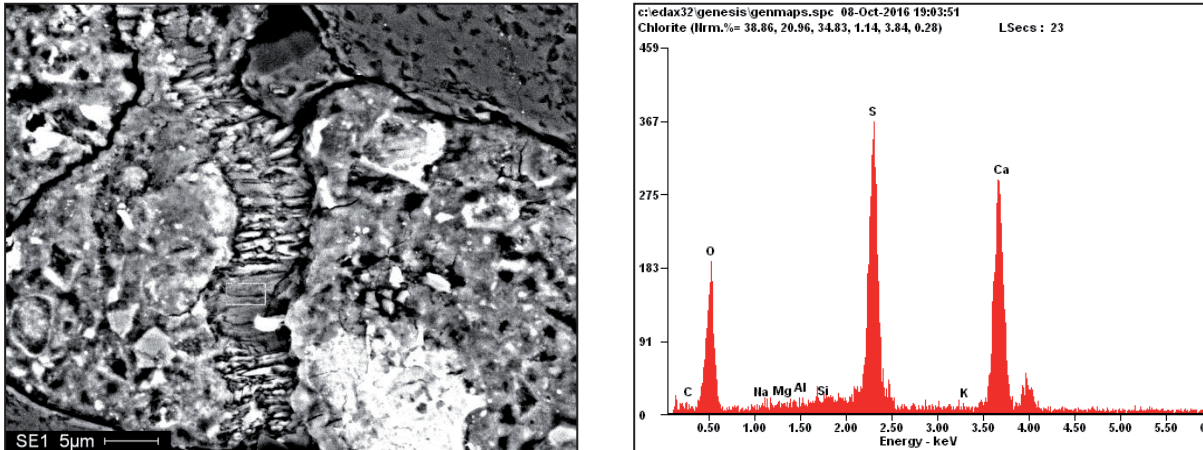
Figure 7. Gypsum deposition in the cracks of OPC immersed in 5 % sodium sulphate solution
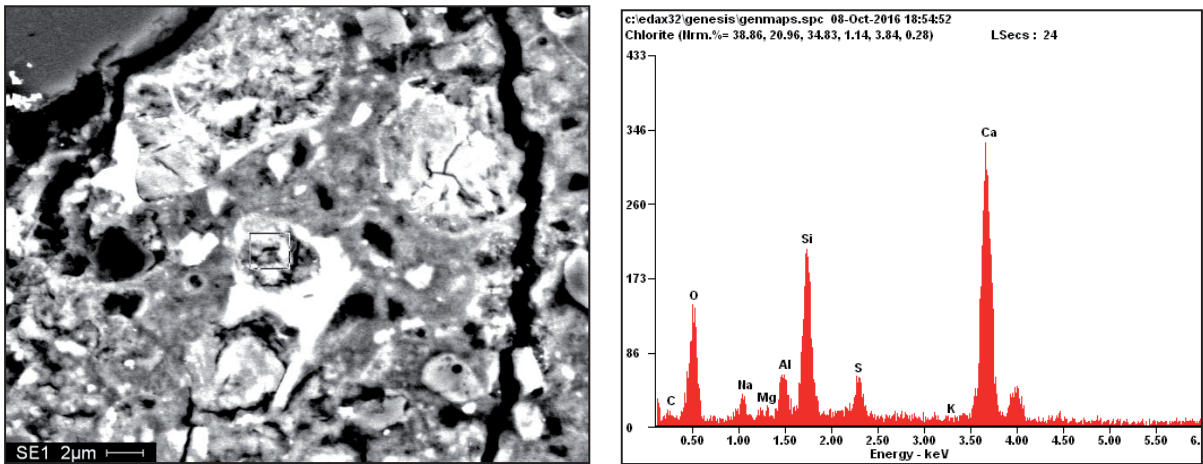
Figure 8. Ettringite embedded in CSH gel of OPC in 5% sodium sulphate solution

CONCLUSIONS

The results up to 66 weeks of exposure confirm that limestone calcined clay blends are highly resistant to sodium sulphate attack. One reason for this good performance is the refinement of pores by the secondary CSH from pozzolanic action and monocarboaluminate produced at the early age from the reaction of limestone and calcined clay. The limestone-calcined clay systems that are prepared using clays with lower kaolin contents (LC3) confirm that calcined clay need not have high purity kaolin to perform well in sodium sulphate environment.

XRD pattern of OPC shows the presence of gypsum and the ettringite, which are also confirmed using the SEM studies. The absence of calcium hydroxide in the LC3 and LCCC system is a clear indication that gypsum formation is impossible in the system. Calcium hydroxide is absent in Fly Ash system which prevents formation of further gypsum.

REFERENCES

[1] Kakali, G., Tsivilis, S., Aggelis E., Bati M., "Hydration products of C3A, C3S and Portland cement in the presence of CaCO3", Cem. Concr. Res., 30, 1073-1077 (2000)

[2] Tsivilis, S., Tsantilas, J., Kakali, G., Chaniotakis E., Sakellariou, A., "The permeability of Portland limestone cement concrete", Cem. Concr. Res.,33, 1465–1471 (2003)

[3] Schutter, G. De., "Effect of limestone filler as mineral addition in self-compacting concrete" 36th Conference on Our World in Concrete & Structures, Singapore, August 14-16 (2011)

[4] Ramezanianpour, A. M., Hooton, R. D. "A study on hydration, compressive strength, and porosity of Portland limestone cement mixes containing SCMs", Cement. Concr.Compos., 51, 1–13 (2014)

[5] Vance, K, Aguayo, M, Oey, T., Sant, G., Neithalath, N., "Hydration and strength development in ternary portland cement blends containing limestone and fly ash or metakaolin" , Cement. Concr.Compos., 39, 93–103 (2013)

[6] Mehta, P.K. and Monteiro P. J.M., "Concrete microstructure, properties and materials", McGraw Hill Education (India) Private Limited, New Delhi., 159-160 (2013)

[7] Antoni, M., Rossen, J., Martirena, F., Scrivener, K.,"Cement substitution by a combination of metakaolin and limestone", Cem.Concr. Res., 42, 1579–1589 (2012)

[8] Al-Akhras, N. M., "Durability of metakaolin concrete to sulfate attack", Cem. Concr. Res., 36, 1727–1734 (2006)

[9] Irassar, E.F., Bonavetti, V.L., Gonzalez, M., "Microstructural study of sulfate attack on ordinary and limestone Portland cements at ambient temperature", Cem. Concr. Res., 33, 31–41 (2003)

[10] Mirvalad, S., Nokken, M., "Minimum SCM requirements in mixtures containing limestone cement to control thaumasite sulfate attack", Constr. Build. Mater., 84, 19–29 (2015)

[11] Yuvarai D., and Santhanam, M., "Phase assemblage in a trial blend of limestone and calcined clay cement", 14th NCB International seminar on cement and building materials, New Delhi, India (2015)

PROCEEDINGS

FIELD ASPECTS

External sulfate attack in Japan: A review

Y. Kawabata[1], N. Yoshida[2], S. Ogawa[3], K. Yamada[4]

ABSTRACT

External sulfate attack (ESA) is one of the pathologies in which concrete is physically or chemically degraded, leading to loss of performance of the structure affected. Although the damage level by ESA is strongly influenced by climate conditions such as temperature history and wetting/drying cycles as well as sulfate concentration of the exposed site, the relation of laboratory tests to field performance remains unclear.

In order to bridge the knowledge gap between laboratory and field performance, it is beneficial to summarize cases of ESA damage to real concrete structures in the field. This paper reviews the real cases in Japan, including some current cases related to ESA.

1.   INTRODUCTION

External sulfate attack (ESA) is one of the pathologies in which concrete is physically or chemically degraded. The damage to concrete induced by ESA leads to a loss of performance of the structure affected.

In Japan, although some cases of ESA have been reported, the influence of climate actions on the actual damage process of the structures remains unclear. Some ESA cases involved other deterioration mechanisms such as acid attack. Since the damage level by ESA is thought to be strongly influenced by climate conditions such as the temperature history and the wetting/drying cycles as well as the sulfate concentration of the exposed site, there is a big gap of knowledge between laboratory and field performance of concrete. In order to bridge the laboratory-performance gap, it is beneficial to collect the cases of real concrete structures in the field damaged by ESA.

This paper presents a review of the real cases of ESA in Japan, especially focusing on the climate conditions. Although most of the cases are physical sulfate attack, some issues either suspected of being related to ESA or related to ESA are also summarized. Major examples of ESA in Japan are physical attack of secondary sulfate ion from sulfides in soil by land reclamation.

[1]   Port and Airport Research Institute, Structural Engineering Department, Japan; kawabata-y@pari.go.jp

[2]   General Building Research Corporation of Japan, Materials laboratory, Japan; e-mail: n-yoshida@gbrc.or.jp

[3]   Taiheiyo Consultant, Sales and Marketing Division, Japan; e-mail: Shoichi_Ogawa@taiheiyo-c.co.jp

[4]   National Institute for Environmental Studies, Radiological Contaminated off-site waste Management Section, Japan; e-mail: yamada,kazuo@nies.go.jp

2. REAL CASES OF ESA IN JAPAN

2.1 Physical sulfate attack

Residential concrete foundation is one of the typical physical sulfate attacks reported in many studies. The cases of damage have been reported since 1980's. The details are presented in the reference [1]. Because of the geological origin of Japan, marine deposits are distributed throughout the country. In all areas, pyrite and other sulfides are frequently identified. During land reclamation for residential construction, these sulfides are inevitably oxidized. Consequently, the ground contains large amounts of water-soluble sulfate although gypsum rich soil is rare. When a concrete structure is constructed on such ground, the concrete is potentially subjected to physical sulfate attack.

Matsushita et al. investigated the sulfate content of the ground in Japan [2], and afterward proposed a risk map of physical sulfate attack based on the geological risk and temperature. Table 1 shows the 3 classifications which are basically identified by temperature and geological classification. When concrete is exposed to high sulfate-bearing ground at high temperature, the risk of physical sulfate attack is extremely high, whereas the risk is reduced at lower temperature.

Figure 1 [2] presents the proposed geological risk map. The map indicates the potential risk of physical sulfate attack due to high sulfate concentration of the ground and the temperature. The locations of real cases are also plotted in the figure [3]. Figure 1 shows a clear trend that most of the real cases are located in classifications A and B.

What is also interesting is that there is no report of physical sulfate attack in the north. One of the reasons for this is difficulty in diagnosing physical sulfate attack. In northern Japan, a concrete structure is subjected to frequent freeze-thaw actions. Therefore, some of the cases might be mistakenly diagnosed as "freeze-thaw damage". Another reason is the influence of temperature. Table 2 summarizes the climate conditions of some cities in Japan [4]. In some areas of Hokkaido, for example, the ground containing high sulfate was identified while no case has been reported. Annual mean temperature in 2015 was 10.0 °C, so that the temperature is thought to be lower for physical sulfate attack. According to the knowledge of the authors, the real case in Iwaki is the highest in latitude. Annual mean temperature in Iwaki is 14.3 °C. However, in Sendai (13.7 °C) where the temperature history is likely to be similar, no case has been reported in spite of a classification B. This indicates that other climate conditions should be taken into account, considering the concentration mechanism of the sulfate ion as well as the expansion mechanism of concrete due to physical sulfate attack.

Contrarily, in Tokyo where the annual mean temperature is 16.4 °C, many cases of physical sulfate attack have been reported. Yoshida investigated the residential concrete foundation around Tokyo and found that the cases of physical sulfate attack damage were plotted on Diluvium and Neogene marine deposits [1, 5]. The results seem to contradict the geological risk map by Matsushita et al. [2]. Yoshida pointed to the construction process, which may be specific in Japan. Most Diluvium and Neogene deposits around Tokyo are located in hilly areas, so they are excavated to flatten the area. This excavating process induces the oxidation of the sulfides and thus increases the risk of physical sulfate attack.

Figure 1 indicates the possible threshold of climate conditions for physical sulfate attack that may exist, while this point remains unclear. The fact that no case of physical sufate attack has been reported in northern Japan, may be attributed to the insufficiency of investigation in the area. It is important to develop a diagnostic method to distinguish freeze-thaw, physical sulfate attack and combined attack. Further investigation is necessary to clarify the threshold.

Table 1 Classification of severity of ESA [2]

	The number of month in which monthly mean temperature exceeds 20 °C	
	≥ 4 months	< 4 month
Alluvium	A (exteremely high)	B (high)
Neogene	B (high)	C (low)
Diluvium	C (low)	- (none)
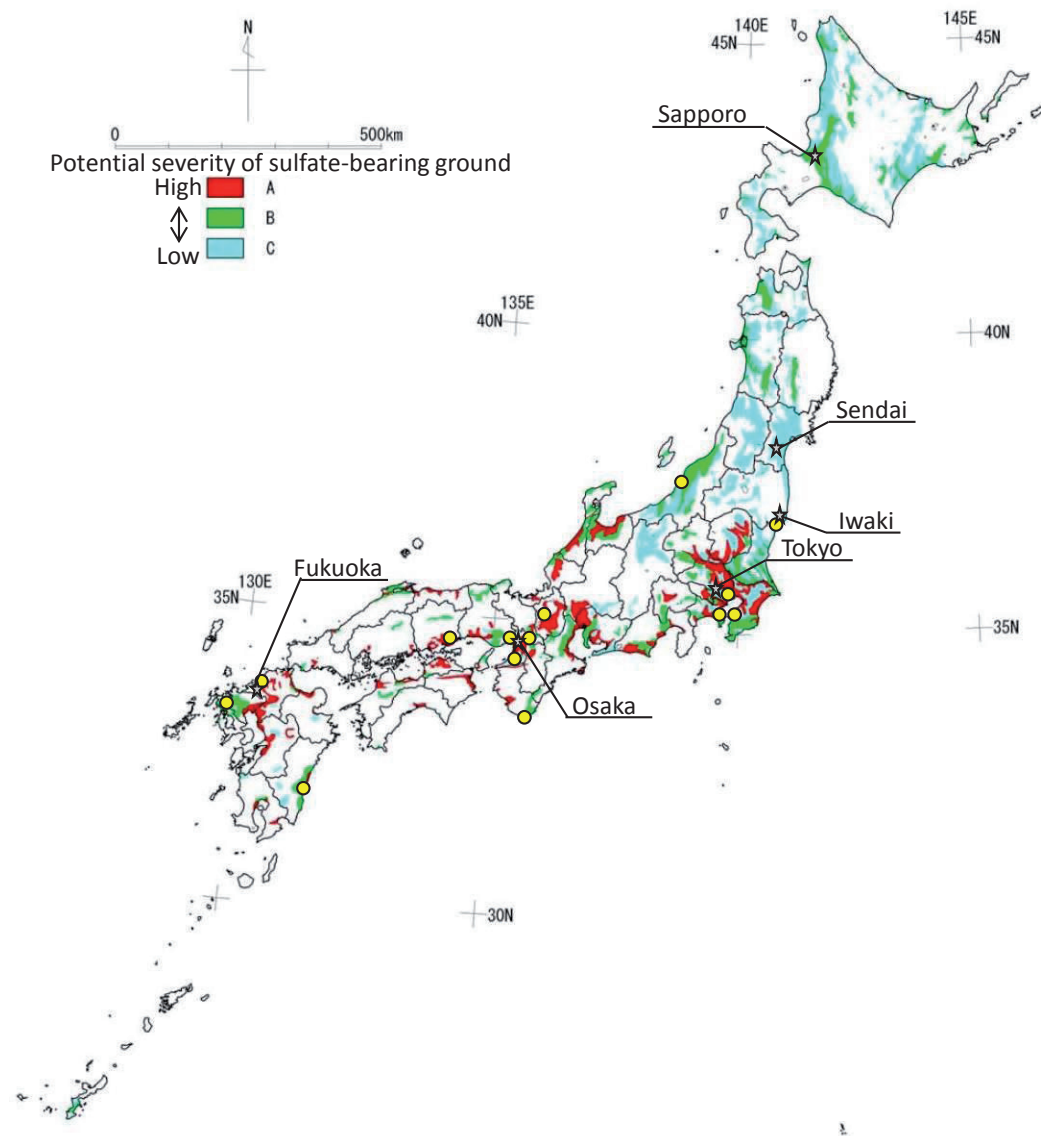
Figure 1 Geological risk map of ESA (yellow plots: real cases). After [2, 3]

Table 2 Climate conditions in 2015 (data from [4])

	Sapporo	Sendai	Iwaki	Tokyo	Osaka	Fukuoka
Annual mean temperature (°C)	10.0	13.7	14.3	16.4	17.2	17.3
Annual mean R.H. (%)	67	69	74	68	66	71
Annual mean precipitation (mm)	1274.5	1444.5	1329.5	1781.5	1648.5	1867.5

*Gray zone: no real case reported

2.2 Thaumasite sulfate attack

One real case of thaumasite sulfate attack (TSA) was reported in Japan [6]. This case was a brick tunnel constructed in 1890 and repaired by shotcreting polymer-modified mortar incorporating a quick setting admixture. The highest and lowest temperature values in a year are 35 °C and -5 °C, respectively. The repair work was performed in the 1990s to prevent water leakage and spalling of the joint fillers. Eight years after the repair work, spalling and delaminating of the mortar were identified. The mortar for repair was 30 mm thick and 15mm at the maximum was degraded (Figure 2). The interface between brick and mortar was mushy-softened and white deposits were observed. XRD with selective dissolution (Na_2CO_3 solution) and SEM/EDS analysis identified the deposits as thaumasite and a minor amount of ettringite (Figure 2).

Analysis of the chemical composition of the water that leaked from the tunnel revealed the sulfate ion concentration of the water to be less than 10 ppm. From this result, the authors concluded that TSA was triggered by sulfate ion from the admixture and carbonate ion from the aggregate or filler. This kind of deterioration was also reported in China [7].

Figure 2 TSA of polymer-modified mortar (left) and XRD before/after treatment using Na_2CO_3 solution [6]

Hosokawa et al. investigated the potential risk of TSA in northern Japan through exposure tests [8].The concrete specimens using limestone coarse aggregate were exposed to three

environments: (1) Seawater without soil, (2) Soil with low-sulfate concentration and (3) container filled with seawater and soil. The main differences were sulfate ion concentration and retention of seaw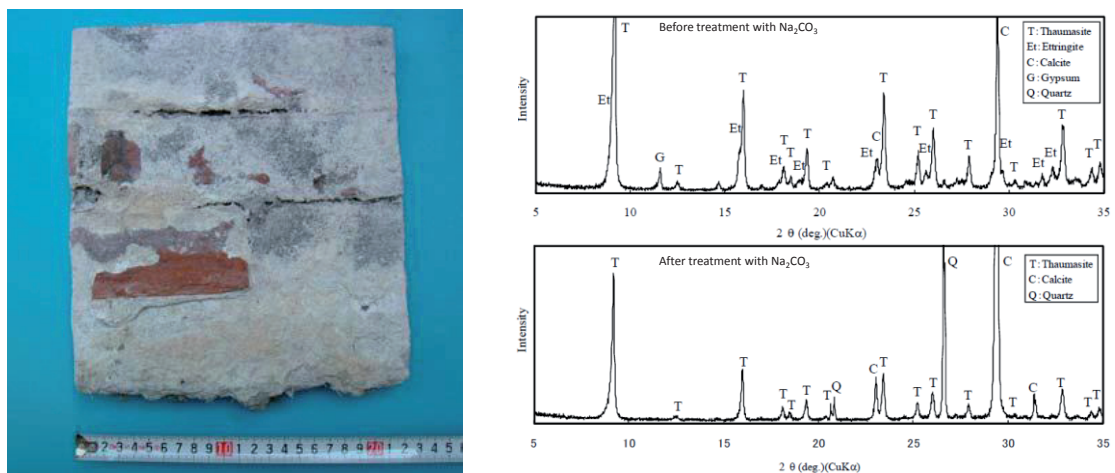ater. Test results after 30 months of exposure showed that only in the case of the "Monbetsu-container" was there deterioration by TSA (Table 3). With retention of seawater, pH of the soak solution increases with increased leaching of alkali from the concrete specimens. This situation is favourable for TSA. The results suggest the possibility that TSA hardly contributes to the main deterioration of marine structures where the seawater is exchanged by wave and tidal actions. This mechanism is consistent with the laboratory test and analytical results [9, 10].

Table 3 Exposure conditions and appearance of specimens after exposure test [8]

	Abashiri- seawater	Monbetsu- underground	Monbetsu- container
Temperature (°C)	5.6	> 12.1	
SO_4^{2-} concentration (ppm)	2650	390	3500
Retention of seawater	No	Yes	
Soil filling	No	Yes	
Appearance of specimen after 30 months			

2.3 Chemical grout-induced sulfate attack

To improve the strength of soft-ground, chemical grouting is usually performed in Japan. There are various materials for chemical grouting, but a combination of waterglass and sulfuric acid as a hardener is commonly used for ground improvement. The strength of soft-ground can be improved by the following reaction.

$$H_2SO_4 + Na_2O \cdot nSiO_{2aq} \rightarrow Si_nO_{2n-1}(OH)_2 + Na_2SO_4 \qquad (1)$$
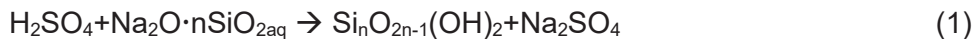
Two grouting methods are practiced. One is the direct mixing method in which the materials are injected to the soil without pre-mixing. This method is problematic in that silica sol starts gelation rapidly, so that the sulfuric acid and waterglass might remain. Therefore, there is a possibility that a considerable amount of sulfuric acid remains in the soil without reaction, leading to deterioration through acid attack. The other method is the indirect mixing method in which the materials are pre-mixed at the plant and then injected into the soil. After soil improvement, a significant amount of sodium sulfate exists in the soil. Concrete ducting combined with this improved soil is also performed.

Figure 3 shows the concrete duct deteriorated by chemical grouting [11]. The concrete duct was constructed by shield tunnelling combined with chemical grouting. The concrete was cracked and water leakage was observed. Chemical analysis of the water leaked through cracks disclosed that the sulfate ion concentration of the water was 1.94%, whereas that from the non-damaged area was 0.02%. XRD analysis on white deposits identified thenardite formation.

This kind of deterioration is rarely reported because it is difficult to inspect concrete structures: most concrete structures are embedded in the soil. Therefore, more cases may exist and hence field investigations should be performed.

(a)Non-damaged area   (b)Damaged area   (c)Damaged area
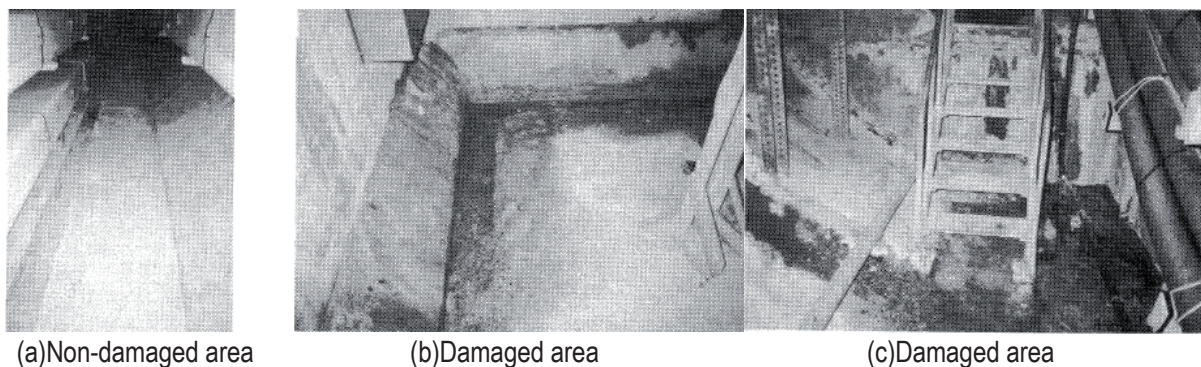
Figure 3 Concrete duct deteriorated by chemical grouting-induced sulfate attack [11]

2.4 Seawater

The marine environment is one of harshness for concrete structures since seawater contains many aggressive ions including sulfate. Yamaji et al. investigated concrete structures subject to long-term service and concrete specimens exposed to seawater [12]. The elemental map of concrete was obtained with an Electron Probe Microanalyzer (EPMA). The profile of Vickers hardness was also investigated. As the result, there is a good relationship between the depth of Mg penetration and the depth where the hardness tends to decrease (Figure 4). This means that the surface of concrete exposed to seawater is weakened by Ca leaching and M-S-H formation. Because the depth of sulfur is larger than that of Mg, it is also clarified that the influence of sulfate in seawater on the deterioration turns out to be limited since no degradation of the hardness was confirmed. A similar result was obtained in recent work in Denmark and Norway [13]. In their work, ettringite, thaumasite and gypsum were identified and considered unlikely to cause cracking.

In contrast, a concrete surface is exposed to wetting-drying cycles with strong solar radiation in Japan. Especially in a splashing zone, the climate condition may be severe for concrete. When no seawater is supplied, the temperature of concrete surface heats up to 60 °C due to solar radiation in summer. When seawater is supplied, the concrete surface cools down to ~ 20 °C. The cycle is repeated day in and day out, following the actual wave and tidal actions, atmospheric temperature and solar radiation.

The Port and Airport Research Institute (PARI) in Japan has a large exposure site which can simulate actual marine environments, such as splashing zones, tidal zones, submerged zones and airborne salt zones. In a splashing zone, cracking on the surface of concrete specimens is frequently observed, irrespective of the specimen materials (Figure 5 (a) & (b)). Surface cracking is typically observed in summer. The backscattered electron image

presented in Figure 5 (c) shows that numerous micro-cracks have developed in the concrete. The concrete surface is subjected to wetting-drying cycles with large temperature variations induced by solar radiation so that a high degree of supersaturation might be generated in this process. The mechanism still remains under discussion and further research is necessary to clarify the matter.
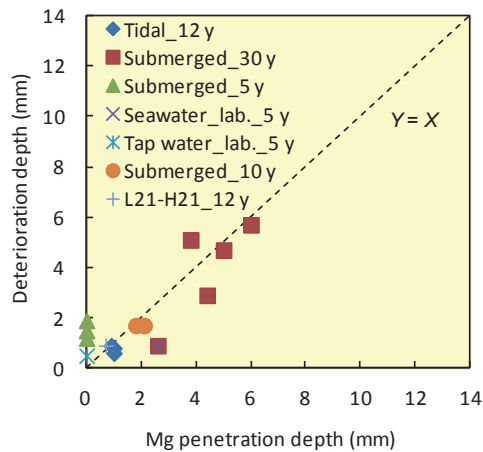
Figure 4 Mg penetration depth vs. deterioration depth estimated with Vickers hardness [12]

(a) Cracking at the angle   (b)Severe cracking   (c) Severe micro-cracking

Figure 5 Cracking of concrete subjected to wetting-drying cycles of seawater with large temperature variations

2.5 Hot spring

There are many hot springs in Japan so that the deterioration of concrete related to hot spring is also of concern. The deterioration has been observed in the situation that the pH of solution was below 3.0 [14]. Therefore majority of the cases of deterioration in hot spring area is thought to be attributed to acid attack although in some cases sulfate may have affected in some degree.

2.6 Other related deterioration

For delayed ettringite formation (DEF) in Japan, the first case was found in 2005 (Figure 6) [15]. While many cases of steam cured precast concrete block such as railway sleepers were experienced but not reported officially, the case of massive concrete structure is hardly reported.

Apart from ESA, the deterioration by $CaCl_2$ is serious issues in Japan. $CaCl_2$ is commonly used as deicing salt. Mori et al. investigated the deteriorated slabs served for more than 30 years (Figure 7) [16]. Concrete was granulated and heavily damaged. Through the investigation, $CaCl_2$ was thought to be involved in the granulation. The reaction of portlandite and $CaCl_2$ results in a formation of $3CaO \cdot CaCl_2 \cdot 15H_2O$ (3-1-15), leading to cracking and delamination of concrete from the surface.

Figure 6 Expansion of concrete block due to DEF [15]
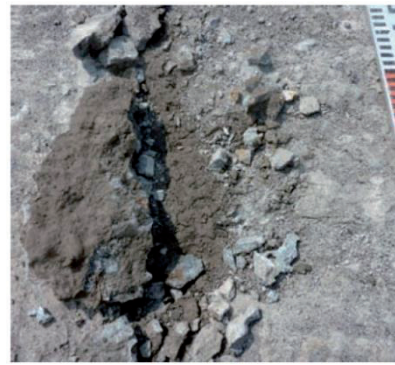
Figure 7 Granulation of concrete due to 3-1-15 formation [16]

3. GAP BETWEEN LABORATORY AND FIELD

One of the difficulties to bridge the gap is to identify the cause of the damage of concrete. In the laboratory, the climate conditions are simplified in general whereas the field concrete structures are subjected to complicated environmental actions and thus multiple deterioration mechanisms. Especially, wetting-drying process has a strong impact on the degree of supersaturation so that simple immersion test may lead to unexpected result against field performance. Regarding physical sulfate attack, partial immersion test successfully performed the laboratory test whose result is well consistent with field [1, 17]. The term ESA has various deterioration mechanisms. It is also difficult to distinguish how much each deterioration mechanism contributes to the damage. Especially, the small ettringite crystals responsible for expansion easily dissolve to reform larger crystals in cracks, voids and other available spaces. Alkali-silica reaction sometimes involves in the deterioration. These complicated situations make diagnosis on field concrete more difficult. Diagnosis on ASR & DEF also remains controversial (e.g., in Thailand [18, 19]). Therefore, appropriate diagnosis such as petrography is necessary with our deep understanding of the mechanisms.

As shown in Figure 1, although there is a potential risk widely in Japan because of sulfate-bearing ground distributed throughout Japan, the report of the real case has been limited. The climate conditions in Japan are compared to some cities in Europe and North America (Figure 8 [20]). Tokyo and Osaka has the higher temperature and more rainy days than other cities in summer. Significant difference between them can hardly be observed. There may be a missing link of climate conditions between laboratory and field. Further experiments focusing on the influence of climate conditions is necessary.

Relatively new deterioration due to chemical grouting or improvement by water glass-sulfuric acid materials for soil or tunnel is also of big concern. Some cases may have not been disclosed in public. The actual situation remains unclear so that more investigation should be carried out. In any case, special attention should be taken when concrete structures are

constructed in chemical-grouted soil. Laboratory tests are also necessary to make clear the mechanisms.

(a) Average temperature per month   (b) Average days with precipitation per month
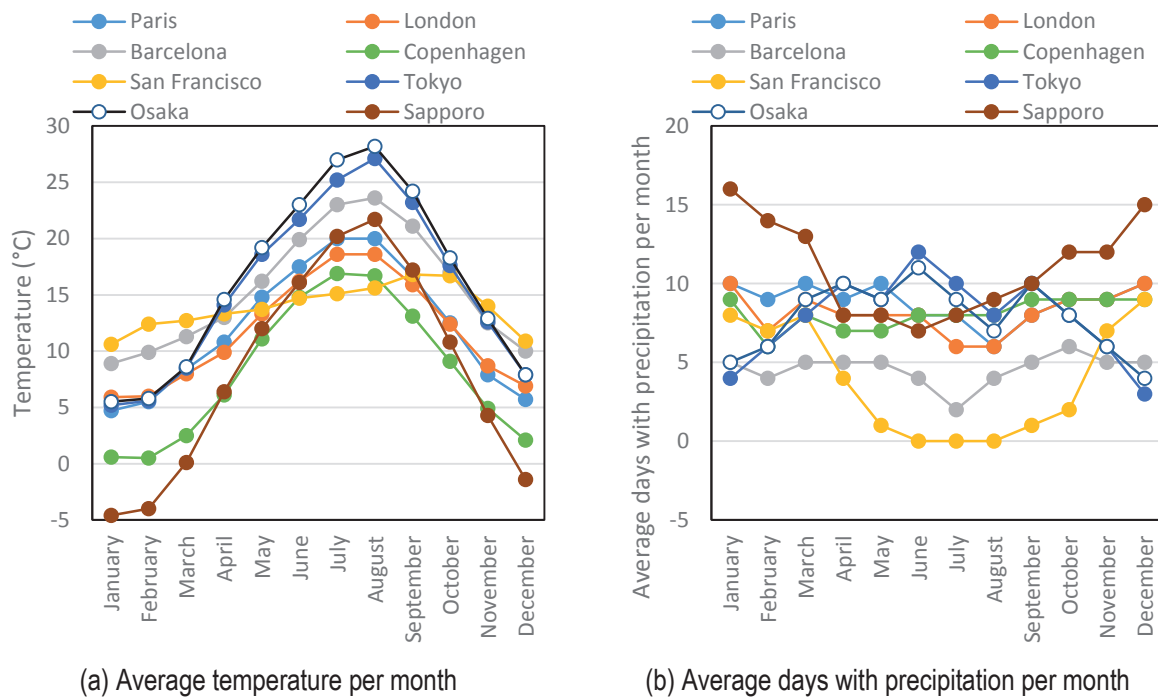
Figure 8 Climate conditions in 2015 [20]

4.   CONCLUSIONS

This paper presents a review on the real cases of ESA in Japan including some related issues. Physical sulfate attack is a main cause of ESA damage in Japan whereas some suspected cases have been reported. However, there may be a missing link of climate condition between laboratory and field so that further study is still necessary.

ACKNOWLEDGEMENT

REFERENCES

[1]   Yoshida, N., Sulfate attack on residential concrete foundations in Japan, Proceedings of Workshop on External Sulfate Attack, Lisbon (2016), (submitted to this conference)

[2]   Matsushita, H., Sagawa, Y. and Sato, T., Classification of probability of deterioration of concrete by suflate attack based on investigation results of sulfate content of ground, Doboku Gakkai Ronbunshuu E 66 (2010) 507-519 (in Japanese)

[3]   Japan Society of Civil Engineers, Concrete Engineering Series 103 (2014)

[4]   http://www.data.jma.go.jp/obd/stats/etrn/index.php (in Japanese)

[5]   Yoshida, N., Matsunami, Y., Nagayama, M. and Sakai, E., Salt weathering in redidential concrete foundations exposed to sulfate-bearing ground, Journal of Advanced Concrete Technology, 8 (2010) 121-134

[6]   Ueda, H., Nishio, S., Watanabe, Y. and Ichijo K., Deterioration of cement-based repair material damaged by thaumasite formation, Proceedings of the Japan Concrete Institute 30 (2008) 687-692 (in Japanese)

[7]   Ma, B., Gao, X., Byars, E. A. and Zhou, Q., Thaumasite formation in a tunnel of Bapanxia Dam in western China, Cem. Concr. Res.36 (2006) 716-722

[8]   Hosokawa, Y., Kitazawa, K., Nozaki, T. and Yamada, K., Possibility of the thaumasite sulfate attack in actual marine environment, Proceedings of the Japan Concrete Institute 33 (2011) 707-712 (in Japanese)

[9]   Nozaki, T., Ogawa, S., Hirao, H., Kono, K. and Yamada,K., A required condition of thaumasite formation in marine environments, 6th International Conference on Concrete under Severe Conditions, Environment and Loading, Merida, Yucatan, Mexico, 1 (2010) 85-90

[10]   Schmidt, T., Lothenbach, B., Romer, M., Scrivener, K., Rentsch, D. and Figi, R., A thermodynamic and experimental study of the conditions of thaumasite formation, Cem. Concr. Res.38 (2008) 337-349

[11]   Japan Society of Civil Engineers, Concrete Engineering Series 91 (2010)

[12]   Yamaji, T., Akira, Y., Hamada, H. and Yamada, K., Study on a deterioration and deterioration indicator of concrete under marine environments, Doboku Gakkai Ronbunshuu E 66 (2010) 21-37 (in Japanese)

[13]   Jakobsen, U. H., De Weerdt, K. and Geiker, M., Elemental zonation in marine concrete, Cem. Concr. Res.85 (2016) 12-27

[14]   Japan Society of Civil Engineers, Concrete Engineering Series 53 (2003)

[15]   Kawabata, Y. and Matsushita, H., A study on DEF-related expansion in heat-cured concrete, Journal of Japan Society of Civil Engineers, Ser. E2 67 (2011) 549-563 (in Japanese)

[16]   Mori, H., Kuga, R., Ogawa, S. and Kubo, Y., Estimating deterioration factors of RC slabs in cold regions, Concrete Research and Technology 24 (2013) 1-9 (in Japanese)

[17]   Scherer, G. W., Stress from crystallization of salt, Cem. Con. Res.34 (2004) 1613-1624

[18]   Hirono, S. et al., ASR found in Thailand and tropical regions of southeast Asia, Proceedings of 15th International Conference on Alkali-Aggregate Reaction in Concrete, 15ICAAR2016_123 (2016)

[19]   Jensen, V. and Sujjavanich, S., ASR and DEF in concrete foundations in Thailand, Proceedings of 15th International Conference on Alkali-Aggregate Reaction in Concrete, 15ICAAR2016_193 (2016)

[20]   https://www.yr.no

Sulfate attack in concrete: State of art in Brazil

R. Schmalz[1], F. G. S. Ferreira[2], A. L. Castro[3], J. P. Moretti[4], A. Sales[5]

ABSTRACT

Sulfate ions are among the main concrete deterioration agents. They chemically react with the cement hydration products ($Ca(OH)_2$ and CSH) causing expansion and cracking in the cement matrix. These damages in matrix facilitates the ions penetration and accelerates the degradation process. Fairly is known about the effects of this aggressive agent, however some issues still raise doubts and controversy. Among them, which is the most effective method to analyze the deleterious potential of these ions and which variables can interfere on the results. Therefore, the present paper presents the state of art of Brazilian researches about sulfate attack. Were analyzed and discussed the factors that can influence the degradation process, the laboratory tests results and, at last, the Brazilian standards that define the requirements for concrete exposed to sulfates.

Keywords: Concrete / Sulfate / State of art

1   INTRODUCTION

Nowadays, cases of premature deterioration of reinforced concrete structures are becoming frequent, including collapses in buildings before the end of its useful life. To reverse this reality, it should be given attention to a number of factors related to concrete and structure, including the concrete quality, taking into account not only the strength, but also its durability.

The durability question is related to the environment in which the structure is inserted. Among the existents aggressive agents are the sulfate ions, that chemically react with hydrated cement pastes, causing the concrete deterioration.

This kind of attack can occur both external, when ions are present in the environment and enter the structure with the water action, and internally, when aggressive agents are present in the concrete mixture. This paper presents and analyzes only the first one.

In recent years, some researches have been done in Brazil about the sulfate attack. However, some differences in their experimental programs limit comparisons between them, such as specimen's dimensions, mixtures proportions, time and curing type, exposure to attack methods and tests carried out to assess material durability.

Therefore, this paper presents the overview of the researches developed in Brazil and describes the factors that influence the sulfate attack, as well as the results of laboratory

[1]   Department of Civil Engineering, Federal University of São Carlos, Brazil; e-mail: rosanaschmalz@gmail.com

[2]   Department of Civil Engineering, Federal University of São Carlos, Brazil; e-mail: fgiannotti@ufscar.br

[3]   Department of Structure Engineering, University of São Paulo, Brazil; e-mail: alcastro@sc.usp.br

[4]   Department of Civil Engineering, Federal University of São Carlos, Brazil; e-mail: julianamoretti88@gmail.com

[5]   Department of Civil Engineering, Federal University of São Carlos, Brazil; e-mail: almir@ufscar.br

tests, with the presentation of Brazilian standards that define the requirements for concrete exposed to sulfates.

2   THE SULFATE ATTACK

Sulfates are present in seawater, groundwater, soil and industrial wastewater and usually manifest themselves in plain areas where the salts have accumulated over time without being carted by underground water flows [25].

According to Neville [18], the salts in solid state do not attack the concrete and the chemical reaction with hydrated cement paste only occurs when they are in solution form. The author also mentions that in soils and groundwater the sulfates of sodium, potassium, magnesium and calcium are more common.

The chemical reactions between the hydrated Portland cement and sulfate ions presents in the environment can cause expansion and cracking of the cement matrix, which increases the permeability and facilitates penetration of water inside it, accelerating the deterioration process. Another manifestation form of this type of attack is the progressive loss of strength and mass resulting from the loss of cohesion of cement hydration products [16].

The concrete that suffers the action of sulfates ions has a whitish appearance and damage begins in the edges and corners, leading to progressive cracking and spalling, culminating in a friable concrete, in other words, capable of being reduced to powder [18].

Costa [11] explains that the major means of sulfate attack to the concrete occur by the reaction with the hydration cement products, which are: hydrate calcium aluminate, calcium hydroxide (CH) and hydrates calcium silicate (CSH), which behavior and resulting substances are detailed in this paper.

3   FACTORS THAT INFLUENCE THE SULFATE ATTACK

3.1   Aggressive solution

The intensity and nature of the attack vary depending on the cation associated with SO_4^{-2} radical (Na^+, Ca^{+2}, Mg^{2+} etc.). Sulfates of calcium, sodium and magnesium are presented in this work due to their high aggressivity and abundance on the environment.

3.2   Calcium sulfate

Calcium sulfate ($CaSO_4$), present in most soils in hydrated form ($CaSO_4.H_2O$), also known as gypsum, is the least aggressive among three sulfates due to its low solubility. It reacts only with hydrated calcium aluminate, forming the ettringite (Equation 1).

$$3Ca0 . Al_2O_3 . 2H_2O + 3CaSO_4 . 2H_2O + 54H_2O \rightarrow 3CaO . Al_2O_3 . 3CaSO_4 . 32H_2O \qquad (1)$$
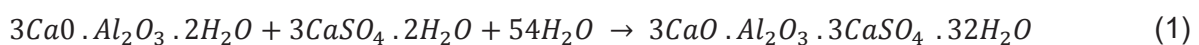
The ettringite formation characterizes an expansive reaction, once its size is 2.5 times greater than the tricalcium aluminate [25]. This expansion in the cementitious matrix

generates cracking and thus increases the concrete permeability, accelerating the degradation process.

3.3 Sodium sulfate

According to Costa [11], the sodium sulfate is about 20 times more soluble than calcium sulfate. When in high concentrations (> 8000 ppm), reacts with portlandite ($Ca(OH)_2$ or CH), forming gypsum and, due to the volume increase, causes expansion and cracking of the cement matrix (Equation 2). As reaction's byproduct, there is the sodium hydroxide that retains the high alkalinity of the system and ensures the stability of the main product of cement hydration, the hydrated calcium silicate (CSH), preventing its decomposition [16].

$$Ca(OH)_2 + Na_2SO_4 . 10H_2O \rightarrow CaSO_4 . 2H_2O + 2NaOH + 8H_2O \tag{2}$$

The authors also claim that there were observed cases where the deterioration of Portland cement paste occurs by gypsum formation, characterizing a process which first leads to reduction system pH, loss of stiffness and strength, followed by expansion and cracking, and finally, the transformation of concrete in a non-cohesive mass.

While at concentrations lower than 1000 ppm SO_4/l, sodium sulfate reacted with hydrated calcium aluminate forming the ettringite and also sodium hydroxide (Equation 3). The consequences to the concrete are the same: expansion and cracking.

$$2(3Ca0 . Al_2O_3 . 12H_2O) + 3(Na_2SO_4 . 10H_2O) \rightarrow \tag{3}$$
$$3CaO . Al_2O_3 . 3CaSO_4 . 32H_2O + 2Al(OH)_3 + 6NaOH + 17H_2O$$
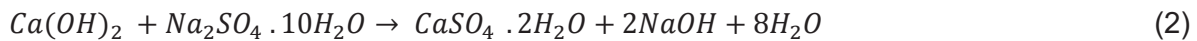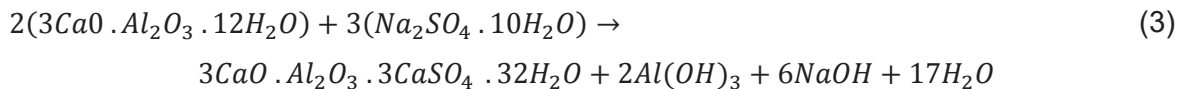
In this context, Souza [26] explains that during the hydration of Portland cement, there is the ettringite formation, originated from the reaction of gypsum (present in the cement as a setting time regulator) with aluminates, which is gradually converted into calcium monossulfoaluminate after all gypsum contained in the mixture is consumed. However, when the hardened cementitious material comes in contact with sulfates present in the environment, the balance is altered and this reaction tends to return to its initial state, forming ettringite.

3.4 Magnesium sulfate

Thirty-five times more soluble than calcium sulfate and considered the most aggressive to the concrete, magnesium sulfate causes a chemical reaction that involves both the SO_4^{-2} anion as Mg^{2+} cation. Both reacts with portlandite forming a surface layer composed of gypsum ($CaSO_4.H_2O$) and brucite ($Mg(OH)_2$) [26]. The reaction is described in Equation 4.

$$Ca(OH)_2 + MgSO_4 + 2H_2O \rightarrow CaSO_4 . 2H_2O + Mg(OH)_2 \tag{4}$$
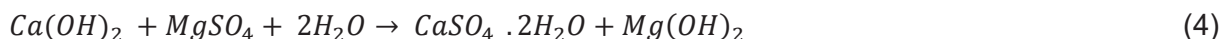
Santhanam [24] explains that the brucite formation process consumes a large amount of CH, causing the reduction of the solution pH contained in the pores. To maintain stability, the C-S-H releases CH in solution, raising again the pH and causing the C-S-H decalcification and, thus, loss of cementitious structure. With destabilization, C-S-H reacts with magnesium sulfate, resulting in gypsum, magnesium hydroxide and silica gel, as shown in Equation 5.

$$3Ca0 . 2SiO_2 . 3H_2O + 8H_2O + 3MgSO_4 \rightarrow \tag{5}$$

$$3(CaSO_4 . 2H_2O) + 3Mg(OH)_2 + 2SiO_2 . H_2O$$
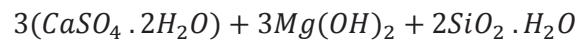
In advanced attack cases, the cation Ca^+ is completely replaced by Mg^{2+}, leading to the magnesium silicate hydrate formation (MSH), which is considered a non-cementitious material [6,7]

Thus, the magnesium sulfate attacks the concrete in the way of expansion and cracking due to the gypsum formation and also the loss of strength by dissolving the CSH. Neville [18] cites the possible occurrence of reaction between the magnesium hydroxide and silica gel, also harmful to concrete.

3.5 Cement type

The cement type used in the mixture can influence the sulfates attack, both in cases of natural attack and laboratory tests. According to Silva Filho [25], it should be limited the C_3A content, because although the expansive reaction of this component is not the only one to occur during aggressive process, it is still the most important factor in common Portland cement resistance to attack sulfates.

Mehta and Monteiro [16] explain that Portland cements with more than 5% C_3A, alumina predominate in the form of hydrated monosulfate ($C_3A.CS.H_{18}$) and above 8%, in the form of $C_3A.CH.H_{18}$. When the hydrated cement paste comes into contact with sulfate ions, due to the presence of calcium hydroxide, both hydrated containing alumina are converted into ettringite ($C_3A.3CS.H_{32}$), as shown in Equations 6 and 7 shown below.

$$C_3A.CH.H_{18} + 2CH + 3S + 11H \rightarrow C_3A.3CS.H_{32} \tag{6}$$

$$C_3A.CS.H_{18} + 2CH + 2S + 12H \rightarrow C_3A.3CS.H_{32} \tag{7}$$

3.6 Concrete permeability
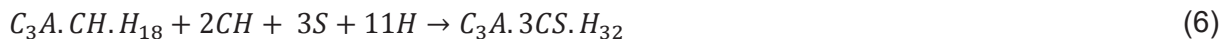
Permeability is the main influence factor on concrete durability, and can be defined as the ease with which fluid - either liquids or gases - can enter and move within it.

The presence of water is decisive in the deterioration cases, and it is known that the greater is the ease with which it penetrates into porous solids, the greater the structure degradation rate will be. As mentioned by Mehta and Monteiro [16], the water molecules are very small, facilitating its penetration into extremely fine pores.

Thus, there comes the importance of searching for concrete with low permeability, lower void ratio and disconnected pores, in order to avoid water flow within the structure, reducing the presence of aggressive ions, their movement and, hence, the degradation process of the concrete structure. Among the factors that influence the distribution system for the concrete pores are: water/cement ratio (w/c), curing, chemical additives and mineral additions [21].

3.7 Water/cement ratio (w/c)

Neville [18] explains that the cement paste permeability varies with the hydration evolution. When the paste is fresh, the water flow is controlled by the size, shape and concentration of the original cement particles. With the hydration progress, the gel fills the pores previously

filled with water and, because of their size approximately 2 times greater than the volume of cement anhydrous, it causes the paste permeability to decrease. Therefore, the smaller the w/c ratio, there will be less voids pores and lower will be material's permeability.

The author mentions that the permeability increases significantly in hydrated cement pastes which w/c ratios are higher than 0.40, as shown in Figure 1, bringing consequences to the material and to its durability, as the access of aggressive agents to their interior is facilitated.
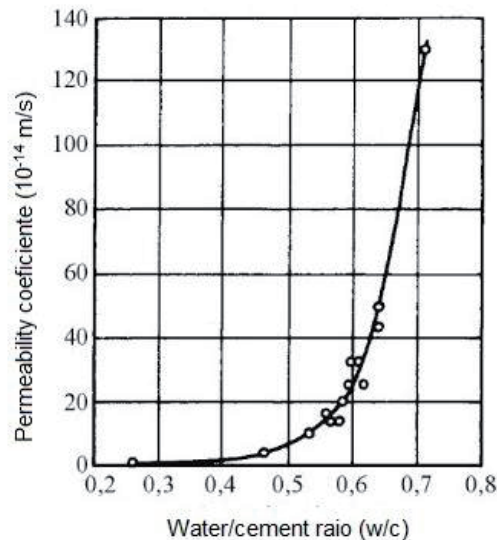
Figure 1: Relation between permeability and water/cement ratio to cement pastes
(Adapted from Neville [18]).

A low w/c ratio is also cited by the American Concrete Institute [4] as one of the main requirements for the concrete sulfate attack resistance, and the limit values are 0.45 and 0.50, ranging according to the aggressiveness class of the environment. The same values are set by the Brazilian Standard (NBR 12655:2015) [2], being 0.45 for severe conditions of exposure and 0.50 for moderate, as can be seen in Table 1.

3.7 Curing

Mehta and Monteiro [16] claim that a proper curing process is essential to reduce the void volume of the cementitious matrix, which in turn, reduces its permeability. The low permeability implies a more durable concrete face to aggressive agents, including sulfates.

The main objective of the curing is to maintain the concrete saturated, or nearly so, until the spaces originally filled with water in the fresh state are filled by the cement hydration products [18]. Thus, it avoids cracking due to retraction, a factor which also leads to an increase in the concrete permeability.

3.8 Additives and mineral additions

The additives and additions use is favorable when it is desired to obtain a concrete with low permeability and greater durability, due to its ability to refine the concrete microstructure.

Plasticizers and superplasticizers additives, also known as water reducers, act on the concrete decreasing the surface tension of the surrounding water to cement particles, increasing the flowability of the mixture [16]. Then, it becomes possible to fix a lower w/c ratio and, as previously mentioned, the lower the w/c ratio, the lower will be the material permeability.

Regarding the benefits of using mineral admixtures in concrete, the authors mention the better resistance to thermal cracking due to the low hydration heat, the pores refinement and the transition zone strengthening, which implies in a greater durability against sulfate attack.

The Conen and Bentur [10] research concluded that when a mineral addition, as the silica fume, is used in the mixtures, there is a pozzolanic reaction that consumes the present CH and in the magnesium sulfate attack case, the reaction reaches quickly descaling CSH phase. However, the permeability reduction and pore refinement overlaps this negative effect, which leads to the importance of an optimal dosing to maximize benefits and minimize the deleterious effects.

3.9 pH

About the pH, Souza [26] claims that the aggressive solution influences the degradation process due to the ettringite stability in pH between 10.5 and 13. Some researchers analyzed how this influence works and the results indicated that a reduction in solution pH also reduces the resistance to sulfate attack, increasing the concrete expansion [8,12].

3.10 Temperature

Besides the pH level, temperature also influences the ettringite stability, which at temperatures above 65 °C, decomposes and forms hydrate monosulfate. This reaction releases sulfate ions which are adsorbed by CSH, then forming the secondary ettringite, which is responsible for the expansion and cracking of concrete [16].

3.11 Specimens geometry

The specimens geometry and how it influences the sulfate attack was studied by Ferraris *et al.* [12]. The authors concluded that the smaller is the specimen, more accelerated will be the attack, and the type of cracking varies according to the geometry, so that in cylindrical and prismatic specimens, due to the existence of sharp edges, there is a superficial cracking followed by spalling. Regarding the spherical specimens, for not having sharp edges, superficial cracking does not result in spalling.

4   BRAZILIAN STANDARDS

In Brazil, there are two rules that approach the question of durability of concrete structure, the NBR 6118:2014 [1] and NBR 12655:2015 [2]. The first establishes the procedures for the concrete structures project, where the environmental aggression is classified taking into account the type of environment in which the structure is inserted, as shown in Table 1. While in respect to the structures durability, the standard limits values for the w/c ratio and for concrete strength class according to the aggressiveness class, as well as the concrete cover values for the concrete structure elements.

Table 1: Environmental aggression classes and projects parameters for the reinforced concrete

Projects parameters	Environmental aggressiveness classes			
	I	II	III	IV
Aggressiveness	Low	Moderate	Severe	Very Severe
Classification	Rural/ Submerged	Urban	Marine/ Industrial	Industrial/ Tidal Splash
w/c ratio	≤ 0.65	≤ 0.60	≤ 0.55	≤ 0.50
Concrete class	≥ 20 MPa	≥ 25 MPa	≥ 30 MPa	≥ 40 MPa
Coverings - beam and column (mm)	25	30	40	50
Coverings - slab (mm)	20	25	35	45

(Source: Adapted from NBR 6118: 2014 [1])

The NBR 12655: 2015 [2] has a more specific approach and establishes the requirements for exposed concrete solutions containing sulfates, limiting the w/c ratio and determining a minimum characteristic compressive strength of concrete (CS) for each exposure condition, which is classified according to the concentration of sulfates present in the solution, as shown in Table 2.

Table 2: Requirements for concrete exposed to solutions containing sulfates

Class of exposure	Water-soluble sulfate (SO_4) in the soil (percent by weight)	Soluble Sulfate (SO4) present in water (ppm)	Maximum w/c ratio	Minimum CS (MPa)
Low	0.00 a 0.10	0 a 150	*	*
Moderate	0.10 a 0.20	150 a 1500	0.50	35
Severe	Over 0.20	Over 1500	0.45	40

* For low conditions of exposure to sulfates, use Table 1 of NBR 12655: 2015, considering only the environmental aggressiveness class.

(Source: Adapted from NBR 12655:2015 [2])

However, Neville [19] shows that not only environmental characteristics and aggressive solution concentrations influence the deterioration, but also the concrete quality.

Regarding the evaluation of the sulfate attack, NBR 13583:2014 [3] describes tests for the determination of dimensional change from Portland cement mortar bars exposed to sodium sulfate solution. The standard establishes a mixture proportion of 1: 3.2 and a w/c ratio of 0.60 for molding specimens, which must undergo an initial period of air-curing for 48 hours,

followed by an intermediate curing in water saturated with lime for 12 hours, and finally immersed in an aggressive solution of sodium sulfate for 42 days. Length's measurements of the bars should be carried out at the 14, 28 and 42 days of immersion, and should also be subjected to visual examination to identify cracks and disaggregation.

As it can be noted, some recent studies have their methodologies based on NBR 13583:2014 [3] guidelines in regard to the means of exposure to aggressive solution and the durability evaluation test by dimensional variation. However, there are still large variations between researches since the 90's to nowadays, which, as mentioned above, hinders the comparative analysis between them.

5   STATE OF ART OF BRAZILIAN RESEARCHES

Brazilian researches about sulfate attack to concrete present a wide variation in mixture proportions parameters, curing conditions and exposure to aggressive agent, as well as the tests realized to analyze the attack consequences.

Tables 3 and 4 bring a review of Brazilian researches, showing these variations between them. The first table presents the variables related to dosage, curing methods and material characterization tests before sulfate attack exposing. Table 4 shows the variations in types of attack and tests performed to evaluate the cementitious composite durability.

Table 5 shows the nomenclatures used in Tables 3 and 4.

Table 3: State of art of Brazilian researches: strength, curing and characterization tests.

| Reference | Dosage | | | Curing | | Characterization tests | | |
	Cement	a/c	Additive / Addition	Type	Time	Test	Ages	Specimen (mm)
Silva Filho (1994)	CP I e CP IV	0.28. 0.43 0.67	SF: 0, 5 e 10%	Moist	28 days	CS WA, VR, PWP	28 days 21, 28 e 63 days	ø100x200 150x150x120
Moura (2000)	CP I-S	0.40. 0.50 0.60	Copper slag 0 e 20%	Moist	28 days		Unrealized	
Gomides (2001)	CP II-F-32	RCC	SF: 0 e 10%	Moist	70 days	CS, TDC. Tração Simples WPUP, WA	7, 28, 63, 70, 91, 154 e 200 days 7, 28 e 63 days 63 days	ø150x300
Centurione e *et al.* (2003)	CP IV-32 CP II-Z-32 CP II-F-32	0.60	-	In air + Immersion	48 h + 12 days		Unrealized	
Costa (2004)	CP II-E-32 CP III-32-RS CP IV-32	0.67 0.42	-	In air + Immersion	24 h + 12 days		Unrealized	
Souza (2006)	Classe G CP II-Z-32	N.I.	-	Immersion at 65°C	28 days		Unrealized	
Linhares (2010)	CP II-E CP II-F	0.35. 0.48 0.70	SF: 5 e 10% Metakaolin: 5 e 10%	Immersion	28 days	CS	1, 3, 7 e 28 days	50x50x50
Alves *et al.* (2010)	CP V-ARI	0.40. 0.50 0.60	-	Moist + In air	1 + 7 days 46 days		Unrealized	
Kulisch (2011)	CP II-F	0.60	-	In air + Immersion	48 h + 12 days		Unrealized	
Rheinheimer e Khoe (2013)	CP IV, CP III CP V-ARI-RS, CP II-Z	0.60	-	In air + Immersion	48 h + 12 days		Unrealized	
Cesário e Vale Silva (2014)	CP V	0.65	Additive SP: 0,7%	Unrealized			Unrealized	
Hoppe Filho *et al.* (2015)	CP V-ARI	0.60	Filler, RHS, SF, metakaolin and ceramic waste	In air + Immersion	48 h + 12 days		Unrealized	
Pereira (2015)	CP II-F-32	0.40	Pyrite:0, 1, 5 e 10% Contaminated aggregate (pyrite): 1 e 3%	In air + Immersion	48 h + 12 days		Unrealized	

Table 4: State of art of Brazilian researches: type of attack and test to evaluated sulfate attack effects.

Reference	Attack				Material	Tests to evaluated sulfate attack		
	Type	Solution	Concentration	Time		Test	Age	Specimen (mm)
Silva Filho (1994)	Immersion	Na_2SO_4	5%	120 days	Concrete	CS, FS, Visual Evaluation	120 days	ø100x200 e 40x40x160
					Mortar	FS Linear Expansion	21, 42, 77 e 120 days 21, 35, 42, 56, 77 e 120 days	10x10x60
Moura (2000)	Immersion	Na_2SO_4	5%	450 days	Concrete	WA, Visual Evaluation Chemical Resistance (R)	90 a 450 days - monthly 450 days	40x40x160
Gomides (2001)	Immersion	Na_2SO_4	5%	130 days	Concrete	CS Linear Expansion SEM, XRD	21, 84 e 130 days 7 a 130 days – weekly 30 days	ø150x300 150x150x600 ø150x300
Centurione et al. (2003)	Immersion	Na_2SO_4	10%	42 days (40±2) °C	Mortar	Dimensional Change	7, 14, 21, 28, 35 e 42 days	25x25x285
Costa (2004)	1 day of immersion and 3 days oy drying	$MgSO_4$	10g/l e 50g/l	180 days	Mortar	Ultrasound, EM, CS, MIP, Chemical Analysis, SEM	28, 90 e 180 days	ø100x200
Souza (2006)	Immersed cure at 65°C	Na_2SO_4 $MgSO_4$	2810ppm (MgNa$_2$) 54424ppm (Mg) 45426ppm (Na$_2$)	28 days	Paste	XRD, TG Specific gravity Chemical Analysis	3, 7 e 28 days	50x50x50
Linhares (2010)	Immersion	Na_2SO_4	5%	105 days	Mortar	Dimensional Change	7, 14, 21, 28, 56, 91 e 105 days	25x25x285
Alves et al. (2010)	3 days of immersion and 4 days of drying	NaCL NaCl+H$_2$SO$_4$ NaCl+H$_2$SO$_4$	1M 1M+0,4% 1M+2%	7 days	Concrete	CS WA, VR	56, 140 e 280 days 72 h	ø100x200
Kulisch (2011)	Immersion	Na_2SO_4	10%	36 days (40±2) °C	Mortar	Dimensional Change	14, 28 e 36 days	25x25x285
Rheinheimer e Khoe (2013)	Immersion	Na_2SO_4	10%	42 days (40±2) °C	Mortar	Dimensional Change, SEM, CS	14, 28 e 42 days	25x25x285
Cesário e Silva (2014)	Exposure: Water, MgSO$_4$, Na$_2$SO$_4$ e FeSO$_4$			182 days	Concrete	CS, SEM, XRD, pH	7, 28, 84, 139 e 182 days 182 days	ø100x200
Hoppe Filho et al. (2015)	Immersion	Na_2SO_4	10%	42 days (40±2) °C	Mortar	Dimensional Change	14, 28 e 42 days	25x25x285
Pereira (2015)	Immersion	Na_2SO_4	10%	42 days (40±2) °C	Mortar	Dimensional Change	7, 14, 21, 28, 35 e 42 days	25x25x285

Table 5: Nomenclatures used in Tables 3 and 4

Nomenclatures			
NI	Not Informed	**TDC**	Traction by diametral compression
RCC	Roled Compacted Concrete	**WPUP**	Water Permeability Under Pressure
SF	Silica Fume	**FS**	Flexural Strenght
SP	Superplasticizer	**SEM**	Scanning Electron Microscopy
RHS	Rice Husk Silica	**XRD**	X-ray Diffraction
CS	Compressive strenght	E_d	Elasticity dynamic modulus
WA	Water Absorption	**MIP**	Mercury Intrusion Porosimetry
VR	Void Ratio	**TG:**	Thermogravimetry
PWP	Pressurized water penetration	**pH**	Potential of Hydrogen

It is noticed that researches differ in the dosage variables, specimen's dimensions, characterization tests, types of aggressive attack and test to evaluated sulfate attack effects. This great variability influences the results and raises difficulties in the comparisons among them.

7   CONCLUSION

It can be concluded that there are several factors that influence the sulfate attack in cementitious matrices, among them: the aggressive solution, its concentration and the cation associated; cement type; concrete permeability, influenced by the water/cement ratio, curing and additive or addiction use; pH of aggressive solution; concrete temperature and the specimens' geometry.

The state of the art of Brazilian researches shows that there is no standard for the researches experimental program, and variations between them range from the mixture proportions until the test for evaluation the attack.

With regard to the evaluation tests of sulfate attack, the NBR 13583:2015 [3] defines an evaluation procedure only based on the dimensional variation of the mortar, with no other tests that measure degradation, such as mechanical strength, microstructural and chemical analysis, as performed by some authors.

This lack of standardization for evaluation the attack by sulfates ions to concrete composites clearly influences the variability of researches and makes comparing among them difficult.

REFERENCES

[1]   ASSOCIAÇÃO BRASILEIRA DE NORMAS TÉCNICAS. NBR. 6118: Projeto de estruturas de concreto armado. Rio de Janeiro, 2014.

[2]   _____. NBR12655: Concreto de cimento Portland – Preparo, Controle, recebimento e aceitação - Procedimento. Rio de Janeiro, 2015.

[3]   _____. NBR 13583: Cimento Portland – Determinação da variação dimensional de barras de argamassa de cimento Portland expostas à solução de sulfato de sódio. Rio de Janeiro. 2014.

[4]   AMERICAN CONCRETE INSTITUTE. INTERNATIONAL ORGANIZATION FOR STANDARDIZATION. Guide to the selection and use of hydraulic cements. (ACI 225R-99).

[5]   ALVES, H. G.; NERI, K. D.; VILAR, E. O. Estudo Mecânico de concretos atacados por cloretos e sulfatos. In: I Encontro Nacional de Educação, ciência e tecnologia; UEPB, Campina Grande, 2012.

[6]   BONEM, D.; COHEN, M. D. Magnesium sulfate attack on Portland cement-paste – I. Microstructural analysis. Cement and concrete research, v. 22, p. 169-180. 1992.

[7]   BONEM, D.; COHEN, M. D. Magnesium sulfate attack on Portland cement-paste – II. Chemical and mineralogical analyses. Cement and concrete research, v. 22, p. 707-718. 1992

[8]   BROWN, P. W. An evaluation of the sulfate resistance of cements in a controlled environment. Cement and Concrete Research, v. 11, p. 719-727, 1981.

[9]   CENTURIONE, S. L.; BATTAGIN, A. F.; KIHARA, Y. Durabilidade de concreto submetido a ataques de ions sulfato. In: XLVII Congresso Brasileiro de Cerâmica, João Pessoa, 2003.

[10]   COHEN, Menashi D.; BENTUR, Arnon. Durability of portland cement-silica fume pastes in magnesium and sodium sulfate solutions. Materials Journal, v. 85, p. 148-157, 1988.

[11]   COSTA, R. M. Análise de propriedades mecânicas do concreto deteriorado pela ação de sulfato mediante utilização do UPV. Tese (Doutorado). Universidade Federal de Minas Gerais, 2004.

[12]   FERRARIS, C. F.; CLIFTON, J. R.; STUTZMAN, GARBOCZI, E. J. Mechanisms of degradation of Portland cement-based systems by sulfate attack.

[13]   GOMIDES, M. J. Ataque por sulfatos ao concreto compactado com rolo. Dissertação (Mestrado). Universidade Federal de Goiás, 2001.

[14]   KULISCH, D. Ataque por sulfatos em estruturas de concreto. Trabalho de Conclusão de Curso. Universidade Federal do Paraná, 2011.

[15]   LINHARES, B. T. Avaliação do desempenho de cimentos CPII E e CPIII F com diferentes teores de pozolana frente ao ataque de íons sulfato. Trabalho de Conclusão de Curso. Universidade Federal do Rio Grande do Sul, 2010.

[16]   MEHTA, P. K.; MONTEIRO, P. J. M. Concreto: microestrutura, propriedades e materiais. São Paulo: IBRACON, 2014.

[17]   MOURA, W. A. Utilização de Escória de Cobre como adição e como agregado miúdo par concreto. Tese (Doutorado). Universidade Federal do Rio Grande do Sul, 2000.

[18]   NEVILLE, A. M. Propriedades do Concreto. Bookman Editora, 2015.

[19] NEVILLE, A. M. The confused world of sulfate attack on concrete. Cement and concrete research, v. 34, p. 1275-1296, 2004.

[20] HOPPE FILHO, J.; SOUZA, D. J.; MEDEIROS, M. H. F.; PEREIRA, E.; PORTELLA, K.F. Ataque de matrizes cimentícias por sulfatos de sódio: adições minerais como agentes mitigadores. Cerâmica. v. 61, p. 168-177, 2015.

[21] PAULON, V., KIRCHHEIM, A. P. Nanoestrutura e Microestrutura do Concreto Endurecido. Concreto: Ciência e Tecnologia. v. 1, cap. 16, p. 585-614. São Paulo: IBRACON, 2011.

[22] PEREIRA, E. Investigação e monitoramento do ataque por sulfatos de origem interna em concretos nas primeiras idades. Tese (Doutorado). Universidade Federal do Paraná, 2015.

[23] RHEINHEIMER, B.; KHOE, S. S. Ataque por sulfatos em estações de tratamento de efluentes. Trabalho de Conclusão de Curso. Universidade Federal do Paraná, 2013.

[24] SANTHANAM, M.; COHEN, M. D.; OLEK, J. Sulfate attack research - Whither now?. Cement and Concrete Research, v. 31, p. 845–851. (2001).

[25] SILVA FILHO, L. C. P. Durabilidade do concreto à ação de sulfatos: análise do efeito da permeação de água e da adição de microssílica. Dissertação (Mestrado). Universidade Federal do Rio Grande do Sul, 1994.

[26] SOUZA, R. B. Suscetibilidade de pastas de cimento ao ataque por sulfatos – método de ensaio acelerado. Dissertação (Mestrado). Universidade de São Paulo, 2006.

[27] CESÁRIO, A. P.; SILVA, B. V. Análise do desempenho do concreto utilizado em fundações submetido a ataque por sulfato. Trabalho de Conclusão de Curso. Universidade do Extremo Sul Catarinense, 2014.

Sulfate resistance in blended cements with fired clay-based additions

E. Asensio[1][1*], C. Medina**[2]**, I.F. Saéz[2], B. Cantero[2], M. Frías[1], M.I. Sánchez de Rojas[1]

ABSTRACT

Binders should be judged not only in terms of their ability to develop hydraulic properties, but also of their interaction with potentially aggressive agents, which may affect their characteristics and performance during service life.

This study analysed the effect of different types of fired clay-based industrial by-product or waste additions on cement sulfate resistance. The additions were characterised both physically and chemically. Blended cement pastes were prepared and, using the Köch-Steinegger method, the durability of the new materials was assessed on the grounds of their corrosion index. New hydration products that might induce specimen mineralogical and morphological decay were also studied by comparing the pastes before and after soaking in a sodium sulfate solution for different test periods. With a few exceptions, the findings showed that including such waste as alternative pozzolans improved cement paste durability.

1.   INTRODUCTION

Binders should be judged not only in terms of their ability to develop hydraulic properties, but also of their interaction with potentially aggressive agents, which may affect their characteristics and performance. All other things being equal, concrete durability varies with the physical and especially the chemical features of the binder used. Consequently, when new cements are designed with non-traditional additions such as waste, their resistance to the environment (aggressive substances and media) to which they will be exposed must be determined, given the direct effect of that property on the service life of concretes and mortars.

Sulfate attack is characterised by the formation of products such as gypsum ($Ca_2SO_4.2H_2O$), ettringite ($3CaO.Al_2O_3.3CaSO_4.32H_2O$), thaumasite ($Ca_3Si(SO_4).(CO_3).(OH)_6.12H_2O$) or combinations of these minerals. Attendant upon the formation of these products is the appearance of ever greater stress that induces the decay and destruction of cementitious matrices.

Fired clay-based materials constitute one type of waste that can be used as an active cement addition. As a rule, initially inert clay minerals exhibit significant pozzolanicity when calcined at temperatures of 500 ºC to 900 ºC and ground to the same fineness as cement [1]. The loss of chemically combined water during calcination destroys the crystalline network of the clay constituents, rendering their components amorphous or vitreous. Such thermodynamic instability is largely responsible for the pozzolanicity of these calcined materials [2].

---

[1]   Eduardo Torroja Institute for Construction Sciences (IETcc – CSIC). 28033 Madrid, Spain

[2]   School of Engineering, UEX – CSIC Partnering Unit, University of Extremadura. 10003, Caceres, Spain

Phyllosilicate research has focused primarily on kaolinite, which undergoes hydroxylation when heated to 450 °C-600 °C. The resulting disorderly phase, known as metakaolin or metakaolinite [3, 4], may also be obtained from other sources, such as thermally activated paper sludge [5, 6].

Other types of fired clay-based materials require no thermal activation, for they are sourced from waste generated during high-temperature manufacturing. Rubble from roof tile and brick manufacture [7, 8] and fired clay-based construction and demolition waste [9, 10] contain such materials.

This study analyses the effect of fired clay-based waste and paper sludge on blended cement resistance to sulfate attack. The additions studied were characterised chemically and mineralogically, after which blended cement pastes were prepared with replacement ratios of 20 %. These materials were then tested and compared to the reference cement further to the Köch-Steinegger method [11], which assesses cements on the grounds of their sulfate corrosion index.

Lastly, mineralogical and morphological studies were conducted to identify expansive phases that may induce severe decay in new blended cement matrices soaked in a sodium sulfate solution.

2.   MATERIALS, METHODS AND TECHNIQUES

2.1. Materials

The following materials were used in this study:

- Ordinary Portland cement (OPC): European standard 197-1 [12] CEM I/42.5 N cement (i.e., clinker content greater than or equal to 95 % and up to 5 % of additional components) was the reference OPC used. The chemical composition and BET specific surface are given in Table I.

- Fired clay-based waste (CW): sourced from fired clay roof tiles, this waste was crushed and ground to a particles size of under 63 μm.

- Construction and demolition waste (C&DW) consisted entirely of fired clay-based material (roofing tiles, bricks…) from a Spanish recycling plant, crushed and ground to a particle size of under 63 μm.

- Activated paper sludge (TAPS): this material was prepared by thermally activating paper mill sludge at a temperature of 650 °C for 2 hours in an electric kiln to obtain recycled metakaolinite with a particle size of under 63 μm.

2.2. Methods

The reference and experimental pastes were prepared with deionised water at a water-to-cement ratio of 0.5. After mixing, they were moulded into 1x1x6 cm prismatic specimens and vibration-compacted. After 1 day at 100 % relative humidity, the specimens were removed from the moulds and cured in deionised water at 20±1 ºC for 21 days. Groups of six specimens were subsequently immersed and suspended in an aggressive solution (0.5 M Na_2SO_4) or deionised water as a reference solution, at 20 ºC for 0, 14 and 56 days.

The sulfate resistance of the new cements was determined from compressive strength tests conducted on the 0, 14 and 56 day specimens. The findings were used to calculate the corrosion index (I_c) and chemical resistance (I_{rq}).

The corrosion index (I_c), which assesses reference cement (OPC) or blended cement (cement + addition) performance in the chosen aggressive medium, is found from the following equation (1):

$$Ic\ (OPC)\ and\ (80wt\%\ OPC + 20wt\%\ waste)\ = \frac{[Rc\ sodium\ sulfate]t}{[Rc\ water]t} \quad (1)$$

where: a) [Rc sodium sulfate] is the compressive strength of the reference cement (OPC) or the blended material (cement + addition) after exposure to the aggressive agent (0.5-M Na_2SO_4) during the test time defined; and b) [Rc water] is the compressive strength of the reference cement (OPC) or the blended material (cement + addition) cured in deionised water for the same period of time.

Chemical resistance (I_{rq}) reveals whether the addition raises ($I_{rq} > 1$) or lowers ($I_{rq} < 1$) performance in the aggressive medium studied. This index is found from the following formula (2):

$$Irq\ (NaSO4)\ = \frac{[Rc\ (80wt\%\ OPC\ +\ 20wt\%\ addition)]t}{[Rc\ OPC]t} \quad (2)$$

where: a) [Rc (80wt% OPC + 20wt% addition)]$_t$ is the compressive strength of the blends (cement + addition) exposed to the aggressive agent for the test time; and b) [Rc OPC]$_t$ is the compressive strength of the reference cement (OPC) exposed to the aggressive agent for the test time.

2.3. Techniques

The pastes were chemically characterised on an S8 Tiger Bruker X-ray fluorescence (XRF) spectrometer fitted with a 4-kW rhodium anticathode tube.

Their mineralogical composition was analysed on a BRUKER AXS D8 GmbH X-ray powder diffractor fitted with a 3-kW (Cu Kα1.2) copper anode and a wolfram cathode X-ray generator. Scans were taken at 2θ angles ranging from 5 to 60° at a rate of 2°/minute. The standard operating conditions for the voltage generator tube were 40 kV and 30 mA.

The morphological changes in cement hydrates due to aggressive attack were studied with a Hitachi S-4800 scanning electron microscope (SEM) fitted with a Bruker EDX energy dispersive X-ray (EDX) analyzer. This procedure furnishes semi-quantitative information on the elemental composition of pastes at the point inspected.

Compressive strength was determined on an IBERTEST AUTOTEST 200/10-SW test frame fitted with an adapter for 1x1x6-cm specimens.

3.   RESULTS AND DISCUSSION

3.1.   Characterisation of materials

Table 1 gives the chemical composition of the ordinary portland cement (OPC) and the waste used in this study (CW, TAPS and C&DW). Note that the fired clay-based waste (CW and C&DW) had high SiO_2 contents (67.03 % and 59.63 %, respectively) and low loss on ignition (0.47 % and 2.15 %, respectively). In contrast, the thermally activated paper sludge exhibited substantially higher loss on ignition (23.36 %) and was CaO-high (38.81 %) and SiO_2-low.

Table 1. Chemical composition (wt%)

Chemical constituent (wt%)	Materials			
	OPC	CW	C&DW	TAPS
SiO_2	19.60	67.03	59.63	21.06
Al_2O_3	4.41	19.95	18.51	13.58
Fe_2O_3	3.30	6.29	5.92	0,54
CaO	63.21	0.11	4.72	37.81
MgO	4.20	1.37	3.12	2.24
Na_2O	0.30	0.21	0.73	0.09
K_2O	0.50	3.54	3.59	0.35
TiO_2	0.15	0.28	0.84	0.25
SO_3	3.00	0,39	0.42	0.29
LOI *(a)*	1.40	0.47	2.15	23.36
Total	99.76	99,64	99.63	99,57

(a) LOI: Loss on ignition

Figures 1-3 show the compounds present in the crystalline structure of the waste studied. The main crystalline compounds in the fired clay rubble included quartz (Q), muscovite (Mu), microcline (M), and hematite (H) (Figure 1). The construction and demolition waste (C&DW), in turn, contained primarily illite (I), quartz (Q), orthoclase (O), anorthite (A), calcite (C), dolomite (D) and hematite (H) (Figure 2). Lastly, calcite (C) and talc (T) were the main crystalline compounds in calcined paper sludge (TAPS) (Figure 3).
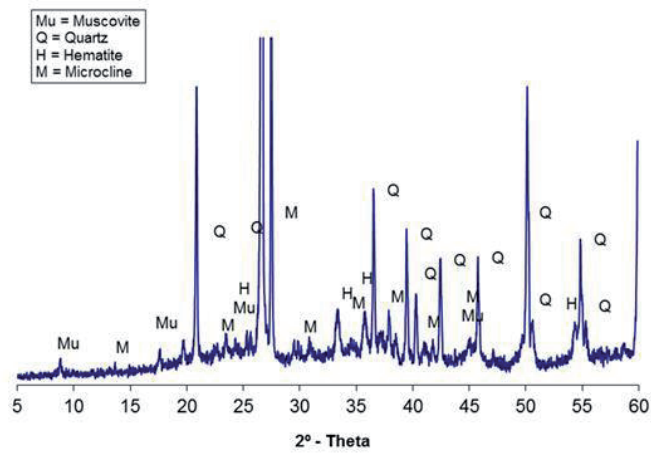
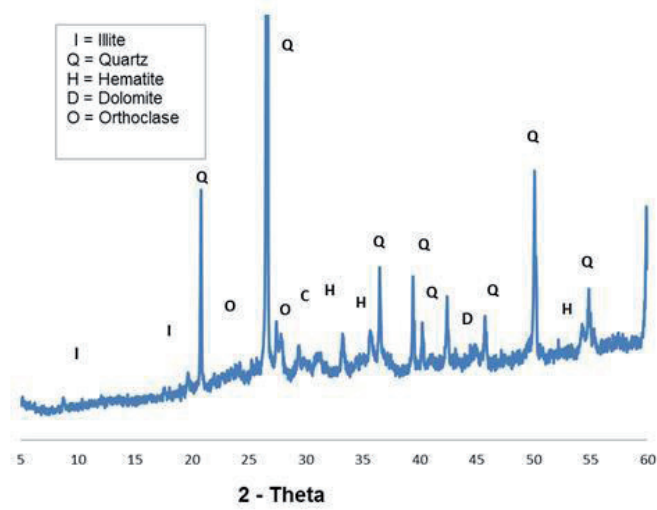Figure 1: XRD pattern for fired clay -based waste (CW)

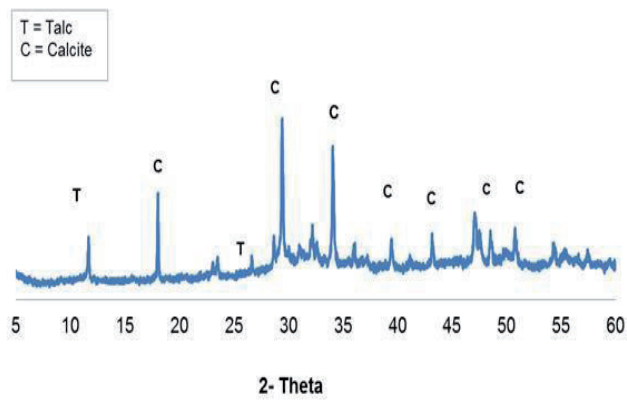Figure 2: XRD pattern for construction and demolition waste (C&DW)

Figure 3: XRD pattern for thermally activated paper sludge (TAPS)

3.2. Sulfate resistance

The corrosion index and chemical resistance values for the blends analysed are found in Table 2 and Figures 4-5.

Table 2. Corrosion index and chemical resistance

Paste	I_c				I_{rq}			
	0 days	14 days	56 days	90 days	0 days	14 days	56 days	90 days
OPC	1	1.20	0,88	0,65	1	1	1	1
CW-OPC	1	1.09	0,94	1,26	0.90	1.04	1.19	1.30
C&DW-OPC	1	0.93	0.98	0,82	0.66	0.86	1.13	1.25
TAPS-OPC	1	1.02	0.7	*	1	1.03	0.8	*

* broken specimens

Further to Table II and Figure 4, the 56 day and 90 days corrosion index (I_c) for the cements bearing fired clay-based waste was close to one, an indication that the inclusion of these additions had no adverse effect on durability. The pastes with 20 % paper sludge (APS), in contrast, exhibited a lower value.

The fired clay-based blended cements (CW and C&DW) exhibited chemical resistance values (I_{rq}) of over one only after 14 days and 56 days respectively, because pozzolanicity is not high at early ages in these additions. The pattern observed in TAPS was the opposite, with sulfate resistance declining over time.
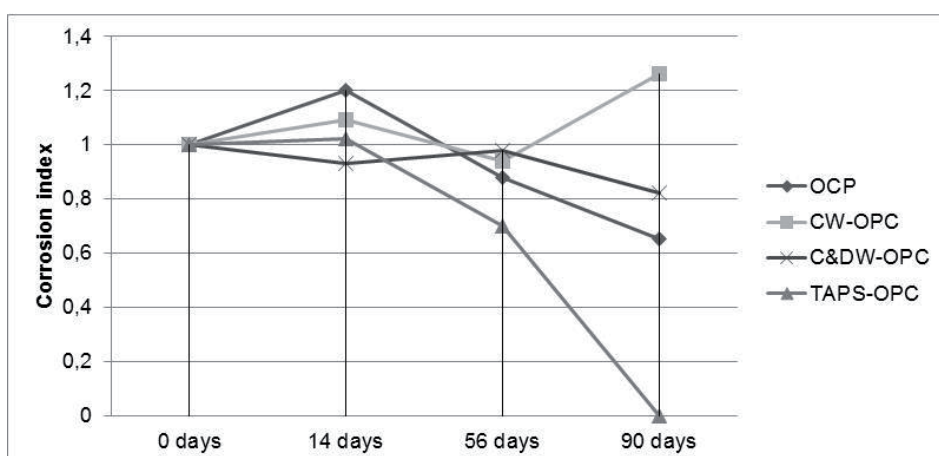

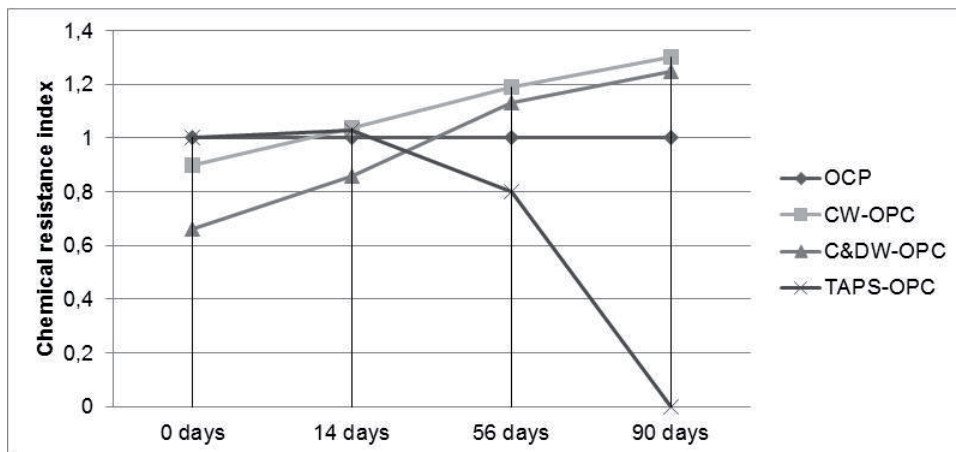Figure 4: Corrosion indices for 0, 14, 56 and 90 day pastes

Figure 5: Chemical resistance in 0, 14, 56 and 90 day pastes

3.3. Sulfate-induced reaction products

The mechanism governing sulfate attack may be broken down into five steps: a) diffusion of SO_4^{2-} and CH leaching, b) ettringite formation, c) gypsum formation and depletion of CH, d) decalcification of C-S-H and e) thaumasite formation [13].

Figure 6 reproduces the XRD patterns for the pastes exposed to sulfates for 56 days. The ettringite formed as a result of paste hydration did not increase significantly after soaking in the sulfate solution [14]. The presence of gypsum observed in the C&DW-OPC paste was due to the aggressive medium, however. Unlike the other pastes, the TAPS-OPC material contained carboaluminates as a result of calcite participation in hydration.
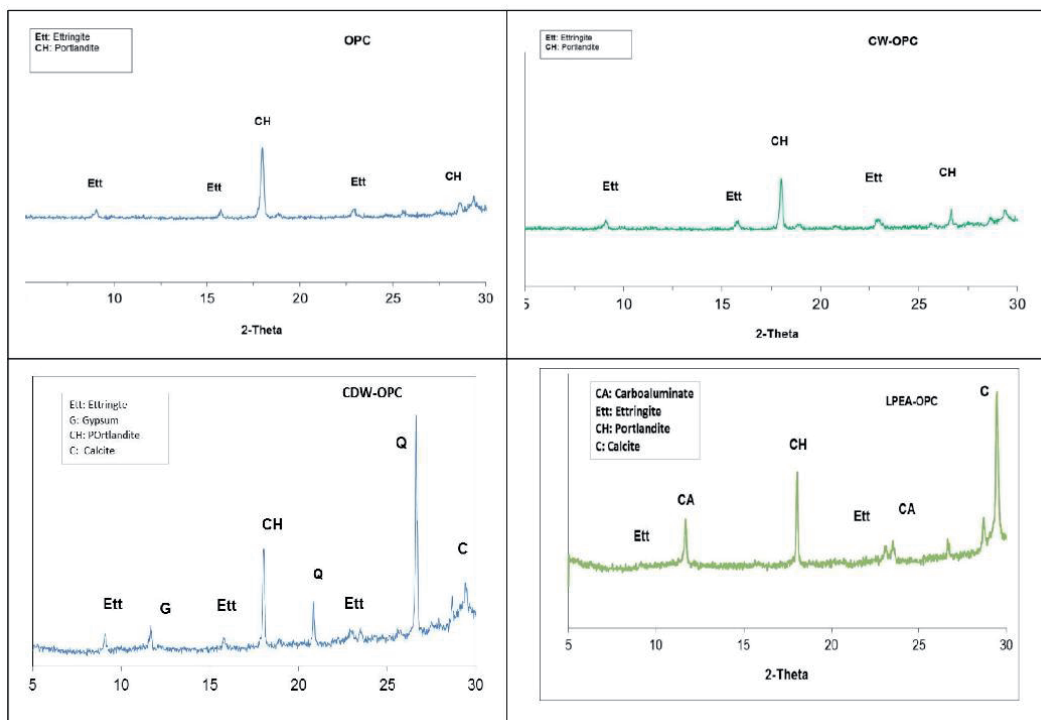

Figure 6: XRD patterns for pastes soaked in a sulfate medium for 56 days
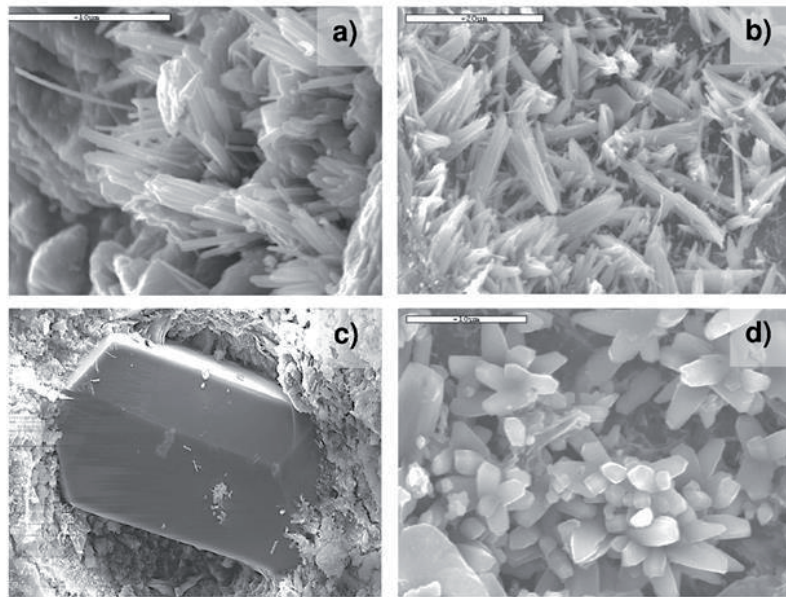
Figure 7: Micrographs of pastes exposed to sulfates for 56 days: a) OPC; b) CW-OPC; c) C&DW-OPC; d) TAPS-OPC

4.   CONCLUSIONS

The conclusions that can be drawn from the present study are set out below.

– The corrosion indices (I_c) for CW- and C&DW-blended cements exposed to sulfates were similar to the values obtained for deionised water, a finding not extensive to the TAPS-blended cements.

– The 56 day chemical resistance (I_{rq}) values were over one for the pastes bearing CW and C&DW, but only 0.8 for the cement containing TAPS.

– The inclusion of paper sludge in the design of new cements did not enhance their sulfate resistance.

– No differences attributable to the inclusion of the waste were observed in the hydration products in the sulfate-soaked pastes, although carboaluminate formation was detected in the TAPS samples due to the presence of calcite in the original material. Gypsum formation but no decay was observed in the cement specimen containing C&DW.

ACKNOWLEDGEMENTS

REFERENCES

[1]   Johansson, S; Andresen, P.J., Pozzolanic activity of calcined moler clay. Cem Concr Res 20 (1990), 447-452 [2]

[2]   He, C.; Osbaeck, B.; Makovicky, E., Pozzolanic reactions of six principal clay minerals: activation, reactivity assessments and technological effects". Cem Concr Res 25 (1995)1691-1702.

[3]   Frías, M; Sánchez de Rojas, MI. The effect of high curing temperature on the reaction kinetics in MK/lime and MK blended cement matrices at 60ºC. Cem Concr Res 33 (2003) 643-649.

[4]   Frías, M. The effect of MK on the reaction products and microporosity in blended cement pastes submitted to long hydration time and high curing temperature. Adv Cem Res 18 (2006) 1-6.

[5]   Rodríguez, O.; Frías, M, Sánchez de Rojas, MI. Influence of the calcined paper sludge on the development of hydration heat in blended cement mortars. J Ther Analy and Calor 92 (2008) 865-871.

[6]   Frías, M, Rodríguez, O; Sánchez de Rojas, MI. Paper sludge, an environmentally sound alternative source of MK based cementitious materials. A review. Const and Buil Mat 74(2015)37-48.

[7]   Sánchez de Rojas, M.I.; Marín, F.; Rivera, J.; Frías, M., Morphology and properties in blended cements with ceramic waste materials recycled as pozzolanic addition. J Am Ceram Soc 89 (2006) 3701-3705.

[8]   Sánchez de Rojas, M.I.; Marín, F.; Frías, M.; Rivera, J., Properties and performances of concrete tiles containing waste fired clay materials. J Am Ceram Soc 90 (2007) 3559-3565.

[9]   Asensio, E.; Median, C.; Frías, M.; Sánchez de Rojas, M.I. (2016). Caracterization of ceramic-based construction and demolition waste: Use as pozzolan in cements. J Am Ceram Soc, Doi 10-111.jace 14437.

[10]   Asensio, E. Medina, C., Sánchez de Rojas, M.I., Frías, M., Blended cements based on C&DW.Influence in the pozzolanicity. : International Conference on Construction Materials and Structures (ICCM 2014). Johannesburg, South Africa. Noviembre 2014

[11]   Koch, A.; Steinegger, U., A rapid Test for Cements for their behaviour under sulphate attack. *Zem-Kalk-Gips*, 7, (1960) 317-24

[12]   EN 197-1. Standards. Cement. Part 1: Composition, specifications and conformity criteria for common cements (2011).

[13]   E. F. Irassar, V. L. Bonavetti, M. González. Microstructural study of sulfate attack on ordinary and limestone Portland cements at ambient temperature. Cem Concr Res, 33 (2003) 31-41.

[14]   Sánchez de Rojas, M.I.; Frías, M; Rodríguez, O., Rivera, O., Durability of blended cement pastes containing ceramic waste as a pozzolanic addition. J Am Ceram Soc, 97 (2014)1543-1551.

PROCEEDINGS

MECHANISMS
AND MODELLING

Artificial neural network modeling of the expansion behaviour of recycled concrete aggregate under external sulphate attack

S. Boudali[1,5], B. Boukhatem[2], B. Abdulsalam[3], S. Poncet[1] , A.M. Soliman[4], D. E. Kerdal[5]

ABSTRACT

Evaluating expansion of self-compacting concrete (SCC) incorporating recycled concrete aggregates (RCA) during production is a commonly used criterion. However, monitoring expansion is a complicated process. In this research, an Artificial Neural Network (ANN) model was developed to predict the expansion of self-compacting concrete (SCC), incorporating recycled concrete aggregates (RCA) and fine recycled aggregates (FRA) as replacement of natural aggregates (NA) and natural pozzolana (NP), respectively, while being exposed to external sulphate attack. For the ANN model, nine input parameters including water content, water-binder ratio, mineral additives (NP,FRA), sand, natural aggregate (NA) ,recycled concrete aggregates contents and immersing period in sodium sulphate (Na_2SO_4) solution. The output parameter of the developed ANN is the expansion change for an investigated period (up to 1 year). The developed ANN model exhibited excellent capability in capturing complex effects and interactions among model inputs on the expansion change of SCC for different levels of RCA replacement.

Keywords: Artificial neural networks / Recycling / sulphate attack / Self-compacting concrete

1   INTRODUCTION

Over the last 50 years, rising volumes of construction and demolition wastes (CDW) has become a cause for growing concern [1]. For this reason, the construction sector has made significant efforts to find ways to reuse the huge amounts of waste generated each year. A practical solution for this problem is the use of recycled concrete aggregates (RCA) to replace natural aggregates (NA) in concrete mixtures.

The mechanical, physical and chemical proprieties of RCA to formulate this type of concrete must be studied in details. Results on the use of RCA for concrete formulation have been encouraging [2][3][4]. Concrete deterioration results from various reasons, including sulphate attack.

---

1   Université de Sherbrooke, Department of f Mechanical Engineering,Canada; sara.boudali@usherbrooke.ca

2   Université de Sherbrooke, Department of Civil Engineering,bakhta.boukhatem2@usherbrooke.ca

3   Western University, Departent of Civil and Environmental Engineering, babdulsa@uwo.ca

1   Université de Sherbrooke, Department of Mechanical Engineering; Sebastien.Poncet@USherbrooke.ca

4   Concordia University, Departent of Building, Civil and Environmental Engineering, ahmed.soliman@concordia.ca

5   Oran University of Science and Technology, Department of Civil Engineering, djkerdal@yahoo.fr

Research on the performance of recycled aggregate concrete (RAC) mainly focused on the effect of introducing the coarse fraction of recycled concrete aggregates (RCA) on the mechanical performance of concrete. Recent investigations focused on the performance of concrete made with coarse [5] and fine [6][7][8] aggregates. Shayan and Xu [9] observed satisfactory sulphate resistance of concrete exposed to untreated or sodium silicate plus lime treated coarse aggregate or fine recycled aggregate along with conventional concrete when concrete samples were stored in a 5% sodium sulphate for 12 months. Limbachiya [10] observed a comparable expansion of two classes of conventional concrete and concrete with 30% replacement of coarse NA by RCA and produce strength of 10 and 20 MPa, when both were immersed in a 3% in sodium sulphate solution for 6 months. However, the sulphate-induced expansion of recycled concrete increased as the replacement level of NA by RCA increased to 50 and 100 %. On other hand, Boudali et al. [11] observed a higher sulphate resistance for SCC contacting the coarse RCA and fine recycled than in conventional concrete when the both SCC concrete were exposed to immersion-drying cycles at 5% sodium sulphate solution for 6 months.

Generally, the free expansion behaviour is influenced by multiple factors such as water-to-binder ratio (W/B), size and type of aggregate, cement content, water content, interfacial zone propriety and other mix design parameters. Prediction of concrete structure expansion behaviour needs long term monitoring using experimental methods, but it is limited to short time nearly 700 days [12][13]. To remove this subjectivity, some criteria must be established as a basis for the prediction process [14][15]. Hence, in this paper, an intelligent-based prediction model using Artificial Neural Network technique was developed and its potential was discussed.

A number of efforts were done on using multi-variable regression models to improve the accuracy of predictions. Previous study applied regression analysis to evaluate relationships among demolished concrete characteristics, properties of their RA and strength of their RAC [16]. An attempt was also made to predict compressive strength of high performance concrete using multiple regressions [17]. The conventional methods for predicting the compressive strength of concrete are based on statistical analysis and involve estimating and choosing an appropriate regression equation [18] [19]. Today, ANNs have been applied to many civil engineering problems with some degree of success as detection of structural damage, modeling of material behavior and predicting properties of compressive strength at long term for concrete in sulphate environment [20]. They have been also successfully tested for predicting the effect of sulphate attack on strength of cement paste [21]. Hence, in this paper, an intelligent-based prediction model using ANN technique was developed and it is potential to predict expansion behavior of SCC with RCA was discussed.

2 ARTIFICIAL NEURAL NETWORKS (ANN$_S$)

ANN is one of the most important soft computing techniques that simulate the behavior of the human brain and nervous system. The basic element in the ANN is a processing element, called artificial neuron or node. Each neuron contains a very limited amount of local memory and performs basic mathematical operations. These neurons are highly interconnected in layers such as an input layer, an output layer and one or more hidden layers. The computational power of ANN comes from this interconnection which makes input data concurrently processed in artificial neurons as shown in Figure 1. The ANN is trained by presenting a set of input-output associated data based on learning or training process.

Generally, in a process of learning, the neurons receive the input data (x1,... xn) and transmit them to the neurons in the hidden layer, which are responsible for simple mathematical

calculations useful involving the weight of connections (W11,..., W1n), bias (b1,…, bn), and the input values. The Back Propagation neural network (BPNN) is the most popular training algorithm often used which is employed in this study. The BPNN consists in one input layer, several hidden layers, and one output layer [22]. Signals can be obtained in an input layer, and then transferred to the first hidden layer for processing. Input values from each input neuron are multiplied by each of the adjustable connection weight linking the input layer neurons to hidden layer neurons. For every neuron of hidden layer, input values be summed, while a bias value is added [23]. The weighted sums of each hidden layer neuron can then be obtained using the method above. The processing is as follows:

$$(net)_j = \sum_{i=1}^{n} w_{ij} x_i + b \qquad (1)$$

Where $(net)_j$ is the weighted sum of jth neuron for input value from the previous layer; wij is the weight between the ith neuron in the previous layer and jth neuron in this layer; xi is the output of ith neuron of previous layer; b is the bias value; and $\sum$ is the sum function[24][25].

The training process uses an algorithm, in which the ANN develops a function between the inputs and outputs.
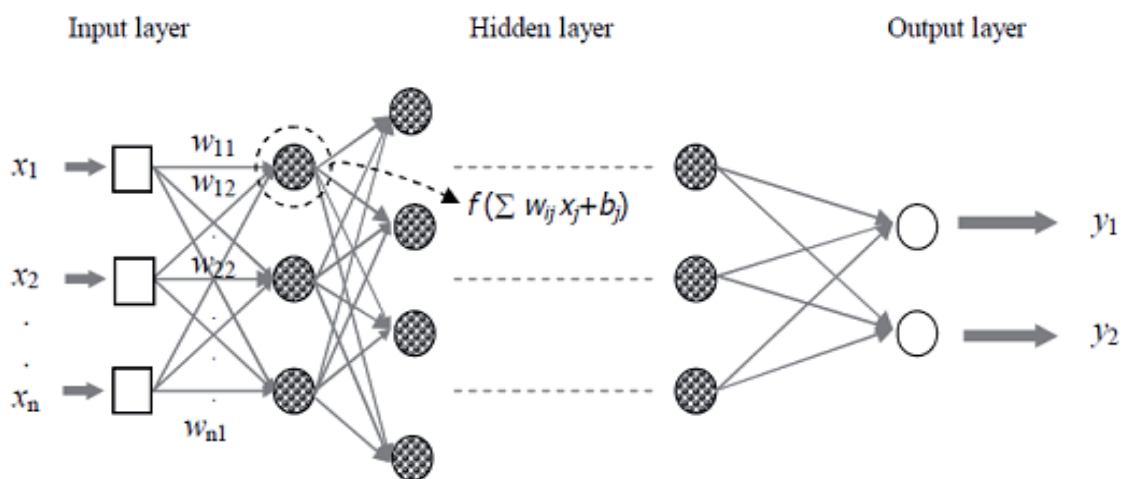

Figure 1: Multi-layer neural network.

3   EXPERIMENTAL DATABASE

The main purpose of this study is to develop an ANN model to predict the expansion behavior of SCC containing recycled aggregate exposed to sulphate attack. To construct this model, an experimental database is constructed based on the authors' experimental results previously published that were performed on SCC mixtures containing RCA under sulphate attack [11][26], where a total of 84 data sets were used.

In this study a total of nine input parameters were used to construct the present ANN model. These input parameters include water-binder ratio (W/C+F), binder content, water (W), two different mineral additives: Natural pozzolana (NP), fine recycled aggregate (FRA), naturel coarse aggregates (NA), recycled concrete aggregates (RCA), sand in addition to the time of immersion under Na_2SO4 solution. The input parameters remained the same for the all the

networks. The output parameter is the expansion change of recycled SCC overtime up to 365-days. The limit values (maximum and minimum) and units of input and output data sets used for developing the ANN model are shown in Table 1. The database was divided into three parts: training (60%), Testing (20%) and validation (20%) [27] to provide the ANN model with good generalization capability. After data division the data were normalized between -1 and +1 before their presentation to NN model to make them consistent with the limits of tangent sigmoid transfer function used in hidden layers and output layer by using the following equation:

$$X_n = \frac{X - X_{min}}{X_{max} - X_{min}}$$

(2)

Where X_{min} is the minimum value of the X data sample, X_{max} is the maximum value of the X data sample, and X_n is the scaled value of the X data sample.

Table 1: Input and output parameters with their maximum and minimum values

No	Input Parameters (unit)	Range of Values(Min-Max)
1	Binder (kg/m3)	490-620
2	Water/(Cement+fines) (W/C+F)	0.34-0.36
3	Water (kg/m3)	175-210
4	Naturel aggregates-NA (kg/m3)	0-791
5	Recycled concrete aggregates- RCA (kg/m3)	0-791
6	Natural Pozzolana NP (kg/m3)	0-200
7	Fine recycled aggregate FRA (kg/m3)	0-200
8	Sand (kg/m3)	887.81-1169
9	Time of immersion (days)	7-365
	Output Parameter	
1	Expansion change (%)	0-1.470

4 METHODOLOGY OF DEVELOPING THE ANN MODEL

The architecture of the ANN model is first described, followed by the determination of the training parameters that optimize its performance. The model was trained and tested respectively with training and testing data sets by using the Back-propagation algorithm. The implementation and simulation were performed using MATLAB neural network toolbox functions [28].

4.1 Choice of the Best Architecture

The optimal appropriate architecture of the proposed ANN model is described in Figure 2. It has nine input parameters, only one hidden layers with seven neurons and one output parameters. It should be noted that the optimal number of neurons in hidden layers was determined by the training process. No reasonable theory has been established to calculate

the appropriate number of neurons in hidden layers. In practice, the number of neurons in hidden layers can be computed using the following function:

$$n = \sqrt{n_i + n_o} + a \qquad\qquad (3)$$

Where n is the number of hidden layer neurons, n_i is the number of input layer neurons, n_o is the number of output layer neurons, and a is a fixed value ranging from 0 to 10.

According to this function, the number of hidden layer neurons can be between 3 and 13. In this research the number of neurons is set to 6.

4.2 Training and testing the ANN model

For building the ANN model, a MATLAB based program was used [29]. Training the ANN is performed by using the Levenberg–Marquardt training algorithm which is considered as the fastest algorithm for training neural networks of moderate size [30]. The various parameters of the present ANN training model developed are summarized in Table 2. This model has been developed with high coefficients of determination were 0.95, 0.93 and 0.91 respectively for the training, testing and validation phases with quite acceptable performance as shown in Figure 3. The results demonstrate that the proposed ANN model is suitable and the predicted expansion values are very close to the experimental values with a total coefficient of determination R^2 of 0.9311 or regression value R of approximately 0.965.
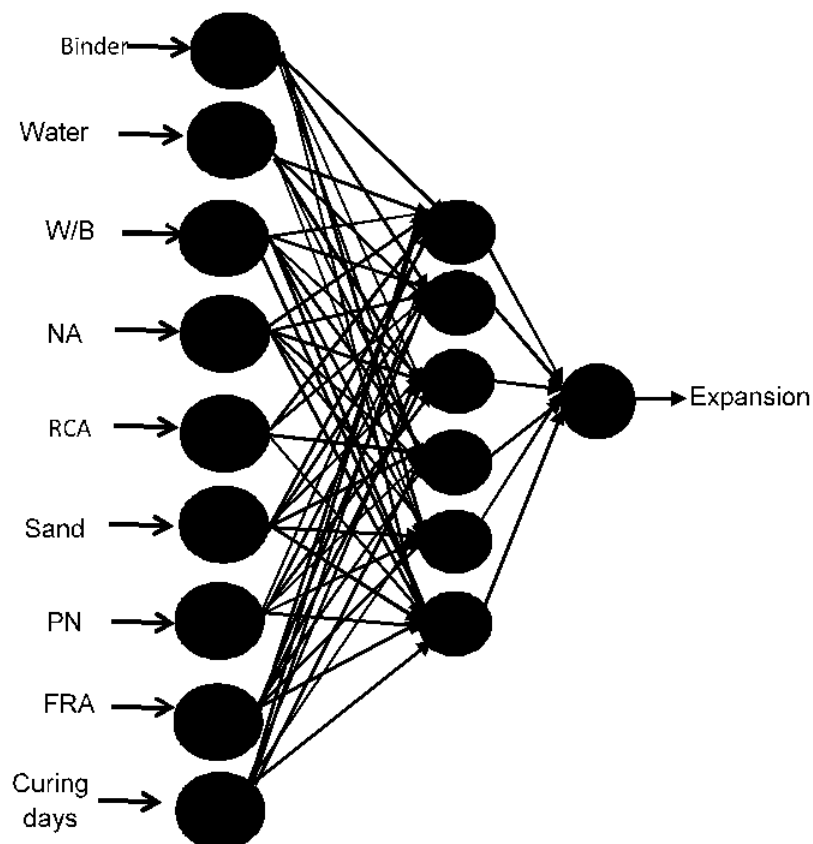

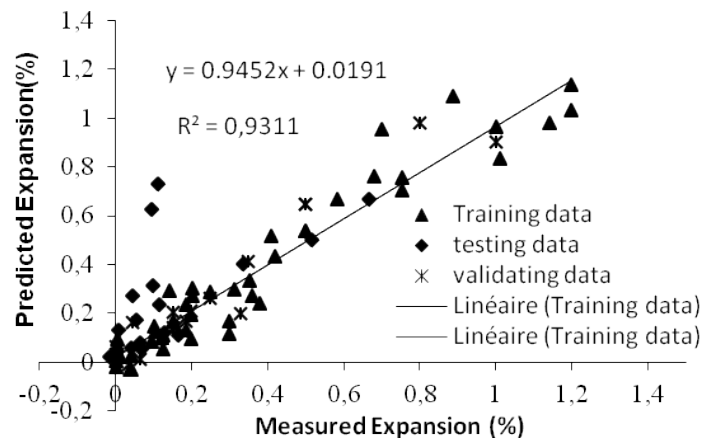Figure 1: The architecture of the ANN model

Figure 2: Response in predicting expansion change values for recycled SCC specimens exposed to sodium sulphate solution.

Table 2: Training parameters of the developed ANN model

Sr.No	Input Parameters	Range of Values(Min-Max)
1	Learning algorithm	trainlm
2	Transfer functions in the hidden layer output layer,	Tansig
3	Transfer functions in the output layer,	Logsig
4	Approximation goal	0.001
5	Learning rate	0.5
6	Learning cycle	200

5   PARAMETRIC ANALYSIS ON ANN MODEL RESULTS

The expansion behavior of recycled concrete aggregate SCC under external sulphate attack is a multiple-parameter mechanism that depends on both exposure conditions and the concrete-mixture proportion. Therefore, providing a reasonable estimation of this behavior requires exploring the effect of these parameters on the expansion changes with the ANN model through sensitivity analysis. In this analysis, only one parameter is varies and the others are kept constant.

5.2   Effect of RCA and FRA replacement level on expansion change

In order to study the effect of RCA replacement level on its expansion of SCC exposed to a sulphate attack, the main variables considered were FRC content and RCA content, binder content and W/B. The different scenarios used to simulate the behavior of the recycled SCC under sulphate attack through ANN in MATLAB program can be seen in Table 3.

Table 3 Different scenarios simulated through ANN

SCC	Binder (kg/m³)	W/B
1. FRC%		
10	385	0.45
20	420	0.41
30	455	0.38
40	490	0.36
2. RCA%		
0	385-490	0.28-0.5
50	385-490	0.28-0.45
75	385-490	0.37-0.45
100	385-490	0.28-0.5

The simulated results of the expansion change for SCC concrete at 7 to 365 days are shown in Figures 4 and 5. In this case, a great effect when the replacement level varies from 30 to 40 % FRA on the outputs parameters was found.

Mixtures with low content of FRA and RCA (Figure 3(a-b)) showed an expansion increase as immersion days extended. This was most probably, due to the increase in the volume of the specimens, usually formed by reaction products between sulphate ion N^{+2} and cement matrix (i.e. calcium hydroxide), which is believed to be the principal cause of the concrete expansion, caused cracking and structural damage. Figures 4(a,b) shows the expansion change of SCC prepared with low content of FRA (10 and 20%) and different levels of RCA (0,50,75,100). The figure indicates that the expansion increased by 0.7-0.8 % when FRA was used with a replacement level of 10% and 100% natural aggregate (NA). This can be attributed to the fact that there is a greater formation of expansive phases (ettringite, gypsum) in the specimens due to the reaction between of SO_4^{-2} and monosulfoaluminate and monocarboaluminate present in the concrete [31]. The present results show that the developed model is capable to predict the results of the experimental program. Mixtures with the highest FRC and RCA content (40 and 100% respectively) exhibited a resistance performance to sulphate attack compared to all other mixtures, as shown in Figure 4-d. This was probably, due to the fact that microstructure nature of RAC is plastic like, due to its higher porosity, and matures enough to resist to excessive expansion and relief stresses especially at the later ages. Similar observations were found in previous studies [32] [33]. Consequently, adding FRA and RCA at rates (30 to 40% and 75-100% respectively) will help to reduce the concrete degradation. This is in agreement with previous studies conducted on recycled concrete [6], [9], [10].
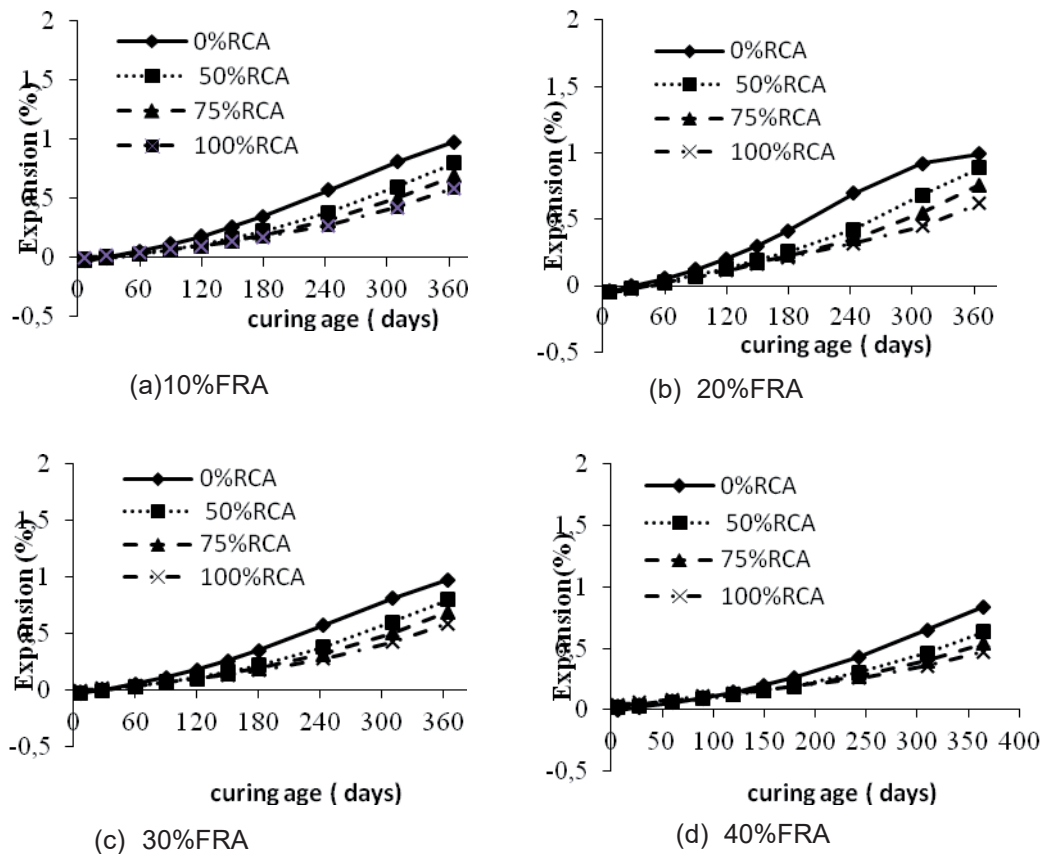
Figure 3 Expansion change against time for different replacement of recycled concrete aggregate (RCA) and (a) 10% fine recycled concrete (FRA), (b) 20% FRA, (c) 30%FRA and (d) 40% FRA.

Figure 4 (c-d) also suggests that at high rate of FRA content and RCA, the expansion change is minimal compared to other mixtures. This can be attributed to the denser microstructure of SCC containing 100% RCA and (30 to 40%) FRA, due to ITZ beneficial effects. In recycled aggregate, there are two interfacial transition zones (ITZ1): an interfacial transition zone between the original aggregate and the old mortar, and another new (ITZ2) between the adhesion mortar and the new mortar. In the present study, the ITZ between the mortar adhesion and the new mortar (ITZ2) affects significantly to the performance of recycled SCC [34].

Figure 5 shows, an increase in the expansion change for all mixes with increasing immersing days. Especially, for mixture content 40% FRA, the expansion at 365 days did not exceed 0.5%. A mixture content of 10% FRA and 100% RCA presented a higher expansion than the mix content of (20 and 30%) FRA, respectively. That was probably due to loss of the binder content (Cement + addition mineral). The loss of the binder content caused a structural degradation because of the existence of the expansive minerals (gypsum and secondary ettringite) and therefore induced a decrease of its strength [35].
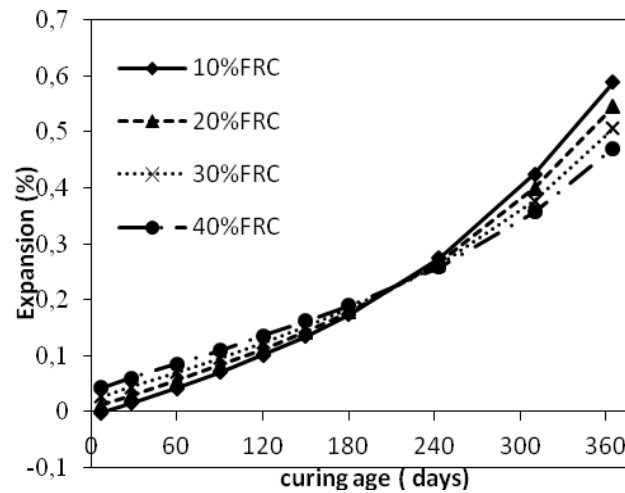
Figure 4: Expansion change against time for different replacement of fine recycled aggregates (RCA) and 100% RCA of SCC concrete exposed to sodium sulphate attack at 365 days.

Mixtures containing 40% FRA and 100% RCA presented higher resistance under sulphate attack. This can be due to a continued matrix hydration at later ages (more than 120 days). It is clear that mixtures incorporating fine and coarse recycled aggregate exhibited higher strength than those with natural aggregate.

6   CONCLUSIONS

The conclusions drawn from the current studies are summarized as follows:

1- Numerical modeling using neural network is obviously a great method to predict recycled self-compacting concrete properties subjected to sulphate attack, with an R2 value of 0.956 for testing a set ANN.

2- The design charts emphasize the importance of using fine (FRA) and coarse recycled aggregates (RCA) by replacement level (30 to 40% and 75 to 100% respectively).

3- By adopting this model there is no need to go through sophisticated and time – consuming laboratory tests to obtain expansion change of self – compacting concrete content different replacement level of RCA and FRA. Further, this research it enables to decrease the experimental costs for design recycled self-compacting concrete.

4- After successfully learning, the ANN model has a good performance with a desirable accuracy for this particular application. It is concluded that ANN is an appropriate tool for modeling the expansion behavior at 1 year. This would help engineering design in using FRA and RCA for concrete application in an aggressive environment.

5- A mix ratio of 40% FRA and 100% RCA provided the best results under sulphate attack.

6- The advantage of using recycled aggregate compared to natural aggregate in SCC concrete production with replacement levels of RCA ranging between 75 at 100 % and 30-40% FRA approved durability at long term.

REFERENCES

[1]   Debieb F, Courard L, Kenai S, Degeimbre R. Mechanical and durability properties of concrete using contaminated recycled aggregates. Cem. Concr. Compos. 32 (2010), 421–426.

[2]   Rao A, Jha KN, Misra S. Use of aggregates from recycled construction and demolition waste in concrete. Resour. Conserv. Recycl. 50 (2007),71–81.

[3]   Tam VWY, Tam CM, Wang Y. Optimization on proportion for recycled aggregate in concrete using two-stage mixing approach. Constr. Build. Mater. 21 (2007),1928–1939.

[4]   Di Niro G.; Dolara, E.; and Cairns R. Properties of Hardened RAC for Structural Purposes," Sustainable Construction: Use of Recycled Concrete Aggregate. Eds R.K. Dhir, N.A. Henderson, and M.C. Limbachiya, Thomas Telford, London; (1998).

[5]   Saeed A and Hammons M. Use of Recycled Concrete As Unbound Base Aggregate in Airfield and Highway Pavements to Enhance Sustainability. Airfield and Highway Pavements (2008), 497–508.

[6]   Khatib JM. Properties of concrete incorporating fine recycled aggregate. Cem. Concr. Res. 35 (4) (2005),763–769.

[7]   Evangelista L, de Brito J. Mechanical behaviour of concrete made with fine recycled concrete aggregates. Cem. Concr. Compos.29 (2007), 397–401.

[8]   Zega CJ, Di Maio AA. Use of recycled fine aggregate in concretes with durable requirements. Waste Manag.31 (2011), 2336–2340.

[9]   Shayan A and Xu A. Performance and Properties of Structural Concrete Made with Recycled Concrete Aggregate. ACI Am. cocrete Inst.100 (2003), 371–380.

[10]   Limbachiya MC. Recycled aggregates: Production, properties and value-added sustainable applications. J. Wuhan Univ. Technol. Mater. Sci. Ed. 25 (2003), 1011–1016.

[11]   Boudali S, Kerdal DE, Ayed K, Abdulsalam B and Soliman AM. Performance of Self-Compacting Concrete Incorporating Recycled Concrete Fines and Ahmad Shayan Aggregate Exposed to Sulphate Attack. Constr. Build. Mater. 124 (2016), 705-713.

[12]   Tam VWY, Kotrayothar D, Xiao J. Long-term deformation behaviour of recycled aggregate concrete. Constr. Build. Mater. 100 (2015), 262–272.

[13]   Kou S-C, Poon C-S, Etxeberria M. Influence of recycled aggregates on long term mechanical properties and pore size distribution of concrete. Cem. Concr. Compos. 33 (2011), 286–291.

[14]   Chase W, F. Brown F. General Statistics, Fourth ed., Wiley, New-York (1999).

[15]   Chapra SC, Canale RP. Numerical Methods for Engineers, Fifth ed., Higher Education, Boston (2010).

[16]   Tam VWY, Wang K, Tam CM. Assessing relationships among properties of demolished concrete, recycled aggregate and recycled aggregate concrete using regression analysis. J. Hazard. Mater. 521 (2008), 703–714.

[17]   Zain MFM. Multiple Regression Model for Compressive Strength Prediction of High Performance Concrete. J. Appl. Sci. 9 (2009), 155–160.

[18]   Muthupriya P, Subramanian K, Vishnuram BG. Prediction of Compressive Strength and Durability of High Performance Concrete By Artificial Neural Networks. Int. J.

Optim. Civil Eng. 1 (2011), 189–209.

[19]   Kim JI, Kim DK. Application of neural networks for estimation of concrete strength. KSCE J. Civ. Eng. 6 (2002), 429–438.

[20]   Diab AM, Elyamany HE, Elmoaty A, Elmoaty MA, Shalan AH. Prediction of concrete compressive strength due to long term sulfate attack using neural network. Alexandria Eng. J. 53 (2014), 627–642.

[21]   Orejarena L, Fall M. The use of artificial neural networks to predict the effect of sulphate attack on the strength of cemented paste backfill. Bull. Eng. Geol. Environ. 69 (2010), 659–670.

[22]   Ozcan F, Atis CD, Karahan O. Uncuoglu F, Tanyildizi H. Comparison of artificial neural network and fuzzy logic models for prediction of long-term compressive strength of silica fume concrete. Adv Eng Software 40(2009):856–63.

[23]   Yuan Z, Wang LN, Ji X. Prediction of concrete compressive strength: Research on hybrid models genetic based algorithms and ANFIS. Adv Eng Software 67(2014),156–63.

[24]   Sarıdemir M, Topcu _IB, Ozcan F, Severcan MH. Prediction of long-term effects of GGBFS on compressive strength of concrete by artificial neural networks and fuzzy logic. Constr Build Mater. 23 (2009), 1279–86.

[25]   Oztas A, Pala M, Ozbay E, Kanca E, Caglar N, Asghar Bhatti M. Predicting the compressive strength and slump of high strength concrete using neural network. Constr Build Mater. 20 (2006), 769–75.

[26]   Boudali S, Abdulsalam B, Soliman AM, Ahmed A, Ayed K, Kerdal DE. Green self-compacting sand concrete exposed to sulfate attack. In Resilient Infrastructure, London (2016), 1–11.

[27]   Barthelemy S. Introduction aux Réseaux de Neurons Neural (2000). http://www.sylbarth.com/nn.php

[28]   Neural Network for user with MATLAB R2016b, the MathWorks Inc, Prentice Hall.

[29]   Alani T, Réseaux de Neurones Tutorial en Matlab,Departement informatique ESIEE-Paris.(2008),1-48.

[30]   Demuth H, Beale M. Neural network toolbox 5, user's guide. MathWorks Inc. Natick. (2007).

[31]   Gollop RS, Taylor HFW. Microstructural and microanalytical studies of sulfate attack. I. Ordinary portland cement paste. Cem. Concr. Res. 22 (1992), 1027–1038.

[32]   Gomez-Soberon JMV. Porosity of recycled concrete with substitution of recycled concrete aggregate – an experimental study. Cem. Concr. Res. 32 (2002), 1301–1311.

[33]   Tam VWY, Tam CM. Diversifying two-stage mixing approach (TSMA) for recycled aggregate concrete: TSMAs and TSMAsc. Constr. Build. Mater.22 (2008), 2068–2077.

[34]   Ryu JS. An experimental study on the effect of recycled aggregate on concrete properties. Mag. Concr. Res. 54 (2002), 7–12.

[35]   Fall M, Benzaazoua M and Sae E. Mix proportioning of underground cemented paste backfill. Int. J. Tunnelling Underground Construction 23, (2008), 80-90.

[36]   Cohen MD, Mather B. Sulfate attack on concrete-research needs. ACI Mater. J. 88 (1) (1991), 88–62.

Simplified model to assess the durability of elements subjected to external sulfate attack: Influence of shape and size of the elements

Ikumi, T.[1], Cavalaro, S.[1], Segura, I.[1, 2], de la Fuente, A.[1], Aguado, A.[1]

ABSTRACT

The mitigation of the external sulfate attack from the standpoint of the design of concrete structures is usually based on the use of cement with limited content of aluminates. Nevertheless, other parameters may affect the final durability, such as the cement content, the geometry and size of the structure. The consideration of these factors is highly complex. Few straightforward methods are available to verify the durability of structures subjected to sulfate ingress. The objective of this paper is to present a simplified model for the verification of the durability, considering variables related with the composition, the exposure and the geometry of the structure. First, a model to simulate the chemical-physical- mechanical phenomenon is proposed and validated. Then, this model is simplified to make it easy to apply. Finally, a parametric study is performed to evaluate the influence of the shape and size of the element on the durability

1.   INTRODUCTION

External sulfate attack (ESA) is one of the most complex degradation process affecting underground concrete structures. This phenomenon is defined by multiple variables related to the penetration process of sulfate ions (sulfate content and pore network characteristics), material reactivity (concrete composition) and mechanical and geometrical properties of the element under attack. Moreover, since ESA normally only affects a fraction of the whole section of the specimen, the processes acting at the micro-scale have to be reflected at the macro-scale by complex mechanical calculations.

Despite the complexity of this phenomenon, most design codes only consider a limitation of the aluminate content by the use of sulfate resistant cements where the sulfate concentration in the groundwater surpass a predefined limit. The limitation of aluminate content in aggressive environments is equal regardless of the cement content in the concrete and the size or structure typology of the element under attack. Indeed, according to current structural codes it seems that the only way to obtain durable materials against the ESA is by the use of a sulfate resistant cement. However, since this phenomenon is defined by multiple parameters, there should be multiple ways to obtain durable materials.

One of the key aspects that might define the final durability of structures exposed to sulfates is the geometrical characteristics of the specimen. Precisely, the ratio between the affected and sound region of the section. It seems common sense that a large pile of 2 m of diameter should resist better the deleterious effects related to ESA than a micro-pile of 30 cm of

---

[1]   Department of Civil and Environmental Engineering, Universitat Politècnica de Catalunya, Barcelona Tech, Jordi Girona 1-3, C1, Barcelona, Spain

[2]   Smart Engineering Ltd., C/Jordi Girona 1-3, Parc UPC – K2M, 08034, Barcelona, Spain

diameter. Unfortunately, the current approach adopted in the structural codes do not allow any differentiation between these two cases. Despite building codes must contain simplified approaches, the application of the current guideline might lead to very penalizing measures in some situations.

This paper presents a simplified methodology that allows a direct assessment of the ESA by considering parameters related to the aggressiveness of the media, the reactivity of the material and the geometrical characteristics of the element under attack. Moreover, a case study is presented to highlight the contribution of the shape and size of the specimen on the durability against the ESA.

2. SIMPLIFIED METHODOLOGY

The methodology proposed is based on the application of a set of simplified equations to assess the extent of the reactive-transport process and the possible mechanical structural failure at a given service life (25 or 50 years). Figure 1 represents a schematic diagram of the methodology.
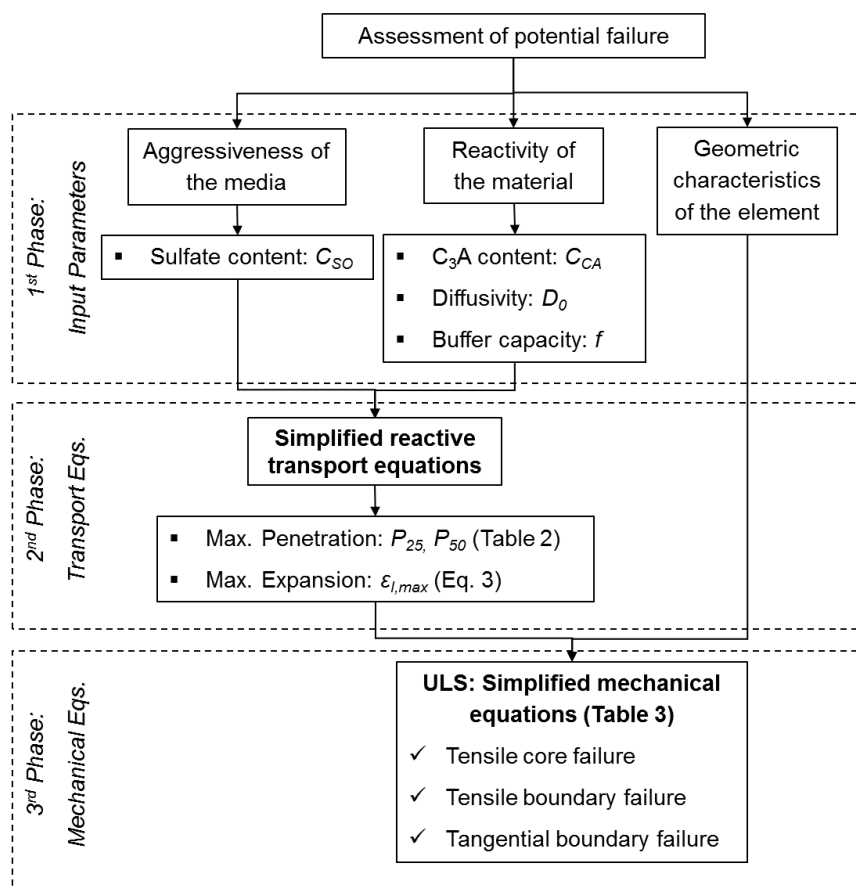

Fig. 1. Outline of the simplified methodology for the durability assessment of the ESA [1].

As can be seen, the assessment proposed takes into account the aggressiveness of the external media, the reactivity of the material and the geometric characteristics of the element under attack. After the definition of the input parameters, the second phase consists on the estimation of the strain profile at a given service life (penetration of the sulfate ions and

magnitude of expansions). Since this methodology consider the geometrical characteristics of the element under attack, it allows the verification of three of the most typical failure modes associated to the ESA. If no mechanical failure occurs and the serviceability is not compromised, it is considered that the structure will comply with the required service life. In this section, the fundamentals and final equations of the simplified methodology are presented. An in-depth description of the derivation process of the simplified equations is available in [1].

2.1-. Simplified transport equations

The simplified equations to quantify the maximum penetration of the sulfate front at 25 and 50 years were deduced from a series of simulations performed in the model presented by T. Ikumi et al. [2] with multiple combinations of the most influencing parameters. Table 1 describes the ranges of the parameters considered. More than 2000 simulations were completed at 25 and 50 years. Once a sufficiently big database of penetration depths was obtained, a nonlinear numerical regression was applied to derive the simplified equations that yield the best fit with the numerical results. Prior description of the transport equations obtained, the general hypothesis adopted during the simulations performed in the comprehensive numerical model [2] are explained below.

Table 1. Ranges of parameters.

Parameter	Description	Minimum	Maximum
C_{SO}	Sulfate Concentration in the media [mol/m³$_{water}$] ([g/l])	6.25 (0.6)	62.5 (6.0)
D_0	Initial diffusivity of sulfates [m²/s]	10^{-12}	10^{-11}
f	Buffer coefficient	0.0	0.4
C_{CA}	Aluminate content in the concrete [mol/m³$_{concrete}$] ([%C₃A])	41 (4)	124 (12)
φ_o	Initial porosity	0.08	0.14
f_{cm}	Compressive strength [MPa]	20	40

2.1.1. Chemical reactions

Sulfate ions (SO_4^{2-}) penetrate the structure and react with calcium hydroxide (CH) to form gypsum ($C\bar{S}H_2$) according with Eq. 1.

$$CH + SO_4^{2-} \rightarrow C\bar{S}H_2 + 2OH^- \tag{1}$$

Gypsum is considered as an intermediate phase that may later react with the aluminate phases to form secondary ettringite ($C_6A\bar{S}_3H_{32}$). Even though several aluminate phases may react with gypsum, to simplify the model it is assumed that all aluminates are in the form of monosulfate ($C_4A\bar{S}H_{12}$) since this should be the predominant phase in the hydrated cement paste at long ages. It is also assumed that the expansions are only caused by the formation of secondary ettringite. The expansive nature of gypsum is not taken into account, as there is still controversy regarding its contribution. By this way, only one single chemical reaction defines the kinetics of the expansive process (Eq. 2).

$$C_4A\bar{S}H_{12} + 2C\bar{S}H_2 + 16H \rightarrow C_6A\bar{S}_3H_{32} \tag{2}$$

2.1.2. Transport process

To simplify the mathematical representation of the transport process, only the penetration of sulfate ions by a concentration gradient and its depletion due to ettringite formation is considered in the model. It is assumed that the system is saturated and all pores are accessible.

The effective diffusivity of the sulfate ions takes into account the pore filling effect and local damage caused by ettringite precipitation. The hyperbolic function proposed by Idiart et al. [3] was adopted to simulate the pore filling process. The value of the diffusivity when the porosity is totally filled by expansive product is set at a tenth of the initial diffusivity and the shape factor β_D is set to 1.5 in accordance with the recommendation from Idiart [3]. On the other hand, the increase of diffusivity due to the local damage generated by ettringite formation is considered through the approach presented by Ikumi et al [2]. The latter considers that the increase of diffusivity is related with the expansions that may be estimated from a stress-strain curve. Such curve is defined by the uniaxial tensile strength of the material and the strain at which the crack becomes stress-free.

For the simulations performed, the upper bound of the diffusivity reached when the material is completely damaged is set to 10^{-10} m^2/s. This value is slightly below the diffusivity of sulfates in free solution, which Gerard and Marchand [4] quantified as 10^{-9} m^2/s for ions able to move freely within cracks. The value of c_1 and c_2 described in [2] were defined respectively as 3 and 6.93, in accordance with the recommendation from [5]. The characteristic cracking length (l_{ch}) is fixed at 26 mm, following the validation by [2].

2.1.3. Expansion mechanism at the micro-scale

It is assumed that the expansion mechanism associated to the ESA is based on the additional volume generated by the ettringite formation. The increase of volume ($\Delta V/V$) is calculated by the stoichiometric constant of the reaction. This calculation gives a 55% volume increase when monosulfate is converted into ettringite. According to this hypothesis, the linear strain (ε_l) is obtained by multiplying the expansion factor by the amount of monosulfate reacted ($C_{C_4A\bar{S}H_{12}}^{react}$), as described in Eq. 3. The term M/ρ corresponds to the molar volume of monosulfate and $C_{C_4A\bar{S}H_{12}}^{react}$ (expressed as a molar concentration). Notice that maximum expansive strain ($\varepsilon_{l,max}$) may be calculated with Eq. 3 by assuming that all monosulfate reacts to form ettringite.

$$\varepsilon_l = \left(1 + \frac{\Delta V}{V}\frac{M}{\rho}C_{C_4A\bar{S}H_{12}}^{react} - f\varphi_0\right)^{1/3} - 1 \tag{3}$$

Since ettringite precipitates within the pore network, the matrix is able to accommodate a certain amount of expansive product without exerting any pressure to the pore walls. The expression presented by Tixier & Mobasher [6] is used to estimate the buffered expansion. This is represented in the second term of Eq. 3, in which φ_0 is the initial porosity of the matrix and f is the fraction of this porosity that may be filled by expansive products before expansions occur. According with Tixier & Mobasher [6], f usually ranges between 0.05 and 0.40.

2.1.4. Simplified reactive - transport equations

Final formulations obtained to estimate the penetration depth at 25 and 50 years (P_{25} and P_{50}) are presented in Table 2. Both equations are applicable as long as the input parameters remain within the ranges defined in Table 1.

Table 2. Simplified reactive-transport equations.

Service Life [years]	Simplified reactive transport formulation [cm]		K_95 [cm]
25	$P_{25} = (7e10D_0 + 0.035C_{SO}) \exp\left(\frac{6.65e11D_0+10.737}{C_{CA}} - \frac{1e-10}{35D_0}f\right)$	(4)	0.65
50	$P_{50} = 1.26P_{25}$	(5)	0.86

The initial diffusivity (D_0) is introduced in m²/s, whereas the aluminate content (C_{CA}) is expressed in mol per cubic meter of concrete. The sulfate content (C_{SO}) is expressed in mol of sulfate per cubic meter of water. As these equations are deduced from the model described by Ikumi et al. [2], sulfate consumption, acceleration of the penetration due to cracking and decrease of diffusivity due to pore filling are indirectly considered.

The simplified transport equations provide a fair approximation of the model [2] with correlation coefficients of 0.91 and 0.90 for 25 and 50 years, respectively. For estimations on the safe side, a statistical analysis was performed in order to assess the error of prediction. A Gumbel distribution of the error estimation was used to assess the minimum penetration depth that had to be summed to the obtained penetration to assure a 95% of probability of achieving values above the calculated with the integrated model by [2]. This additional value (K_{95}) is shown in Table 2 and should be directly added to Eq. 4 and Eq. 5 in case a safer estimation is required.

2.2. Strain profile

Typical strain distributions have complex profiles, as they are defined by the aluminates reacted at each depth. Figure 2 shows in continuous lines a typical strain profile caused by ESA.
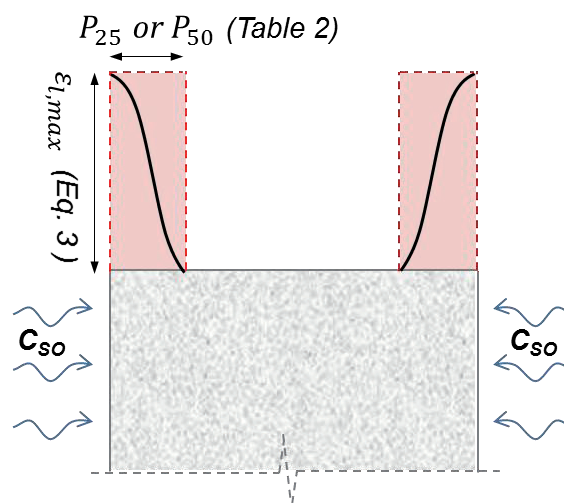

Fig. 2. Strain profile for symmetric sulfate exposure

To simplify the structural consideration, the strain profile depicted with the red discontinuous line is used instead. It assumes that the whole penetrated region estimated by Eq. 4 and Eq. 5 is affected by the same expansions. The magnitude of this expansions is calculated by Eq. 3 assuming that all monosulfate has reacted to form ettringite, which is a hypothesis on the safe side.

2.3. Simplified mechanical equations

Although expansion due to ettringite formation is concentrated in the superficial layers, strains also appear in the sound core of the element to ensure compatibility. In fact, the sound core acts as a restriction that reduces the expansion calculated with Eq. 3. An auto-balanced tension state is generated, leading to possible mechanical failures outside the zone directly affected by the sulfate penetration. Three failures modes are distinguished; tensile failure of the sound core (Figure 2a), tangential failure (Figure 2b) and tensile failure in the boundary between the surficial layers and the sound core (Figure 2c). The compressive stresses generated in the external layers are not considered as a failure mode. However, these are considered indirectly in the simplified transport equations by a degradation of the elastic modulus in the affected region.
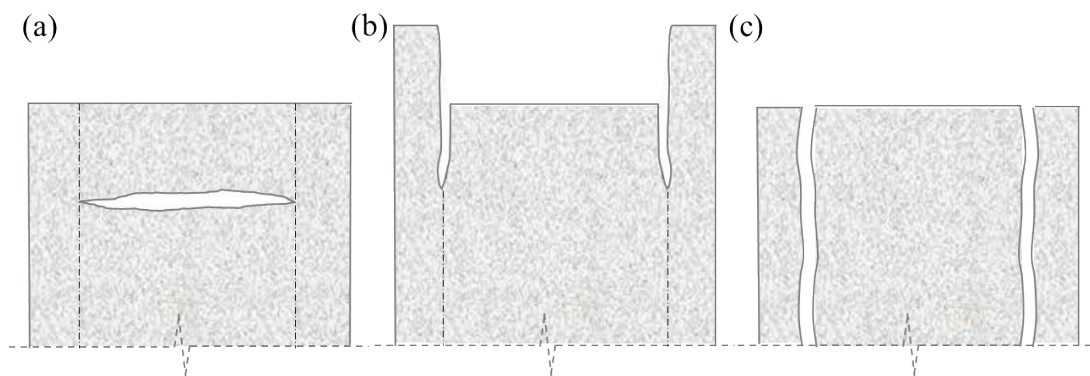

Fig. 2. (a) Tensile core (b) Tangential boundary and (c) Tensile boundary failure mode.

Table 3 includes the final expressions for the assessment of the three failure modes in linear and surface elements under different exposure conditions. This section presents a brief description of the derivation process, a detailed explanation can be found in [1].

2.3.1. Tensile failure of the sound core

Expansions generated by ettringite formation in the external layers are constrained by the sound region of the element. As a result of the interaction, normal compressive stresses (σ_c) rise at the surficial layers, while normal tensile stresses (σ_{tc}) appear at the sound inner core. If σ_{tc} reaches the tensile strength of concrete, the inner core might crack. This might produce a release of the restricted strains and an abrupt displacement of the structure. Figures 3a and 3b depict the stress distribution for symmetric and 1 face sulfate exposure conditions. By assuming equilibrium and compatibility of strains, Eqs. 6-8 are obtained to predict the maximum tensile stresses acting at a certain time in the cross-section (see Table 3).

In the case of piles, R represents the total radius of the cross-section and R_i is the radius of the sound core given by the difference between R and the penetration depth P calculated with Eq. 4 or 5. In the case of diaphragm walls or tunnels, b represent the half thickness of the element.

Table 3. Simplified equations to predict the maximum stresses due to ESA

Struct. typology	Sulfate exp.	Tensile failure of the sound core	Tangential boundary failure		Tensile boundary failure
Piles (linear elements)	Full	$\sigma_{tc} = \frac{E_0 E_e \varepsilon_l (R^2 - R_i^2)}{E_e(R^2 - R_i^2) + E_0 R_i^2}$ (6)	$\tau_b = \frac{E_0 E_e \varepsilon_l (R^2 - R_i^2) R_i \beta_r}{2(E_e(R^2 - R_i^2) + E_0 R_i^2)} tanh\left(\frac{\beta_r l}{2}\right)$ (9) $\beta_r = \sqrt{\frac{2G}{E_0 R_i^2 ln\left(\frac{R}{R_i}\right)}}$ (10)		$\sigma_{tb} = \frac{\varepsilon_l E_e P}{R_i}$ (13)
Diaphragm walls or tunnels (surface elements)	2 faces	$\sigma_{tc} = \frac{E_0 E_e \varepsilon_l P}{E_e P + E_0 (b-P)}$ (7)	$\tau_b = \frac{E_0 E_e \varepsilon_l P b_i \beta}{E_e P + E_0 (b-P)} tanh\left(\frac{\beta l}{2}\right)$ (11)		--
	1 face	$\sigma_{tc} = \frac{E_0 \varepsilon_l P(3P^2 - 9Pb + 8b^2)}{4b^3}$ (8)	$\beta = \sqrt{\frac{G}{E_0(b-P)P}}$ (12)		

2.3.2 Tangential boundary failure

Elements attacked by ESA commonly present a layered spalling of the external surface [7]. Such failure mode might be explained by the tangential stresses that appear at the top and bottom edge of the specimen due to the difference in terms of vertical displacement between the attacked and sound region of the section. These stresses should guarantee the compatibility of displacements at the extremities of the element as the normal stresses do not act at these locations. If the tangential stresses reach the tangential strength of the material, cracks might appear leading to delamination of the structure. Figures 3c and 3d depict the tangential stress distribution for symmetric and 1 face sulfate exposure. Final equations of maximum tangential stresses (τ_b) for symmetric exposure conditions derived from the classical Mixing Theory for short fibers [8-9] are listed in Table 3.

The same formulation is also adopted when elements are exposed to the sulfate ingress only in one face. The curvature introduced by the asymmetric load increases the macroscopic strain in the external damaged layer and reduces the compressive stresses in this region. Therefore, the tangential stresses transmitted to the sound core are reduced, leading to an assessment on the safe side. It is important to remark that the length of the element (l) only affects the assessment of the tangential stresses if it is below a critical value (around 1 m for most structures). For bigger values of l, the maximum tangential stress at the extremities of the element will remain approximately constant.

2.3.3 Tensile boundary failure

In linear structures fully exposed to sulfates, the spalling of the external layers might be also caused by a tensile stress failure at the boundary between the sound and damage regions. As shown in Figure 3e, tensile stresses (σ_{tb}) are induced by the restrictions of the sound core to the expansions experienced by the affected layers in the cross-sectional plane.

The simplified expression to assess this phenomenon is obtained by an analogy with the thin-walled cylinders subjected to internal pressure (penetration depth tends to be significantly smaller than the radius of the element). In order to obtain the maximum tensile stress, it is assumed that the sound core restrains all the expansions in the cross sectional plane, that is, ε_{ce} equals 0. This gives Eq. 13, which should be used for the assessment of σ_{tb} (see Table 3).
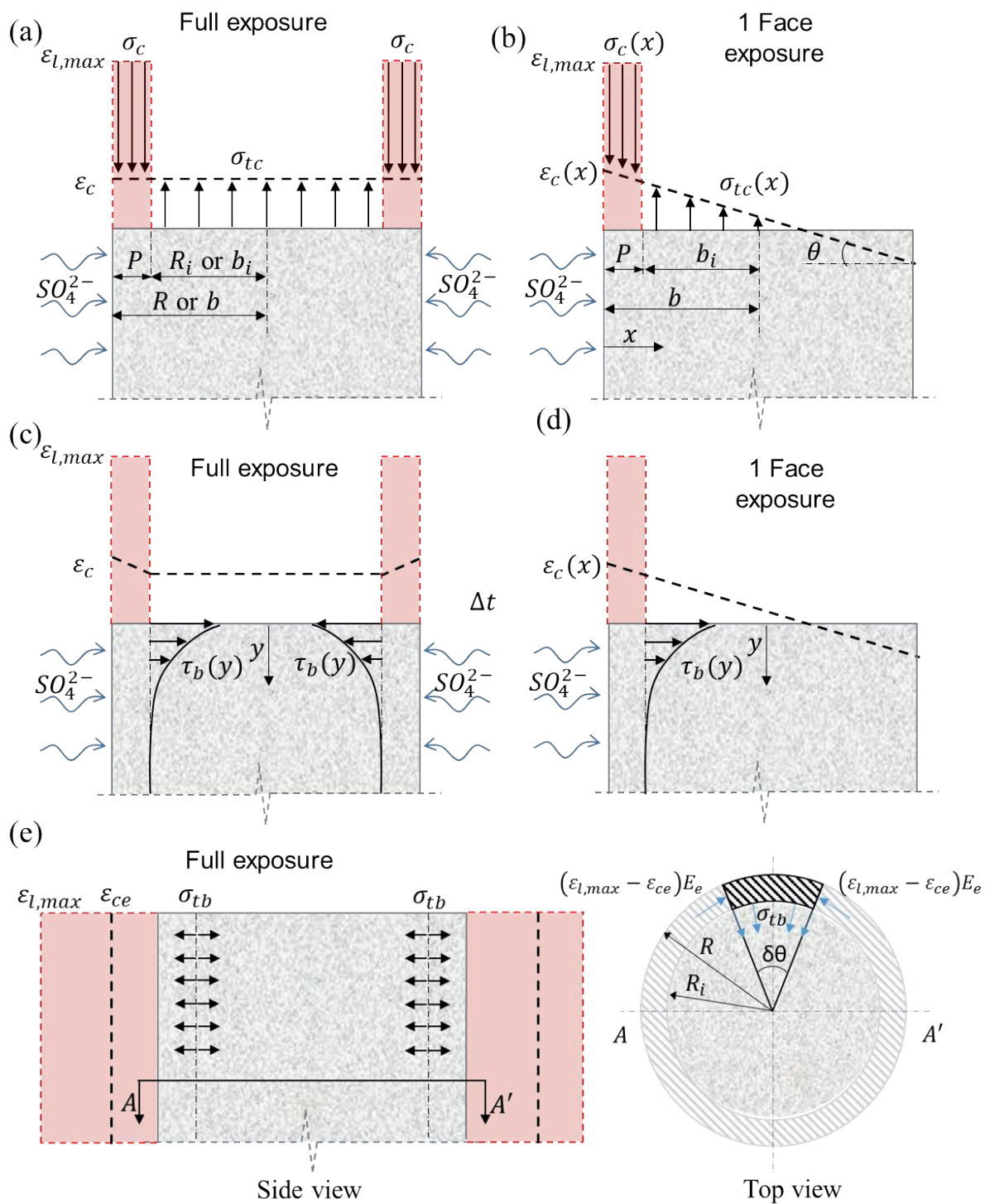
Fig. 3. Stress distribution for (a) Tensile core (b) Tangential boundary and (c) Tensile boundary failure modes under symmetric or 1 face sulfate exposure.

3.   CASE STUDY: INFLUENCE OF SHAPE AND SIZE OF THE ELEMENT

One of the main features of the simplified methodology is that it allows the consideration of the geometrical characteristics of the specimen under attack. By this way, it is possible to take into account the positive contribution of the sound region of the element. In this section, the C_3A limit content prior failure is evaluated for piles and diaphragm walls of different sizes at 25 and 50 years. The results obtained are compared to the criteria from current structural codes.

The sulfate concentration (C_{SO}) was fixed at 3g/l, which correspond a highly aggressive exposure class according to UNE EN 206-1. Initial diffusivity and the buffer capacity of the matrix are fixed at 10^{-12} m^2/s and 0.10, respectively. The length (*l*) of the structural element is fixed at 5 m, which is above the critical length for the assessment of the tangential stresses. This means that the results derived from the parametric study also apply to elements with bigger values of *l*.

To ease the interpretation of the graphs, the different failure modes are represented as the ratio between the stress and its corresponding strength (Ψ). The compressive strength and the elastic modulus of concrete are fixed at 30 MPa and 28000 MPa, respectively. The elastic modulus was considered the same at the sound core and at the superficial layer affected by ESA. This consideration is on the safe side since it provides higher internal stresses in the equations from Table 3. The tensile strength of the material is approximated through the formulation included in the Model Code. The formulation proposed by Kaneko et al. [10] is used to estimate the shear strength, which gives a τ_{max} of 7.1 MPa. This value is in agreement with experimental tests performed by Djazmati [11]. The aluminate content depicted in Figures 4-6 correspond to concretes with 350 kg/m^3 of cement with 80% of clinker. In these figures, the first failure mode is depicted with a discontinuous red line.

Figure 4 depicts the stress/strength ratio for different C_3A contents in piles with 90, 60 and 30 cm of diameter at 25 and 50 years. All curves present similar trends, showing minimum degrees of damage for low contents of C_3A. However, once a threshold content is reached, all stress/strength ratios increase abruptly, indicating a high risk of failure. Notice that this behavior is in agreement with the criteria included in structural codes, which establish a limiting C_3A content for sulfate resistant cements. Below this limit it is assumed that no significant damage occurs.

Results suggests that the size of the element play a very important role on the limit aluminate content. Failure is predicted to occur at C_3A contents around 9%, 8% and 7% for pile diameters of 90, 60 and 30 cm, respectively. Therefore, the limit content of aluminate prior failure decreases along the decrease of size. The failure modes predicted also depend on the size of the element. Large diameters seems to promote the delamination of the external layers due to the tangential stresses in the boundary of the sound and affected regions. On the other hand, for smaller diameters tensile failure in the core might be the predominant failure mode.
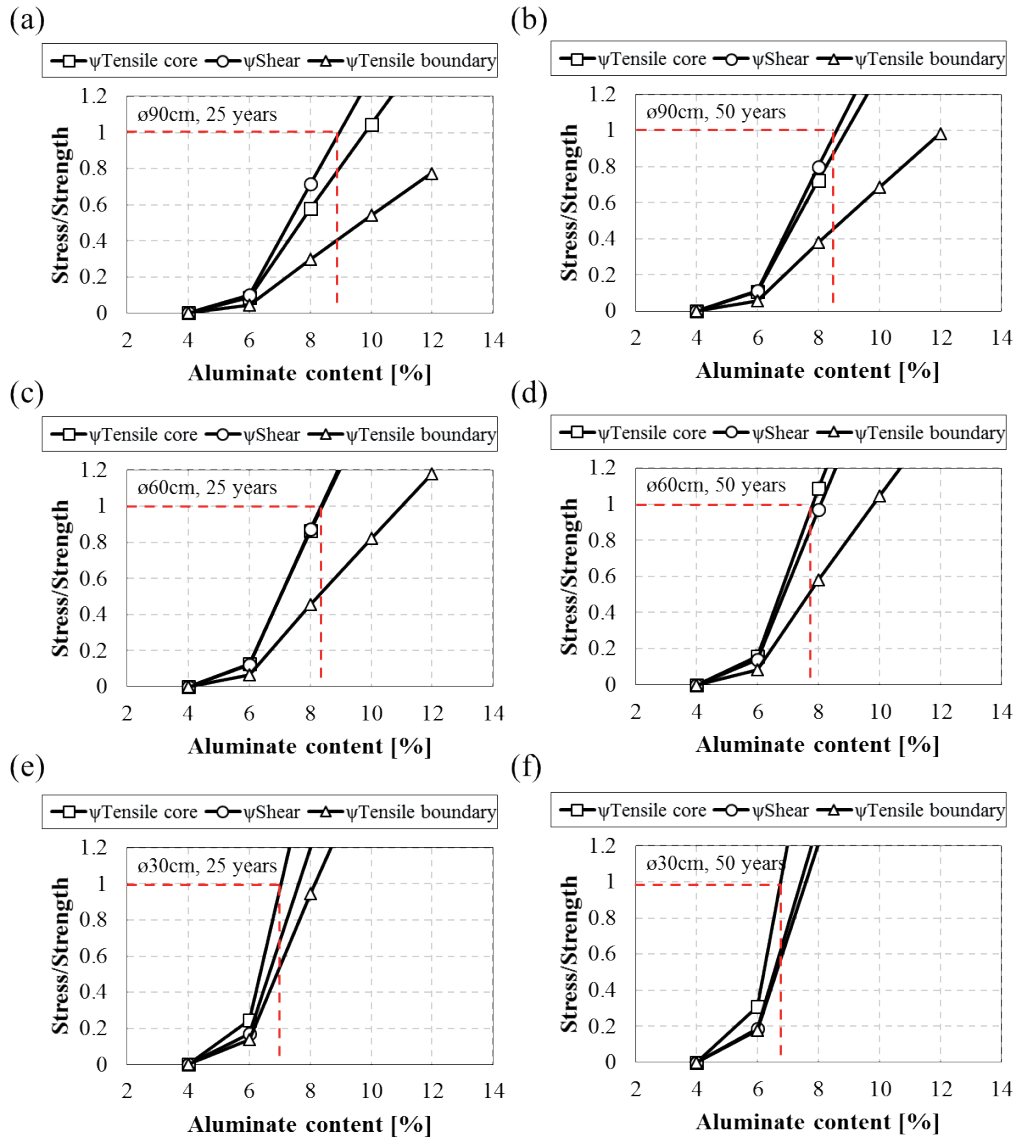
Fig. 4. Stress/strength ratio for piles under full exposure.

Figure 5 shows the stress/strength ratio for different C_3A contents in diaphragm walls of 90, 60 and 30 cm of thickness exposed on the two faces at 25 and 50 years. In this case, only two failure modes are displayed as the tensile boundary failure cannot occur. All curves follow the same trend as the one depicted for the piles. However, in this case the aluminate content at failure is slightly bigger, with allowed contents around 10%, 9% and 8% for 90, 60 and 30 cm of thickness, respectively. Spalling of the external layers is predicted for walls of 90 and 60 cm. In the case of walls of 30 cm, tensile failure in the sound core might be the predominant failure mode.

Notice that according to most design codes, a maximum aluminate content of around 5% should be used for all cases, as the exposure class defined by the sulfate concentration demands the use of a sulfate resistant cement regardless of the size or shape of the element under attack.
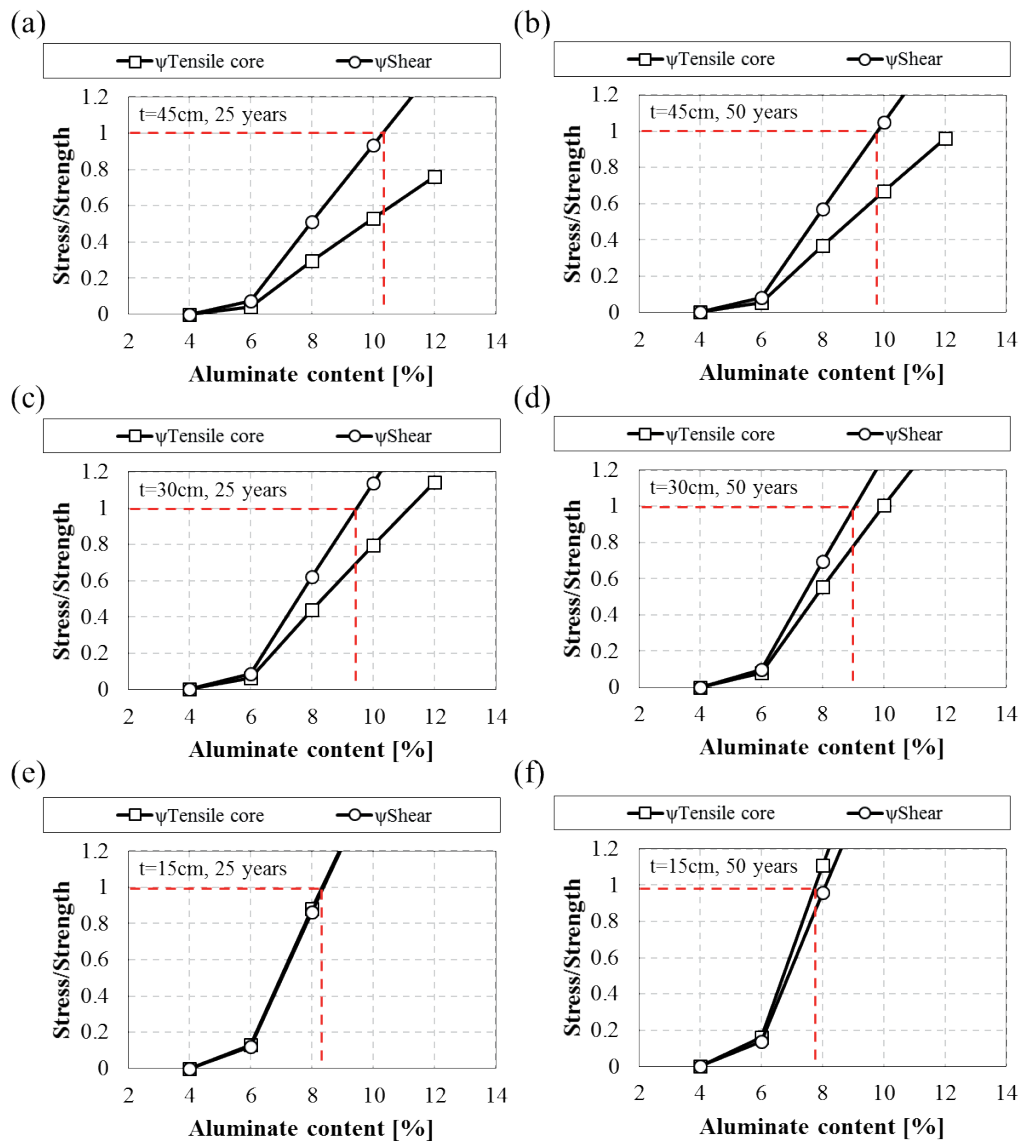
Fig. 5. Stress/strength ratio for diaphragm walls exposed to 2 faces.

4. CONCLUSIONS

A direct and straightforward methodology is developed for the evaluation of the durability of structures exposed to the ESA. This methodology allows a more detailed evaluation of this phenomenon since the specific conditions and expected service life are considered. As a result, an optimized definition of precautionary measures may be obtained for each application.

- Results highlight the influence of the dimensions and structural typology of the element under attack for the assessment of the durability.

- The simplified methodology suggests the existence of a C_3A threshold above which a high risk of structural damage occurs. This threshold increases with the increase of the size of the element and decreases with the desired service life.

- Results indicate that spalling of the external layers due to the tangential stresses might be the predominant failure mode in large elements. However, for slender elements, tensile failure in the core might occur prior delamination.

- Results suggest that the application of the prescriptions described in current design codes might lead to unnecessary penalizing measures in some situations.

ACKNOWLEDGMENTS

REFERENCES

[1]   T. Ikumi,, S.H.P. Cavalaro, I. Segura, A. de la Fuente, A. Aguado, Simplified methodology to evaluate the external sulfate attack in concrete structures, Mat. Des. 89 (2016), 1147-1160.

[2]   T. Ikumi, S.H.P. Cavalaro, I. Segura, A. Aguado, Alternative methodology to consider damage and expansions in external sulfate attack modeling, Cem. Concr. Res. 63 (2014), 105–116.

[3]   A.E. Idiart, C.M. López, I. Carol, Chemo-mechanical analysis of concrete cracking and degradation due to external sulfate attack: A meso-scale model,» Cem. Concr. Compos. 33 (2011), 411–423.

[4]   B. Gérard, J. Marchand, Influence of cracking on the diffusion properties of cement-based materials. Part I: Influence of continuous cracks on the steady-state regime, Cem. Concr. Res. 30 (2000), 37–43.

[5]   D.A. Hordijk, Local Approach to Fatigue of Concrete, Phd Thesis, Delft University of Technology (1991).

[6]   R. Tixier, B. Mobasher, Modeling of Damage in Cement-Based Materials Subjected to External Sulfate Attack. I: Formulation, J. Mater. Civ. Eng. 15 (2003), 305–313.

[7]   S.T. Lee, R.D. Hooton, H. Jung, D. Park, C.S. Choi, Effect of limestone filler on the deterioration of mortars and pastes exposed to sulfate solutions at ambient temperature, Cem. Concr. Res. 38 (2008) 68–76.

[8]   A. Jayatilaka, Fracture of engineering brittle materials, Applied Science Publishers (1979).

[9]   S. Oller, Simulación numérica del comportamiento mecánico de los materiales compuestos, CIMNE 74 (2003).

[10]   Y. Kaneko, H. Mihashi and S. Ishihara, Shear failure of plain concrete in strain localized area, Proceeding of the Fifth International Conference on Fracture Mechanics of Concrete and Concrete Structures, Colorado, USA, V.C. Li, C.K.Y. Leung, K.J. Willam and S.L. Billington (ed.), 12-16 Vol.1 (2004), 383-390.

[11]   B. Djazmati and J.A. Pincheira, Shear stiffness and strength of horizontal construction joints, ACI Structural J. 101 (2004), 484-493.